Cambridge Books Online

http://ebooks.cambridge.org/

Principles of Magnetohydrodynamics

With Applications to Laboratory and Astrophysical Plasmas

J. P. Hans Goedbloed, Stefaan Poedts

Book DOI: http://dx.doi.org/10.1017/CBO9780511616945

Online ISBN: 9780511616945

Hardback ISBN: 9780521623476

Paperback ISBN: 9780521626071

Chapter

7 - Waves and instabilities of inhomogeneous plasmas pp. 300-383

Chapter DOI: http://dx.doi.org/10.1017/CBO9780511616945.008

Cambridge University Press

7

Waves and instabilities of inhomogeneous plasmas

7.1 Hydrodynamics of the solar interior

We have studied the MHD waves for homogeneous plasmas in Chapter 5. This theory was transformed in Chapter 6 to the higher level of spectral theory in order to facilitate the much more complicated analysis of inhomogeneous plasmas, which we want to undertake in the present chapter. Plasma inhomogeneity is not just a complication in the analysis, but also provides qualitatively new physical phenomena like wave damping, wave transformation, and, most important of all, a very wide class of global MHD instabilities of magnetically confined plasmas.

Explicit examples of inhomogeneous plasma dynamics abound in the solar system, as we will see in Chapter 8. For the Sun, a number of important phenomena may be described neglecting the magnetic field. Therefore, before we turn to magnetized plasmas in Section 7.3, we will first simplify the model to a purely hydrodynamic one and study the effects of sound and gravity separate from the three MHD waves. Since the hydrodynamic waves are clearly identified in solar observations, we will be able to clarify the potential of observing MHD wave propagation for the investigation of astrophysical objects in general (Section 7.2.4).

We summarize some basic facts of *the standard solar model* (see Priest [190], Stix [217] or Foukal [69]). The Sun is a sphere of hot material, mainly plasma, of radius $R_\odot = 7.0 \times 10^8\,\mathrm{m}$ and mass $M_\odot = 2.0 \times 10^{30}\,\mathrm{kg}$. The total radiation power output of the Sun, *the solar luminosity*, is $L_\odot = 3.86 \times 10^{26}\,\mathrm{W}$. At the Earth, i.e. at a distance of $1\,\mathrm{AU}$ ($= 1.5 \times 10^{11}\,\mathrm{m}$), this results in a heat flux of $L_\odot/[4\pi \times (1\,\mathrm{AU})^2] = 1.36\,\mathrm{kW\,m^{-2}}$: *the solar constant*. This number roughly corresponds to a crude estimate which one would make on the basis of sunbathing experience. Through the work of H. A. Bethe and C. F. von Weizsäcker (1939) we know that this enormous amount of energy is not produced by gravitational contraction but by *thermonuclear reactions*.

Downloaded from Cambridge Books Online by IP 152.2.176.242 on Mon Apr 29 20:09:08 WEST 2013.
http://dx.doi.org/10.1017/CBO9780511616945.008
Cambridge Books Online © Cambridge University Press, 2013

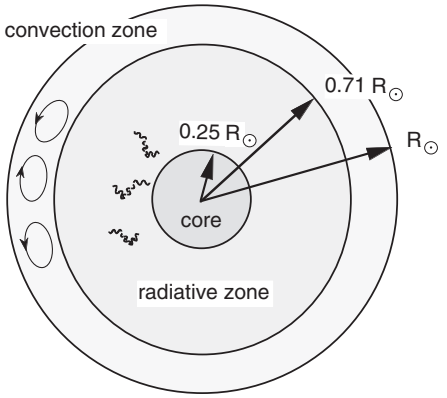

Fig. 7.1. Internal structure of the Sun: thermonuclear energy production in the core, radiation transport in the radiation zone, and convection in the outermost layer.

The thermonuclear energy source is located in *the core* ($r \leq 0.25 R_\odot$) of the Sun (Fig. 7.1), where the values of the temperature and the density are $T_0 = 1.6 \times 10^7$ K and $\rho_0 = 1.6 \times 10^5\,\mathrm{kg\,m^{-3}}$, respectively. This is sufficient for *the* p–p *fusion reaction chain* to occur, described by the equations (1.7) and (1.8) of Section 1.2.1. (Recall that these fusion reactions are completely different, with vastly different time scales, from the ones exploited in thermonuclear laboratory experiments.) The energy produced in the form of gamma radiation is transported through *the radiative zone* ($0.25 R_\odot \leq r \leq 0.713 R_\odot$) to the outer layers. As mentioned in Chapter 1, on average, this process takes millions of years per photon and the wavelengths gradually shift to those of UV and visible light. Finally, the radiative transport is exceeded by convection in the outermost layer of the Sun, *the convection zone* ($0.713 R_\odot \leq r \leq R_\odot$), for reasons that soon will become clear.

7.1.1 Radiative equilibrium model

Let us first consider the process of radiation transport of the thermonuclear power produced in the core to the outer layers of the Sun. This requires the formulation of a *radiative equilibrium model* which can predict the static equilibrium distributions of the different variables characterizing the interior of the Sun. For that purpose, the equations of magnetohydrodynamics presented in Section 4.1 should be enhanced with radiation terms (see Section 4.4.2), whereas the magnetic field contributions can be neglected.

For generality, we first present *the time-dependent hydrodynamic equations*, extending the equations (4.12)–(4.14) of MHD with internal energy production and

Downloaded from Cambridge Books Online by IP 152.2.176.242 on Mon Apr 29 20:09:08 WEST 2013.
http://dx.doi.org/10.1017/CBO9780511616945.008
Cambridge Books Online © Cambridge University Press, 2013

radiation transport, but ignoring the magnetic field ($\mathbf{B} = 0$). The equation of mass conservation (4.12) is unchanged:

$$\frac{\partial \rho}{\partial t} + \nabla \cdot (\rho \mathbf{v}) = 0 \,. \tag{7.1}$$

In the momentum conservation equation (4.13), the gravitational attraction is specified to be spherically symmetric:

$$\rho \frac{\mathrm{D}\mathbf{v}}{\mathrm{D}t} + \nabla p - \rho \mathbf{g} = 0 \,, \qquad \text{where} \quad \mathbf{g} = -g\mathbf{e}_r \,, \quad g = g(r) = G\,\frac{M(r)}{r^2} \,. \tag{7.2}$$

Here, the gravitational constant $G = 6.67 \times 10^{-11}\,\mathrm{N\,m^2\,kg^{-2}}$ and $M(r)$ is the mass inside a sphere of radius r, which is related to the density ρ by means of the obvious differential equation

$$\frac{dM}{dr} = 4\pi r^2 \rho \,. \tag{7.3}$$

For the present purpose, it is convenient to replace the pressure evolution equation (4.14), which is a consequence of the entropy conservation equation, by the appropriate generalization of the internal energy equation (4.19), given by Eq. (4.138):

$$\rho \frac{\mathrm{D}e}{\mathrm{D}t} + p\nabla \cdot \mathbf{v} = \nabla \cdot [\,\lambda \nabla (kT)\,] + \rho\varepsilon \,, \qquad \text{where} \quad e \equiv \frac{1}{\gamma - 1}\,\frac{p}{\rho} \,. \tag{7.4}$$

The right hand side now contains two additional terms which are due to *radiative transport*, governed by *the thermal conduction coefficient*, $\lambda(r)$,[1] and *the thermonuclear energy production per unit mass*, $\varepsilon(r)$. In general, the latter will be strongly dependent on the temperature and the concentration of hydrogen.

At this point, it becomes clear that the radiative model actually requires more than just one fluid since thermonuclear energy production and thermal conduction depend on the concentration of the different particle species. This aspect of the problem will be approximated by means of an equation of state, relating the pressure and the temperature, that is modified to take the different masses of the particles into account. For a plasma consisting of electrons and one kind of ion with equal temperatures ($T \equiv T_e = T_i$), the expression for the pressure may be converted by means of the charge neutrality relation, $n_e = Z_c n_i$, and the definition for the density, $\rho \equiv n_e m_e + n_i m_i$:

$$p = (n_e + n_i)\,kT = n_i(1 + Z_c)\,kT = \frac{1 + Z_c}{m_i(1 + Z_c m_e/m_i)}\,\rho kT \approx \frac{1 + Z_c}{A}\,\frac{\rho kT}{m_p} \,. \tag{7.5}$$

[1] To stick to conventions in the literature, we had to introduce notations conflicting with those of previous chapters: the thermal conductivity λ of the present chapter was called κ in Sections 3.3.2 and 4.4.2, but the symbol κ will here be used for the opacity (see below).

Downloaded from Cambridge Books Online by IP 152.2.176.242 on Mon Apr 29 20:09:08 WEST 2013.
http://dx.doi.org/10.1017/CBO9780511616945.008
Cambridge Books Online © Cambridge University Press, 2013

Here, A is the mass number (in multiples of the proton mass, $m_i = Am_p$) and Z_c is the charge number (in multiples of e) of the ions. The latter quantity is subscripted with the letter c since, in this context, the bare symbol Z is used for another quantity, to be introduced shortly.

So far, the equation of state (7.5) is just the usual one for a plasma consisting of electrons and one kind of ion, so that Z_c and A are constants. Now, we modify the equation of state by permitting different ion species that are radially distributed according to a function called the *mean molecular weight* μ, so that

$$p = \frac{1}{\mu}\frac{\rho kT}{m_p}, \quad \text{where } \mu \equiv \frac{A}{1+Z_c} \text{ is no longer constant.} \tag{7.6}$$

The mean molecular weight μ measures the average weight of the constituent particles in units of m_p: $\mu = 1/2$ for ionized hydrogen ($Z_c = A = 1$), $\mu = 4/3$ for ionized helium ($Z_c = 2$, $A = 4$), and $\mu \approx 2$ for the completely ionized heavier atoms ($Z_c \gg 1$, $A \approx 2Z_c$). For a plasma with a mixture of these ions, $\mu \approx (2X + \frac{3}{4}Y + \frac{1}{2}Z)^{-1}$, where X is the mass fraction of hydrogen, Y is the mass fraction of helium, and Z indicates the mass fraction of the heavier elements. Hence, $\mu = \mu(\rho(r), T(r))$ is now a function of position reflecting the abundance of the different elements in the Sun and their degrees of ionization, to be determined by Saha equations of the type discussed in Section 1.4.1. Note that the dependence of p on μ implies that the pressure decreases when hydrogen is converted into helium by the mentioned thermonuclear reactions.

To construct a *static* equilibrium model of the Sun from these equations, one sets $\mathbf{v} = 0$ and $\partial/\partial t = 0$. The mass conservation equation (7.1) is then trivially satisfied, whereas Eqs. (7.2) and (7.3) provide the equations for *hydrostatic equilibrium:*

$$\frac{dp}{dr} = -\rho g = -G\frac{\rho M}{r^2} \quad \Rightarrow \quad \frac{1}{r^2}\frac{d}{dr}\left(\frac{r^2}{\rho}\frac{dp}{dr}\right) = -\frac{G}{r^2}\frac{dM}{dr} = -4\pi G\rho\,. \tag{7.7}$$

In static equilibrium, the LHS of the internal energy equation (7.4) vanishes so that

$$\frac{1}{r^2}\frac{d}{dr}\left[r^2\lambda\frac{d(kT)}{dr}\right] = -\rho\varepsilon\,, \tag{7.8}$$

which expresses *radiative equilibrium*: the produced thermonuclear energy is transported outward by radiative transfer. The set of differential equations (7.7)–(7.8) is complete when supplemented with the equation of state (7.6) and equations determining the functions $\mu(r)$, $\lambda(r)$, and $\varepsilon(r)$.

Although the hydrostatic model is now complete, it is useful to relate the differential equation (7.8) for the temperature with the fundamental quantities of radiative transport, viz. luminosity, radiation pressure and opacity. Radiative

Downloaded from Cambridge Books Online by IP 152.2.176.242 on Mon Apr 29 20:09:08 WEST 2013.
http://dx.doi.org/10.1017/CBO9780511616945.008
Cambridge Books Online © Cambridge University Press, 2013

equilibrium implies that the local value of *the luminosity*, $L(r)$, which is the net radiation flux per unit of time through a spherical surface, is given by

$$L(r) = \int_0^r \varepsilon(r')\, dM = 4\pi \int_0^r \rho\, \varepsilon r'^2\, dr' . \tag{7.9}$$

To relate this expression to the temperature gradient appearing in Eq. (7.8), we introduce *the radiation pressure*[2]

$$q \equiv p_{\rm rad} = \left(\frac{4\sigma}{3c}\right) T^4 , \tag{7.10}$$

where $\sigma \equiv 2\pi^5 k^4/(15c^2h^3) = 5.67 \times 10^{-8}\,{\rm W\,m^{-2}\,K^{-4}}$ is the Stefan–Boltzmann constant, and we exploit the fundamental relationship between the gradient of the radiation pressure and the absorbed radiation,

$$\frac{dq}{dr} = -\left(\frac{1}{4\pi c}\right) \frac{\kappa \rho L}{r^2} , \tag{7.11}$$

where κ is *the opacity*, i.e. the absorption coefficient of the radiation per unit mass and per unit length. Hence,

$$L(r) = -\left(\frac{16\pi\sigma}{3}\right) \frac{r^2}{\kappa\rho} \frac{dT^4}{dr} . \tag{7.12}$$

From Eqs. (7.9) and (7.12) we again obtain a differential equation for the temperature, which, of course, should be equivalent to Eq. (7.8). This implies that the thermal conductivity λ is inversely proportional to the opacity κ ,

$$\lambda = \left(\frac{16\sigma}{3k}\right) \frac{T^3}{\kappa\rho} . \tag{7.13}$$

The opacity is a microscopic quantity determined by quite a number of different scattering processes between photons and atoms, ions or electrons, averaged over frequency. To compute radiative equilibrium, one considers $\kappa = \kappa(\rho, T)$ to be a known function, obtained in the form of a table from the extensive numerical calculations that have been developed for this purpose [217].

Finally, we need an explicit relation for the thermonuclear energy production rate by proton–proton reactions, as given, e.g., by Zirin [250]:

$$\varepsilon = \varepsilon(X, \rho, T) = 0.25\, \rho X^2 \left(\frac{10^6}{T}\right)^{2/3} \exp\left\{-33.8\, (10^6/T)^{1/3}\right\} , \tag{7.14}$$

[2] The effect of the radiation pressure is here only taken into account as far as the radiation transport is concerned, but neglected in the hydrostatic equilibrium equation. Actually, one should replace p in Eq. (7.7) by the total pressure $P \equiv p + q$, but one easily checks that this effect is negligible for relatively cool stars like the Sun. With $T_0 = 1.6 \times 10^7$ K, $n_0 = 10^{32}\,{\rm m^{-3}}$, and $T_{\rm ph} = 6000\,{\rm K}$, $n_{\rm ph} = 2.4 \times 10^{23}\,{\rm m^{-3}}$, the value of q/p ranges from 7.4×10^{-4} in the centre to 1.6×10^{-5} at the photosphere.

Downloaded from Cambridge Books Online by IP 152.2.176.242 on Mon Apr 29 20:09:09 WEST 2013.
http://dx.doi.org/10.1017/CBO9780511616945.008
Cambridge Books Online © Cambridge University Press, 2013

where the dimensions of the quantities are given by $[\rho] = \mathrm{kg\,m^{-3}}$, $[T] = \mathrm{K}$, and $[\varepsilon] = \mathrm{J\,kg^{-1}\,s^{-1}}$. It is clear that the function $\varepsilon(X, \rho, T)$ is strongly concentrated in the central regions of the Sun where the temperature is high: thermonuclear burn only occurs in *the core region* of the Sun ($r \leq 0.25 R_\odot$).

▷ **Exercise.** Estimate the fraction of the total solar mass participating in the thermonuclear energy production, using the values of $M(R_\odot)$, $L(R_\odot)$ and ρ_0 given in this section. ◁

The standard solar model consists of the two second order differential equations (7.7) and (7.8), supplemented with the equation of state (7.6) and numerically obtained values of the functions $\mu(\rho, T)$, $\kappa(\rho, T)$, and $\varepsilon(X(\rho, T), \rho, T)$. For the latter quantity one should exploit Eq. (7.14), which evidently spoils the possibility of obtaining explicit analytic solutions, even when mild assumptions are made about μ and κ.

Since two second order ODEs are equivalent to four first order ODEs, one may choose, for example, to solve for the following ODEs for the four quantities $M(r)$, $L(r)$, $p(r)$ and $T(r)$:

$$\begin{aligned} \frac{dp}{dr} &= -G\,\frac{\rho M}{r^2}, \qquad \text{where } \rho = \left(\frac{m_p}{k}\right)\frac{\mu p}{T}, \\ \frac{dM}{dr} &= 4\pi\, r^2 \rho\,, \\ \frac{dT}{dr} &= -\left(\frac{3}{64\pi\sigma}\right)\frac{\kappa \rho L}{r^2 T^3}, \\ \frac{dL}{dr} &= 4\pi\, r^2 \rho \varepsilon\,. \end{aligned} \tag{7.15}$$

Appropriate boundary conditions for these equations are

$$p(R_\odot) \approx 0\,, \quad M(0) = 0\,, \quad T(R_\odot) \approx 0\,, \quad L(0) = 0\,. \tag{7.16}$$

Of course, the solution obtained should reproduce the known value of the solar mass, $M(R_\odot) = M_\odot$, and of the solar luminosity, $L(R_\odot) = L_\odot$, at the known position $r = R_\odot$ of the solar radius. Also, the values p_0 and T_0 should correspond to the numbers cited for the central density and temperature to yield thermonuclear burn. This procedure actually turns out to provide quite realistic solutions (see Fig. 7.2), except for one feature, viz. the assumption of hydrostatic equilibrium *up to the solar surface*.

7.1.2 Convection zone

In the outer layers of the Sun, cooling is so strong that the absolute value of the temperature gradient exceeds a certain threshold given by the Schwarzschild

Downloaded from Cambridge Books Online by IP 152.2.176.242 on Mon Apr 29 20:09:10 WEST 2013.
http://dx.doi.org/10.1017/CBO9780511616945.008
Cambridge Books Online © Cambridge University Press, 2013

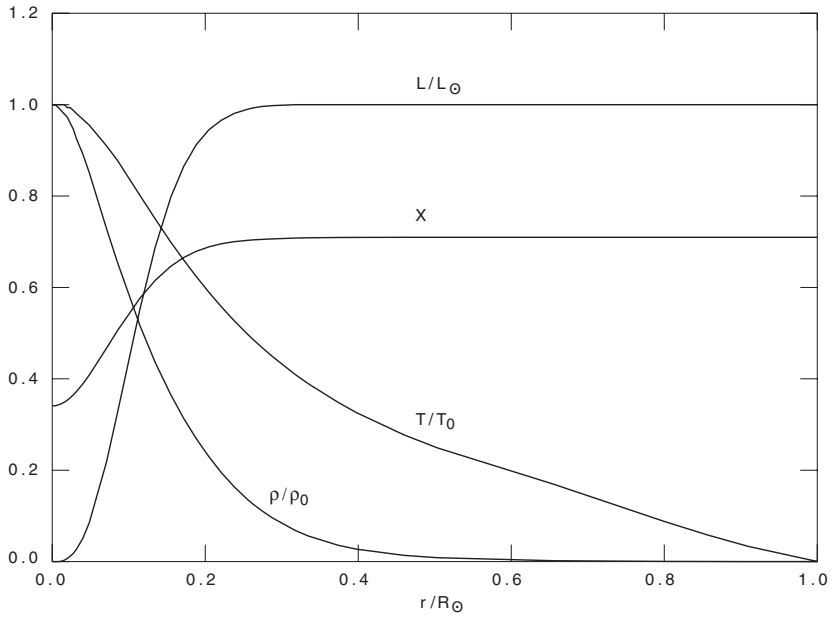

Fig. 7.2. Radial distributions of the physical quantities for a standard solar model. (From Foukal [69], using data of Bahcall and Ulrich, *Rev. Mod. Phys.* **60**, 297 (1988).)

criterion for convective stability. Since the temperature gradient is negative, that criterion is best discussed in terms of the quantity $-dT/dr$. Convective stability is achieved when $-dT/dr$ does not exceed a critical value, which is obtained as follows.

Introducing the mean particle mass, $m \equiv \mu m_p$, the ratio of the Boltzmann constant k and m may be abbreviated as a kind of gas constant, $\mathcal{R} \equiv k/m$. Anticipating the outcome of the present section, $\mathcal{R}$ is actually constant in the convection zone because of the strong mixing that occurs, so that $\mu \approx$ const there. Consequently, the equation of state (7.6) may be written as

$$p = \mathcal{R}\rho T\,. \tag{7.17}$$

Hence, the temperature gradient is related to the density and pressure gradients by

$$-\frac{dT}{dr} = \frac{1}{\mathcal{R}}\left(\frac{p}{\rho^2}\frac{d\rho}{dr} - \frac{1}{\rho}\frac{dp}{dr}\right) \qquad \left[= \frac{1}{\mathcal{R}}\left(\frac{p}{\rho^2}\frac{d\rho}{dr} + g\right)\right], \tag{7.18}$$

where the equilibrium relation (7.7), $dp/dr = -\rho g$, has been inserted in the

Downloaded from Cambridge Books Online by IP 152.2.176.242 on Mon Apr 29 20:09:10 WEST 2013.
http://dx.doi.org/10.1017/CBO9780511616945.008
Cambridge Books Online © Cambridge University Press, 2013

rightmost equality. Here, and below, we put square brackets around such equalities to indicate that this additional equilibrium information has been exploited.

The critical value for convective stability is obtained from the consideration that motions of the gas are neutrally stable only if the fluid is *isentropic*, i.e. if the value of the specific entropy is constant throughout the pertinent region of space:

$$S \equiv p\rho^{-\gamma} = \text{const} \quad \Rightarrow \quad \frac{d\rho}{dr} = \frac{\rho}{\gamma p}\frac{dp}{dr} \qquad \left[= -\frac{\rho^2 g}{\gamma p} \right], \tag{7.19}$$

so that

$$-\left(\frac{dT}{dr}\right)_{\text{isentr.}} = -\frac{1}{\mathcal{R}}\,\frac{\gamma-1}{\gamma}\,\frac{1}{\rho}\frac{dp}{dr} \qquad \left[= \frac{1}{\mathcal{R}}\,\frac{\gamma-1}{\gamma}\,g \right]. \tag{7.20}$$

Convective instability occurs when the actual temperature gradient $-dT/dr$ exceeds this value, i.e. when *the Schwarzschild criterion for convective stability*,

$$-\frac{dT}{dr} \le -\left(\frac{dT}{dr}\right)_{\text{isentr.}} \quad \Rightarrow \quad \frac{d\rho}{dr} - \frac{\rho}{\gamma p}\frac{dp}{dr} \le 0 \quad \left[\Rightarrow \quad \frac{d\rho}{dr}g + \frac{\rho^2 g^2}{\gamma p} \le 0 \right], \tag{7.21}$$

is violated. Interestingly enough, the criterion for gravitational stability (in square brackets) of Section 6.5.4 is recovered: convective and gravitational (Rayleigh–Taylor) instabilities amount to the same.

Note that we here exploit the term 'isentropic' rather than the more usual term 'adiabatic' since we wish to stress that the background equilibrium state is not isentropic in general but that the assumption of adiabatic fluid *motion*, i.e. $DS/Dt = 0$, may still be made. Recall that this assumption is underlying the whole analysis of Chapter 6, including the derivation of the gravitational stability in Section 6.5.4. Hence, adiabatic motions are stable or unstable according to whether the condition (7.21) is satisfied or violated. Only at marginal stability do the two concepts coincide: the equilibrium is then characterized by constant entropy in space and marginal motion ($\omega = 0$) does not change this distribution.

In the Sun, the Schwarzschild criterion (7.21) is violated in the region $0.713R_\odot \le r \le R_\odot$, which is called *the convective region* for that reason. In this region turbulent mixing occurs, i.e. eddies of hot material are carried up and eddies of cool material are carried down so as to maintain the temperature gradient at the value given by the RHS of the first expression (7.21). Consequently, rather than applying the boundary conditions (7.16) at the solar surface ($r = R_\odot$), one obtains a more realistic solar model by separating the interior in the regions $r \le 0.713R_\odot$ (core and radiative zone), bounded by a surface where the boundary condition

$$-\frac{dT}{dr} = -\left(\frac{dT}{dr}\right)_{\text{isentr.}} \qquad (\text{at } \; r = 0.713R_\odot) \tag{7.22}$$

Downloaded from Cambridge Books Online by IP 152.2.176.242 on Mon Apr 29 20:09:10 WEST 2013.
http://dx.doi.org/10.1017/CBO9780511616945.008
Cambridge Books Online © Cambridge University Press, 2013

is imposed, and the convective region which is governed by a completely different set of equations. In particular, the assumption of static equilibrium is not appropriate for the convective region so that one should return to the time-dependent equations (7.1)–(7.6), where the flow also destroys the spherical symmetry of the problem. Unfortunately, there is little one can do about solving this problem without recourse to a large computer and, even then, there remains a large uncertainty about the nature of the solutions in the convection zone.

Ironically, there appears to be more certainty about the structure of the interior of the Sun, which is completely opaque (recall that the mean free path of photons is only a few centimetres there), than the outer regions. Also, the magnetic field, which we have ignored until now, turns out to play an important role in the outer layers of the Sun. In particular, the origin of the solar magnetic field, i.e. *the solar dynamo*, is thought to be situated at the bottom of the convection zone. The dynamo problem involves differential rotation, spherical geometry, and magnetic fields. This significantly adds to the complexity of the problem since magnetic fields cannot be fitted in a spherically symmetric geometry. This fact is very evident from the huge number of complex magnetic structures that can be observed in the atmosphere of the Sun, viz. in the photosphere, the chromosphere and the corona.

In conclusion, it appears hopeless to try to find solutions for the interior of the Sun, by means of the theoretical approach discussed so far, starting from such a complicated boundary. Fortunately, a powerful observational and analytical tool has become available that can probe the deep structure of the Sun, viz. *helioseismology*, which will be treated in the following section.

7.2 Hydrodynamic waves and instabilities of a gravitating slab

The convective layer derives its name from the convective instability which arises when the Schwarzschild criterion (7.21) is violated. Since this is associated with the transition from stability to instability of gravity waves, at this point it is instructive to consider the more general subject of solar oscillations. Here, we will consider the Sun as a whole and, again, neglect the presence of magnetic fields. The symmetry of the problem would involve the treatment of wave propagation in spherically inhomogeneous systems (background quantities depending on the radial coordinate r), leading to the occurrence of spherical harmonics in the analysis. However, we will avoid these technical complications and just consider *the gravito-acoustic waves in a planar stratification* (background quantities depending on the vertical coordinate x). Obviously, the expressions derived require a generalization to spherical stratification if one wishes to compare calculated frequencies with observed ones. Our goal is to demonstrate how spectral analysis relates to

Downloaded from Cambridge Books Online by IP 152.2.176.242 on Mon Apr 29 20:09:10 WEST 2013.
http://dx.doi.org/10.1017/CBO9780511616945.008
Cambridge Books Online © Cambridge University Press, 2013

practical applications, not to treat the subject of solar and stellar oscillations in detail. (The interested reader should consult the texts by Christensen-Dalsgaard [56] or Unno *et al.* [234].)

7.2.1 Hydrodynamic wave equation

Again, we exploit the equations of gas dynamics. We now keep the adiabatic law so that the relevant equations become

$$\frac{\mathrm{D}\rho}{\mathrm{D}t} + \rho\nabla\cdot\mathbf{v} = 0\,, \tag{7.23}$$

$$\rho\,\frac{\mathrm{D}\mathbf{v}}{\mathrm{D}t} + \nabla p - \rho\mathbf{g} = 0\,, \tag{7.24}$$

$$\frac{\mathrm{D}p}{\mathrm{D}t} + \gamma p\nabla\cdot\mathbf{v} = 0\,. \tag{7.25}$$

Note that this implies that, for the study of waves, we neglect the RHS of Eq. (7.4), i.e. *non-adiabatic effects* caused by thermal conduction and thermonuclear energy production. Also, for simplicity, we consider the gravitational acceleration as a given constant, i.e. we neglect perturbations of the gravitational potential (which is called the *Cowling approximation*):

$$\mathbf{g} = (-g, 0, 0)\,, \qquad g = \text{const}\,.$$

We will again assume a static background equilibrium, i.e. $\mathbf{v} = 0$ and $\partial/\partial t = 0$, so that the only restriction on the equilibrium comes from the momentum equation (7.24):

$$\nabla p_0 = \rho_0\mathbf{g} \quad \Rightarrow \quad p_0'(x) = -\rho_0(x)g\,, \tag{7.26}$$

where the prime indicates differentiation with respect to x.

Linearization leads to the following equations:

$$\frac{\partial\rho_1}{\partial t} + \mathbf{v}_1\cdot\nabla\rho_0 + \rho_0\nabla\cdot\mathbf{v}_1 = 0\,, \tag{7.27}$$

$$\rho_0\,\frac{\partial\mathbf{v}_1}{\partial t} + \nabla p_1 - \rho_1\mathbf{g} = 0\,, \tag{7.28}$$

$$\frac{\partial p_1}{\partial t} + \mathbf{v}_1\cdot\nabla p_0 + \gamma p_0\nabla\cdot\mathbf{v}_1 = 0\,. \tag{7.29}$$

These equations are straightforward generalizations of Eqs. (5.5)–(5.7) with additional terms due to gravity and the associated inhomogeneity. Hence, we could derive the wave equation, corresponding to Eq. (5.8) for the homogeneous case, by differentiating Eq. (7.28) with respect to t and inserting the expressions

Downloaded from Cambridge Books Online by IP 152.2.176.242 on Mon Apr 29 20:09:10 WEST 2013.
http://dx.doi.org/10.1017/CBO9780511616945.008
Cambridge Books Online © Cambridge University Press, 2013

for $\partial\rho_1/\partial t$ and $\partial p_1/\partial t$ from Eqs. (7.27) and (7.29). However, we rather exploit our newly obtained instrument of integrating by means of the displacement vector $\boldsymbol{\xi}$ (Section 6.1.2), where $\mathbf{v}_1 = \partial\boldsymbol{\xi}/\partial t$, so that $\rho_1 = -\nabla\cdot(\rho_0\boldsymbol{\xi})$ and $p_1 = -\boldsymbol{\xi}\cdot\nabla p_0 - \gamma p_0 \nabla\cdot\boldsymbol{\xi}$. Inserting these expressions into Eq. (7.28), and cancelling some terms by exploiting the equilibrium relation (7.26), we obtain *the wave equation for gravito-acoustic waves in a plane stratified medium*:

$$\rho\frac{\partial^2\boldsymbol{\xi}}{\partial t^2} - \nabla(\gamma p\nabla\cdot\boldsymbol{\xi}) - \rho\,\nabla(\mathbf{g}\cdot\boldsymbol{\xi}) + \rho\mathbf{g}\,\nabla\cdot\boldsymbol{\xi} = 0\,. \tag{7.30}$$

We have omitted the subscripts 0 and 1 for the equilibrium and perturbed quantities since there can be no confusion any more: perturbed quantities are expressed in $\boldsymbol{\xi}$, all other quantities refer to the background. The wave equation (7.30) generalizes Eq. (5.8) with two additional terms related to gravity. Of course, Eq. (7.30) is also obtained as the special case $\mathbf{B} = 0$ of the general MHD equation of motion (6.23), exploiting the appropriate expression (6.50) for the force operator.

Considering normal mode solutions of the form

$$\boldsymbol{\xi}(\mathbf{r}, t) = \hat{\boldsymbol{\xi}}(x)\,\mathrm{e}^{\mathrm{i}(k_y y + k_z z - \omega t)}\,, \tag{7.31}$$

Eq. (7.30) may be written in matrix form as

$$\begin{pmatrix} \rho\omega^2 + \dfrac{d}{dx}\gamma p\dfrac{d}{dx} & \mathrm{i}k_y\left(\dfrac{d}{dx}\gamma p + \rho g\right) & \mathrm{i}k_z\left(\dfrac{d}{dx}\gamma p + \rho g\right) \\ \mathrm{i}k_y\left(\gamma p\dfrac{d}{dx} - \rho g\right) & \rho\omega^2 - k_y^2\gamma p & -k_y k_z\gamma p \\ \mathrm{i}k_z\left(\gamma p\dfrac{d}{dx} - \rho g\right) & -k_y k_z\gamma p & \rho\omega^2 - k_z^2\gamma p \end{pmatrix} \begin{pmatrix} \hat{\xi}_x \\ \hat{\xi}_y \\ \hat{\xi}_z \end{pmatrix} = 0\,. \tag{7.32}$$

Since there is no preferred horizontal direction in the system, there is no loss in generality if we rotate the coordinate system such that $k_z = 0$, so that $\rho\omega^2\hat{\xi}_z = 0$. Hence, ignoring marginal shifts ($\omega^2 = 0$, $\hat{\xi}_z \neq 0$), all terms with k_z and $\hat{\xi}_z$ may be neglected and $\hat{\xi}_y$ may be eliminated:

$$\hat{\xi}_y = -\mathrm{i}k_0\frac{\gamma p\hat{\xi}_x' - \rho g\hat{\xi}_x}{\rho\omega^2 - k_0^2\gamma p}\,, \tag{7.33}$$

where $k_0 \equiv \sqrt{k_y^2 + k_z^2}$ ($= k_y$ now) is the horizontal wave number. Inserting this expression in the first component of Eq. (7.32) gives a *second order differential*

Downloaded from Cambridge Books Online by IP 152.2.176.242 on Mon Apr 29 20:09:10 WEST 2013.
http://dx.doi.org/10.1017/CBO9780511616945.008
Cambridge Books Online © Cambridge University Press, 2013

equation for the unknown $\hat{\xi}_x$:

$$\frac{d}{dx}\left(\frac{\gamma p\,\rho\omega^2}{\rho\omega^2 - k_0^2\gamma p}\,\frac{d\hat{\xi}_x}{dx}\right) + \left[\rho\omega^2 - \frac{k_0^2\rho^2 g^2}{\rho\omega^2 - k_0^2\gamma p} - \left(\frac{k_0^2\gamma p\,\rho g}{\rho\omega^2 - k_0^2\gamma p}\right)'\right]\hat{\xi}_x = 0\,. \tag{7.34}$$

To solve this differential equation one should specify the vertical profiles $p(x)$ and $\rho(x)$, which should satisfy the equilibrium condition (7.26), and the boundary conditions.

▹ **Alternative expression.** The last term of Eq. (7.34) may be written as

$$-\left(\frac{k_0^2\gamma p\,\rho g}{\rho\omega^2 - k_0^2\gamma p}\right)' = \rho' g - \left(\rho g\,\frac{\rho\omega^2}{\rho\omega^2 - k_0^2\gamma p}\right)'.$$

This more readily exhibits the correspondence with the expressions for spherical geometry (Eq. (7.58) of Section 7.2.4) and for magnetized plasmas (Eq. (7.91) of Section 7.3.2). ◃

Formulation of the appropriate boundary conditions obviously would involve the spherical geometry of the original problem. Since we have ignored that part of the problem, the next logical step is to consider modes that do not sensitively depend on the choice of the boundary. Such modes are obtained by the assumption that the boundaries are far away. In other words: we should study modes of finite extent in the y- and z-directions (either arbitrary wave numbers k_y and k_z, or quantized if one wishes to consider the y- and z-directions as periodic), but *sufficiently localized in the direction of inhomogeneity*. Hence, imposing rigid wall boundary conditions,

$$\hat{\xi}_x(x=0) = \hat{\xi}_x(x=a) = 0\,, \tag{7.35}$$

where $x = 0$ would correspond to the centre and $x = a$ to the surface of the Sun, only makes sense if a is large as compared to the typical 'wavelengths' in the x-direction. (Quotation marks here since we strictly cannot define a wave vector in a direction of inhomogeneity.) For example, we might consider modes which rapidly oscillate in the x-direction:

$$\hat{\xi}_x(x) \sim \mathrm{e}^{\mathrm{i}qx} \quad \text{with} \quad qa \gg 1\,. \tag{7.36}$$

Of course, there are no walls on the Sun, and the boundary conditions (7.35) just serve to define a region of localization of the modes. In more general terms, one would consider so-called *cavity modes*, where the background pressure and density distributions create a kind of potential well in which the modes are confined.

The differential equations (7.34) with the boundary conditions (7.35) permit the study of the instabilities ($\omega^2 < 0$) and stable waves ($\omega^2 > 0$) which originate from the peculiar interaction of the sound and gravity terms. For the solar context, these two cases are exemplified by the convective instabilities of the convection zone

Downloaded from Cambridge Books Online by IP 152.2.176.242 on Mon Apr 29 20:09:10 WEST 2013.
http://dx.doi.org/10.1017/CBO9780511616945.008
Cambridge Books Online © Cambridge University Press, 2013

and the solar acoustic-gravity waves (the p- and g-modes), respectively. We treat these two examples in Subsections 7.2.2 and 7.2.3.

7.2.2 Convective instabilities

Since time scales of gravitational instabilities are much longer than time scales of acoustic oscillations, we may assume $\rho\,|\omega^2| \ll k_0^2 \gamma p$ for the study of these instabilities. The wave equation (7.34) then simplifies to

$$\frac{d}{dx}\left(\frac{\rho\omega^2}{k_0^2}\frac{d\hat{\xi}_x}{dx}\right) - \rho\left(\omega^2 - N^2\right)\hat{\xi}_x = 0\,, \tag{7.37}$$

where N is *the Brunt–Väisäläa frequency*:

$$N^2 = N^2(x) \equiv -g\left(\frac{1}{\rho}\frac{d\rho}{dx} - \frac{1}{\gamma p}\frac{dp}{dx}\right) \qquad \left[\,= -\frac{1}{\rho}\left(\rho' g + \frac{\rho^2 g^2}{\gamma p}\right)\right]. \tag{7.38}$$

Since ρ and N^2 depend on x through $\rho(x)$ and $p(x)$, of which at least one function is completely arbitrary, in general, the solution of the differential equation (7.37) can only be obtained by numerical integration. However, assuming rapid spatially oscillatory modes of the kind expressed by Eq. (7.36) with $q \gg |\nabla| \sim 1/a$, where $|\nabla|$ represents a typical gradient scale length of the equilibrium, one obtains the following estimate for the eigenfrequencies of the local instabilities:

$$\omega^2 \approx \frac{k_0^2}{k_0^2 + q^2}\,N^2(x)\,. \tag{7.39}$$

Hence, the system is locally unstable in the range of x where $N^2 < 0$.

It will have been noticed that the bracket in the definition (7.38) for N^2 is just the expression entering the gravitational stability criterion derived in Section 6.5.4 by application of the energy principle. We now have additional information on this instability, viz. an estimate of the growth rates. (Note that this required application of the alternative to method (3) of Section 6.4.4, viz. the differential equation approach associated with the normal-mode analysis.)

We have already seen in Section 7.1.2 that the Schwarzschild criterion (7.21) for convective stability and the gravitational stability criterion coincide when the equilibrium conditions are taken into account. This is now immediately evident from the connection with the Brunt–Väisäläa frequency:

$$\frac{dT}{dx} - \left(\frac{dT}{dx}\right)_{\text{isentr.}} = \frac{T}{g}\,N^2 \geq 0 \qquad \left[\,\Rightarrow\; -\frac{T}{\rho g}\left(\rho' g + \frac{\rho^2 g^2}{\gamma p}\right) \geq 0\right]. \tag{7.40}$$

Hence, $N^2 \geq 0$ is nothing else than the Schwarzschild criterion.

Downloaded from Cambridge Books Online by IP 152.2.176.242 on Mon Apr 29 20:09:10 WEST 2013.
http://dx.doi.org/10.1017/CBO9780511616945.008
Cambridge Books Online © Cambridge University Press, 2013

If the Schwarzschild criterion is violated, i.e. $N^2 < 0$, Eq. (7.39) tells us that we should expect convective instabilities exponentially growing as $\exp(\sqrt{-\omega^2}\,t)$. Of course, such modes rapidly enter the nonlinear domain, where the assumptions underlying the given derivation break down. This is associated with the formation of convective cells, which may be nonlinearly stable. However, the onset of this phenomenon is correctly predicted by the linear theory. On the other hand, if $N^2 > 0$, Eq. (7.39) provides us with the expression for the frequency of slow gravitational modes (the g-modes). These will be treated in a slightly more general context, without the assumption of smallness of ω^2 made in this subsection.

7.2.3 Gravito-acoustic waves

An instructive special case of gravito-acoustic waves in an inhomogeneous medium is obtained for an *exponentially stratified medium with constant sound speed*:

$$\rho = \rho_0 \mathrm{e}^{-\alpha x}\,, \quad p = p_0 \mathrm{e}^{-\alpha x}\,, \qquad \text{so that} \quad c^2 = \frac{\gamma p}{\rho} = \frac{\gamma p_0}{\rho_0} = \text{const.} \tag{7.41}$$

From the equilibrium equation (7.26) this implies that $p' = -\alpha p = -\rho g$ (where we recall that g is also assumed constant), so that

$$\alpha = \frac{\rho g}{p} = \frac{\rho_0 g}{p_0} = \frac{\gamma g}{c^2} = \text{const.} \tag{7.42}$$

The spectral equation (7.34) then reduces to

$$\frac{c^2\omega^2}{\omega^2 - k_0^2 c^2}\,\frac{d}{dx}\left(\mathrm{e}^{-\alpha x}\,\frac{d\hat{\xi}_x}{dx}\right) + \left(\omega^2 - \frac{k_0^2 g^2}{\omega^2 - k_0^2 c^2} + \alpha\frac{k_0^2 c^2 g}{\omega^2 - k_0^2 c^2}\right)\mathrm{e}^{-\alpha x}\,\hat{\xi}_x = 0\,. \tag{7.43}$$

The expression (7.38) for the square of the Brunt–Väisäläa frequency here simplifies to

$$N^2 = \alpha g - \frac{g^2}{c^2} = (\gamma - 1)\frac{g^2}{c^2} > 0\,, \tag{7.44}$$

so that we will only find stable waves. By means of this expression, Eq. (7.43) transforms to

$$\frac{d^2\hat{\xi}_x}{dx^2} - \alpha\,\frac{d\hat{\xi}_x}{dx} + \frac{\omega^4 - k_0^2 c^2\,\omega^2 + k_0^2 c^2 N^2}{c^2\,\omega^2}\,\hat{\xi}_x = 0\,. \tag{7.45}$$

This is a differential equation with constant coefficients so that its solution becomes trivial.

Downloaded from Cambridge Books Online by IP 152.2.176.242 on Mon Apr 29 20:09:10 WEST 2013.
http://dx.doi.org/10.1017/CBO9780511616945.008
Cambridge Books Online © Cambridge University Press, 2013

This is another occasion of blind luck (cf. Section 6.6.4) which, we repeat, is *not at all typical* for the problem of wave propagation in inhomogeneous media. One should be aware of the limitations intrinsic to the use of special cases that are analytically solvable. Frequently, one comes across so-called 'intuition', based upon insight obtained from such cases, which may be very misleading. For example, here we have lost the important possibility of convective instability, discussed in the previous subsection, simply because $N^2 > 0$ due to the assumption of an exponential medium. In general, for arbitrary pressure and density profiles, the differential equation to be solved is just a general ODE, where numerical solution is the appropriate procedure.

The solutions of Eq. (7.45) are exponentials of the form $\hat{\xi}_x = C\mathrm{e}^{(\frac{1}{2}\alpha \pm \mathrm{i}q)x}$, where

$$q \equiv \sqrt{-\frac{1}{4}\alpha^2 + \frac{\omega^4 - k_0^2 c^2\,\omega^2 + k_0^2 c^2 N^2}{c^2\,\omega^2}}\,. \tag{7.46}$$

Clearly, the expression under the square root sign has to be positive in order to obtain spatially oscillatory solutions that can satisfy the boundary conditions (7.35). The latter conditions imply that q has to be quantized:

$$qa = n\pi \quad (n = 1, 2, \ldots). \tag{7.47}$$

The *dispersion equation of the gravito-acoustic waves* is then obtained by inverting the expression (7.46) for q :

$$\omega^4 - (k_0^2 + q^2 + \tfrac{1}{4}\alpha^2)c^2\omega^2 + k_0^2 c^2 N^2 = 0\,, \tag{7.48}$$

having the solutions

$$\omega_{p,g}^2 = \tfrac{1}{2}k_{\mathrm{eff}}^2 c^2 \left[\, 1 \pm \sqrt{1 - \frac{4k_0^2 N^2}{k_{\mathrm{eff}}^4 c^2}}\,\right], \qquad k_{\mathrm{eff}}^2 \equiv k_0^2 + q^2 + \tfrac{1}{4}\alpha^2\,, \tag{7.49}$$

where k_{eff} is the effective total 'wave number' (quotation marks since the vertical dependence of the perturbations does not correspond to a plane wave) and k_0 is the horizontal wave number. The branch with the $+$ sign refers to *the acoustic waves* or *p-modes* (pressure driven), and the branch with the $-$ sign refers to the *gravity waves* or *g-modes* (gravity driven).

In Fig. 7.3 we have drawn the curves for $\omega^2 = \omega^2(k_0^2)$ for different values of the vertical 'wave number' q. The curves for $q^2 = 0$ (dotted), which represent the so-called *turning point* frequencies ω_{p0}^2 and ω_{g0}^2, mark the boundaries between propagation (q real) and evanescence (q imaginary) of the waves. For increasing values of q^2, the eigenfrequencies ω^2 of the p-modes monotonically increase with an *accumulation* or *cluster point* at ∞ : $\omega_p^2 \to \omega_P^2 = \infty$. This monotonicity of the eigenfrequency with the number of nodes of the eigenfunctions, so-called

Downloaded from Cambridge Books Online by IP 152.2.176.242 on Mon Apr 29 20:09:10 WEST 2013.
http://dx.doi.org/10.1017/CBO9780511616945.008
Cambridge Books Online © Cambridge University Press, 2013

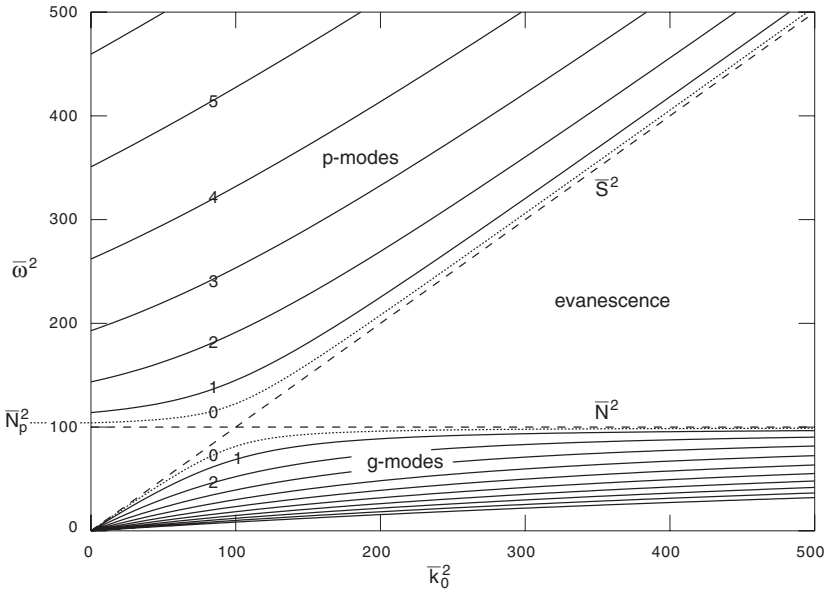

Fig. 7.3. Dispersion diagram for the p- and g-modes of a plane, exponential, atmosphere. The squared frequencies in normalized units, $\bar{\omega}^2 = \bar{\omega}^2(\bar{k}_0^2, \bar{q}^2)$, are plotted for ten values of the vertical 'wave number' $\bar{q} = n\pi$ $(n = 1, 2, \ldots, 10)$. The normalized Brunt–Väisäläa frequency $\bar{N} = 10$, the normalized acoustic cutoff frequency $\bar{N}_p = \frac{1}{2}\bar{\alpha} = 10.21$. Dotted curves represent the turning point frequencies $(n = 0)$, dashed curves are the asymptotic values for $\bar{k}_0 \to \infty$.

Sturmian behaviour, is a well-known property of sound waves and musical instruments. On the other hand, the eigenfrequencies of the g-modes monotonically decrease (*anti-Sturmian* behaviour) with an accumulation point at 0: $\omega_g^2 \to \omega_G^2 = 0$. The lowest branch $(q^2 = 0)$ of the p-modes crosses the ω^2 axis at the value N_p^2, given by

$$N_p^2 \equiv \omega_{p,\mathrm{cut}}^2 \equiv \omega_{p0}^2(k_0^2{=}0) = \tfrac{1}{4}\alpha^2 c^2 = \frac{\gamma^2 g}{4c^2} \quad \left(\geq N^2\right), \tag{7.50}$$

which is called *the acoustic cutoff frequency*. For $k_0^2 \to \infty$, the acoustic branches asymptotically tend to the ordinary sound wave frequency, which is called the Lamb frequency in this context, $\omega_p^2 \approx S^2 \equiv k_0^2 c^2$, whereas the g-modes asymptotically tend to the Brunt–Väisäläa frequency, $\omega_g^2 \approx N^2$ (dashed curves).

The split in Sturmian $(\partial\omega^2/\partial q^2 > 0)$ and anti-Sturmian $(\partial\omega^2/\partial q^2 < 0)$ discrete modes is a quite general one for wave propagation in inhomogeneous media. We will prove in Section 7.5.1, for the more general MHD case, that this difference is

Downloaded from Cambridge Books Online by IP 152.2.176.242 on Mon Apr 29 20:09:11 WEST 2013.
http://dx.doi.org/10.1017/CBO9780511616945.008
Cambridge Books Online © Cambridge University Press, 2013

associated with the sign of the coefficient in front of the highest derivative of the differential equation, i.e.

$$\frac{\rho c^2 \omega^2}{\omega^2 - k_0^2 c^2}\,, \tag{7.51}$$

for the gravito-acoustic waves described by Eq. (7.34). Hence, the marginal frequency ($\omega^2 = 0$) of the numerator and the Lamb frequency ($\omega^2 = k_0^2 c^2$) of the denominator delimit the frequency ranges where the modes are Sturmian or anti-Sturmian.

For the interpretation of the dispersion curves of Fig. 7.3, note that all frequencies and wave numbers have been made dimensionless by means of the sound speed c and the height a of the layer: $\bar{\omega} \equiv (a/c)\,\omega$, $\bar{k}_0 \equiv k_0 a$, $\bar{q} \equiv qa$, etc. To get estimates for the p-mode frequencies of the Sun, let us choose $a \equiv R_\odot = 7 \times 10^8$ m and a value for the sound speed c somewhere in the interior of the Sun (using data from Unno *et al.* [234]):

$$r = 0.5 R_\odot\,, \quad c = 3 \times 10^5\,\mathrm{m\,s^{-1}} \quad \Rightarrow \quad f_p \equiv \frac{c}{2\pi a} = 6.8 \times 10^{-5}\,\mathrm{Hz}\,. \tag{7.52}$$

With the factor f_p we may convert the normalized angular frequencies $\bar{\omega}$ into the actual frequencies ν of the modes, e.g.

$$\begin{aligned} l = \;\; 0\,, \quad n = \;\; 0 \quad &\Rightarrow \quad \nu_{p,\mathrm{cut}} \equiv \bar{N}_p \cdot f_p = 0.68\,\mathrm{mHz}\,, \\ l = \;\; 0\,, \quad n = 20 \quad &\Rightarrow \quad \nu_p \approx n\pi \cdot f_p = 4.3\,\mathrm{mHz}\,, \\ l = 100\,, \quad n = \;\; 1 \quad &\Rightarrow \quad \nu_p \approx \;\; l \cdot f_p = 6.8\,\mathrm{mHz}\,, \end{aligned}$$

where $l \approx \bar{k}_0$ is the number of nodal lines on the spherical surface and $n = \bar{q}/\pi$ is the radial quantum number. These frequencies lie in the range of the observed *5 minute oscillations* ($\nu_p = 3.3$ mHz). To go beyond these order of magnitude estimates, one has to consider the spherical geometry and the actual inhomogeneities of the Sun.

▷ **Free-boundary modes.** The addition of a separate low-density layer on top of the exponential one we considered so far would permit the investigation of surface modes, analogous to the analysis of the Rayleigh–Taylor instability of Section 6.6.4. In the solar context, these oscillations are called *f-modes*, which are free-boundary oscillations of the solar surface involving both the interior and the atmosphere of the Sun. Their frequency is intermediate between the lowest n branches of the p- and g-modes so that the f-mode could be considered as the common $n = 0$ branch of these modes. However, an estimate of the short-wavelength limit of the frequency of incompressible surface waves (which remains valid for compressible fluids) shows that the mechanism is really gravitational:

$$\omega_f^2 \approx k_0 g\,. \tag{7.53}$$

Notice that, in contrast to the problem of Section 6.6.4, gravity is now pointing into the heavier fluid so that the waves are stable. Inserting the value of the gravitational acceleration at the solar surface, we obtain the following approximation of the frequency of the

Downloaded from Cambridge Books Online by IP 152.2.176.242 on Mon Apr 29 20:09:11 WEST 2013.
http://dx.doi.org/10.1017/CBO9780511616945.008
Cambridge Books Online © Cambridge University Press, 2013

f-modes:

$$\nu_f \equiv \frac{\omega_f}{2\pi} \approx \sqrt{l}\cdot f_f\,, \qquad f_f \equiv \frac{1}{2\pi}\sqrt{\frac{GM_\odot}{R_\odot^3}} \approx 0.1\,\mathrm{mHz}\,. \tag{7.54}$$

Since helioseismology actually depends on surface oscillations for detection, the extension with free-boundary modes is an important step towards reality of the model. For further discussion of surface modes, and generalization to MHD, see the review by Roberts [193]. ◁

7.2.4 Helioseismology and MHD spectroscopy

For educational purposes, we have treated the p- and g-modes in a highly idealized medium, characterized by constant values of the sound speed and the gravitational acceleration. Of course, in the Sun these conditions are not valid. Moreover, one should treat the problem in *spherical geometry*. This gives rise to a quantization condition for the horizontal wave number: $k_0 R_\odot = \sqrt{l(l+1)}$, where l is the degree of the mode, whereas the vertical wave number q and associated quantization condition (7.47) also require a modification to account for the inhomogeneities of the interior of the Sun.

▷ **Spherical geometry.** For spherical symmetry, the normal mode expansion (7.31) is to be replaced by

$$\begin{aligned}
\xi_r(r,\theta,\phi,t) &= \hat{\xi}(r)\,Y_l^m(\theta,\phi)\,\mathrm{e}^{-\mathrm{i}\omega t}\,,\\
\xi_\theta(r,\theta,\phi,t) &= \left[\,\hat{\eta}(r)\,\frac{\partial Y_l^m}{\partial\theta} + \hat{\zeta}(r)\,\frac{1}{\sin\theta}\frac{\partial Y_l^m}{\partial\phi}\,\right]\mathrm{e}^{-\mathrm{i}\omega t}\,,\\
\xi_\phi(r,\theta,\phi,t) &= \left[\,\hat{\eta}(r)\,\frac{1}{\sin\theta}\frac{\partial Y_l^m}{\partial\phi} - \hat{\zeta}(r)\,\frac{\partial Y_l^m}{\partial\theta}\,\right]\mathrm{e}^{-\mathrm{i}\omega t}\,,
\end{aligned} \tag{7.55}$$

where $Y_l^m(\theta,\phi)$ are spherical harmonics, well known from quantum mechanics of spherically symmetric systems. Like in quantum mechanics, the actual eigenfrequencies are determined from the radial wave equation which brings in the radial mode number n (number of nodes of the radial wave function). The degree l (total number of nodal circles on the spherical surface) takes the place of the horizontal wave number k_0, and the system is degenerate with respect to the longitudinal order m (number of nodal circles through the poles, $|m| \le l$). This degeneracy is lifted when differential rotation is taken into account.

In the Cowling approximation, where perturbations of the gravitational potential are neglected, the original vector eigenvalue problem in terms of $\boldsymbol{\xi}$ may be reduced to the solution of just one ODE for $\hat{\xi}$, the radial wave equation. Similar to the plane case of Section 7.2.1, one of the three variables $\hat{\xi},\ \hat{\eta},\ \hat{\zeta}$ vanishes:

$$\omega^2\hat{\zeta} = 0 \quad\Rightarrow\quad \hat{\zeta} = 0 \quad (\text{if } \omega^2 \neq 0)\,, \tag{7.56}$$

i.e. when marginal toroidal shifts are ignored ($\omega^2 = 0\,,\ \hat{\zeta} \neq 0$). Then, the component $\hat{\eta}$ may be eliminated,

$$\hat{\eta} = -\frac{(c^2/r^2)(r^2\hat{\xi})' - g\hat{\xi}}{r^2(\omega^2 - S^2)}\,, \tag{7.57}$$

Downloaded from Cambridge Books Online by IP 152.2.176.242 on Mon Apr 29 20:09:11 WEST 2013.
http://dx.doi.org/10.1017/CBO9780511616945.008
Cambridge Books Online © Cambridge University Press, 2013

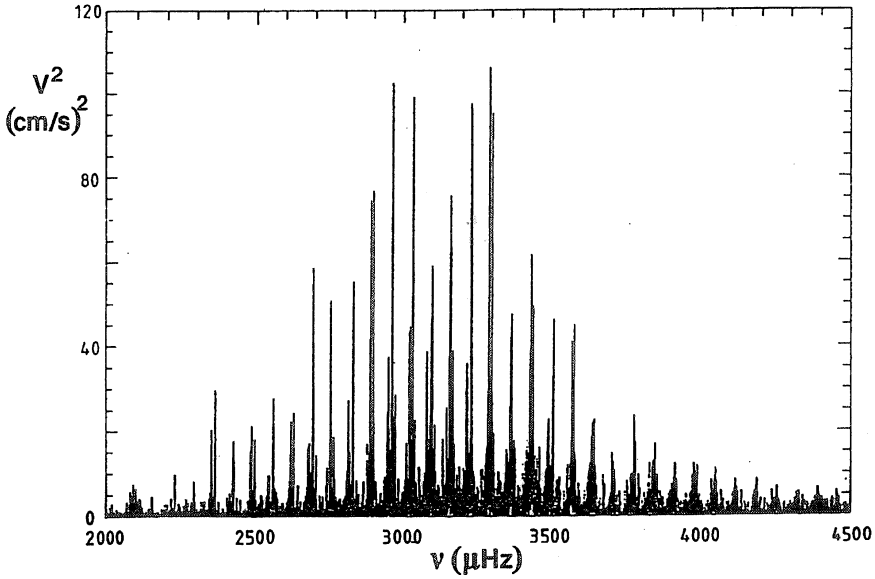

Fig. 7.4. Power spectrum of solar oscillations, obtained from Doppler velocity measurements in light integrated over the solar disc. (From Christensen-Dalsgaard [56], citing A. Claverie, G. R. Isaak, C. P. McLeod, H. B. van der Raay, P. L. Palle and T. Roca Cortes, *Mem. Soc. Astron. Ital.* **55**, 63 (1984).)

which, upon substitution, yields the radial wave equation

$$\frac{d}{dr}\left(\frac{\omega^2}{\omega^2 - S^2}\frac{\gamma p}{r^2}\frac{d}{dr}(r^2\hat{\xi})\right) + \left[\rho\omega^2 - \frac{\rho g^2}{r^2}\frac{l(l+1)}{\omega^2 - S^2} + \rho' g - r^2\left(\frac{\rho g}{r^2}\frac{\omega^2}{\omega^2 - S^2}\right)'\right]\hat{\xi} = 0, \tag{7.58}$$

where $S^2 \equiv l(l+1)c^2/r^2$ is the Lamb frequency. Note the similarity with the analogous equation for the H-atom in quantum mechanics, but also notice that there is considerably more structure to this problem (due to the presence of three background fields $\rho(r)$, $p(r)$, $g(r)$, and the reduction of a vector eigenvalue problem to a scalar wave equation, with a much more complicated dependence on the eigenvalue parameter). ◁

When the theory is modified in this manner and applied to the observations of the p-mode spectra, it provides a powerful tool for probing the interior of the Sun, called *helioseismology*; see Christensen-Dalsgaard [56] or Harvey [105]. Broadly speaking, this is done by 'inversion' of the observed spectra to obtain the equilibrium profiles that produced them. Fig. 7.4 shows a typical example of a *classical* spectrum of solar oscillations observed by means of a measurement of the Doppler shifts of the *quantum mechanical* spectral lines of the sunlight. At this point, it is important to realize that the Doppler shifts themselves are the object of study here since they are directly related to the radial oscillations of the photosphere. With observed radial velocities $\tilde{v}_r \sim 1\,\mathrm{km}/s$, it is quite all right to exploit linear

Downloaded from Cambridge Books Online by IP 152.2.176.242 on Mon Apr 29 20:09:11 WEST 2013.
http://dx.doi.org/10.1017/CBO9780511616945.008
Cambridge Books Online © Cambridge University Press, 2013

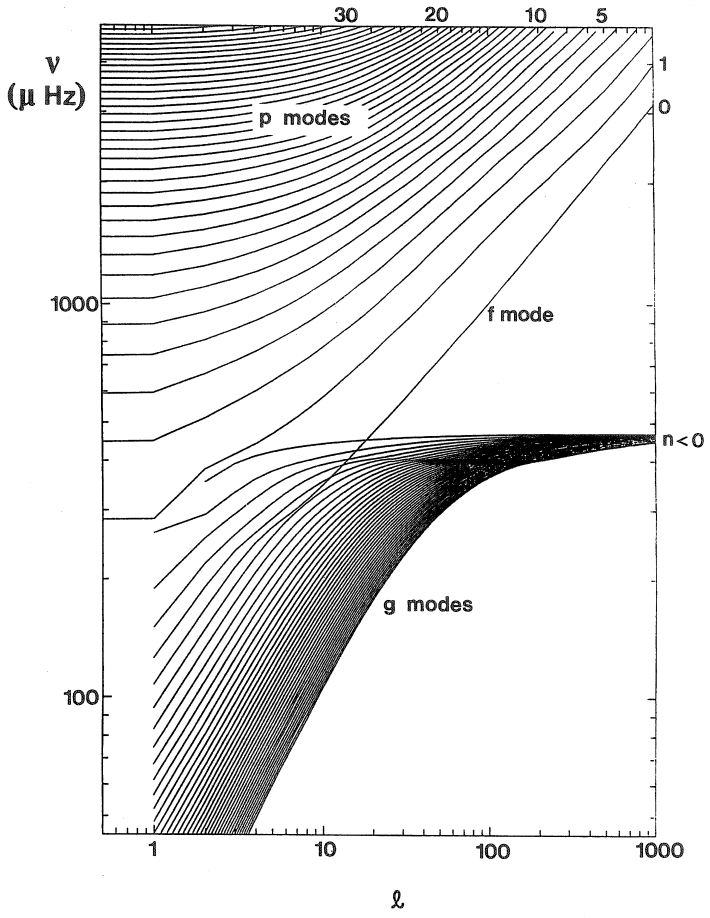

Fig. 7.5. Solar oscillations for a standard solar model: computed frequency as a function of the degree ℓ for different values of the radial mode number n. (From Christensen-Dalsgaard [56].)

theory since the amplitudes reached in typical 5 min periods are not larger than $5 \times 10^{-4} R_\odot \ll R_\odot$.

Above, 'inversion' of the solar oscillation spectrum is put in quotation marks to indicate that it is not a mechanical procedure that can be applied blindly. Whereas computing a spectrum for a particular equilibrium can be carried out numerically (see, e.g., Fig. 7.5), virtually to any degree of accuracy desired, the inverse problem requires a much larger effort. (It is not so difficult to take fingerprints at the site of the crime, but it is usually quite difficult to catch the criminal that produced them.) It consists of computing the spectrum while iterating on infinitely many possible values of the equilibrium input parameters until matching is obtained.

Downloaded from Cambridge Books Online by IP 152.2.176.242 on Mon Apr 29 20:09:11 WEST 2013.
http://dx.doi.org/10.1017/CBO9780511616945.008
Cambridge Books Online © Cambridge University Press, 2013

This procedure is ill-posed, a mathematical way of expressing that it is really a kind of art.

Also notice that a spectrum of solar oscillations, like that shown in Fig. 7.4, does not exhibit the modes on an equal footing. First, out of the infinity of modes that are possible, only a finite number are observed that have been excited by some mechanism, which, in itself, is part of the puzzle. Second, the spectral peaks observed do not correspond to the energy contents of the modes but to the amplitudes of the eigenfunctions at the position where the Doppler shifts are produced, that is in the photosphere. Hence, there is strong biasing towards modes that have a sizeable amplitude there.

One finds that p-modes of low order l penetrate the deep interior of the Sun, whereas high l modes in general are more localized towards the outside. This high l localization is most outspoken for the f-modes, which are free-boundary gravitational oscillations of the solar surface. (Note that the frequency estimate given in Eq. (7.54) checks quite well with the numbers of Fig. 7.5.) In general, g-modes are *cavity modes* trapped in the region interior to the convection zone and, hence, quite difficult to observe. The spectrum of p-modes, however, has been determined with surprising accuracy. It has been compared with computed values based on theoretical solar models. It turns out that the frequencies deduced from the Doppler shifts of spectral lines agree with the calculated ones for the p-modes to within 0.1%! This impressive agreement serves as an example for what is possible in a purely classical (as opposed to quantum mechanical) kind of spectroscopy.

▹ **Caveat on the analogy with quantum mechanical spectral theory.** In Section 6.5.4, we have stressed that the analogy of MHD (and, hence, HD) spectral theory with quantum mechanics is through the mathematics of linear operators, not through the physics of the systems. Consequently, one should be careful not to make tacit assumptions on the physical interpretation of the spectra. For example, the (accidental) degeneracy of the energy levels $E(n, l)$ of the hydrogen atom (due to the Coulomb potential), with the restriction $l \leq n$, and the association of l with the angular momentum operator are strictly limited to the quantum mechanical interpretation of the radial wave equation for $\psi(r)$. From Fig. 7.5 it is evident that the eigenfrequencies $\nu(n, l)$ of the solar oscillations do not exhibit this degeneracy and restriction on l. They are obtained from the radial wave equation (7.58) for the fluid displacement $\xi(r)$, which not only has a completely different radial structure but also a completely different physical interpretation. In particular, whereas l is associated with the number of nodal lines on the sphere in both cases, the quantum mechanical association with the angular momentum operator certainly does not carry over to fluid dynamics. ◃

On the basis of this successful example of fluid dynamical spectroscopy, we have proposed a similar activity for laboratory fusion plasmas, called *MHD spectroscopy* [88]. In order to understand the common feature, the procedure of helioseismology has been summarized in Fig. 7.6 to provide a kind of model example for other physical systems, like laboratory fusion machines. Notice that for the birth of helioseismology it was not sufficient to have collected a great number of

Downloaded from Cambridge Books Online by IP 152.2.176.242 on Mon Apr 29 20:09:11 WEST 2013.
http://dx.doi.org/10.1017/CBO9780511616945.008
Cambridge Books Online © Cambridge University Press, 2013

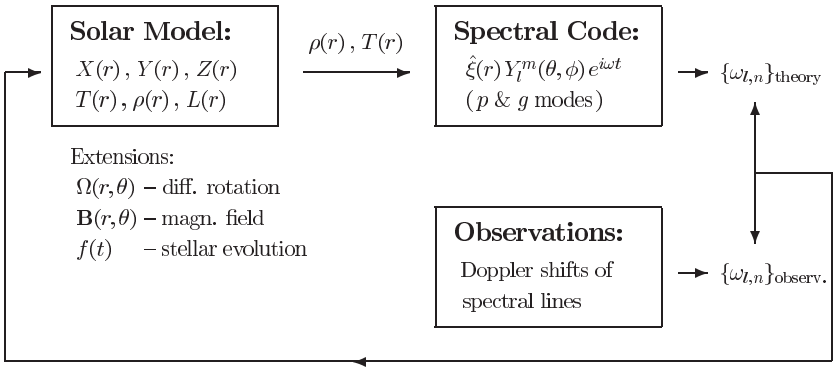

Fig. 7.6. Systematics of helioseismology.

observations of solar oscillations or to have calculated many spectra, but rather that the two activities should have matured to a sufficient degree to allow for a unique correlation between calculated and observed spectra. This interplay between theory and observations is illustrated in the figure. To leading order, the Solar Model is spherically symmetric with the equilibrium depending on the abundance of the different chemical elements H, He, and the heavier ones (indicated by the symbols X, Y, and Z), the temperature T, the density ρ, the luminosity L, etc. Perturbations of this equilibrium are studied by means of a Spectral Code which determines the collection $\{\omega_{l,n}\}$ of the frequencies of the different modes. Observations provide values of the same quantities. The discrepancies between the two then bring about improvement of the Solar Model, where the non-spherical symmetry due to the presence of differential rotation (Ω) and magnetic fields ($\mathbf{B}$) plays an important role. Of course, the final interest is in stellar evolution, i.e. the very slow time-dependence of all the equilibrium quantities that are determined on a snapshot basis by helioseismology.

It is not difficult to recognize the counterparts of the three activities depicted in Fig. 7.6 for laboratory fusion research: transport models to describe the slow evolution of the background equilibrium, spectral calculations of the fast MHD modes, and diagnostics to determine the frequencies and other characteristics of these modes. Clearly, the success of the similar activity of MHD spectroscopy hinges on improved diagnostics and spectral calculations. Helioseismology provides the paradigm demonstrating that fluid dynamical states can be predicted with high accuracy. We will see in a later chapter that this should be realizable for tokamaks as well. Another example of this kind of HD or MHD spectroscopy has been developed in the solar context with the aim of determining the hydrodynamical and magnetohydrodynamical properties of sunspots from the absorption of sound waves propagating in the photosphere. This activity has been called *sunspot*

Downloaded from Cambridge Books Online by IP 152.2.176.242 on Mon Apr 29 20:09:12 WEST 2013.
http://dx.doi.org/10.1017/CBO9780511616945.008
Cambridge Books Online © Cambridge University Press, 2013

seismology by Bogdan [34, 33]. Many other plasma-astrophysical objects may be investigated this way, e.g. there is a recent proposal to initiate *magneto-seismology of accretion discs* by Keppens *et al.* [124].

At this point in our exposition, it might appear that extension of the 1D spherical HD model to MHD with magnetic effects is the next logical step. However, recall that spherically symmetric magnetic fields are incompatible with $\nabla \cdot \mathbf{B} = 0$ (Section 1.3.4). Hence, incorporation of magnetic fields in spherical geometry inevitably involves 2D magnetic configurations (as indicated by the extensions listed outside the 1D Solar Model box in Fig. 7.6). In the following sections we will stay with 1D geometry and introduce magnetic fields in the plane slab model. This will give rise to plenty of new phenomena associated with plasma inhomogeneity. The further complications of two-dimensionality will be the subject of later chapters in Volume 2.

7.3 MHD wave equation for a gravitating magnetized plasma slab

7.3.1 Preliminaries

With the instructive examples of hydrodynamic waves and instabilities in ordinary fluids of Section 7.2, we now turn to the influence of inhomogeneity on the spectrum of waves and instabilities in *magnetized* plasmas. Macroscopic plasma dynamics inevitably involves effects of the *finite* geometry of the magnetic confinement volume. This substantially complicates the analysis since the assumption (made in Chapter 5 for homogeneous plasmas) of plane waves represented by uncoupled Fourier harmonics breaks down. Waves with different wave numbers $\mathbf{k}$ couple through plasma inhomogeneity so that *wave transformation* takes place. It is perfectly well possible to have a wave that should be characterized as a fast magneto-sonic wave in one part of the plasma volume, but which exhibits Alfvén wave properties in another part.

More important yet, from a fundamental as well as from a practical point of view, is the occurrence of two new phenomena, viz. *instabilities* and *continuous spectra*. Both are essentially due to plasma inhomogeneity, but instabilities (as the hydrodynamic convective instability encountered in Section 7.2.2) obviously occur for $\omega^2 < 0$, whereas continua are mainly located on the stable side ($\omega^2 > 0$) of the spectrum in ideal MHD. These phenomena are extremely important for a wide class of laboratory and astrophysical plasmas. This will be extensively demonstrated in the later chapters, but first we have to get acquainted with the necessary analytical tools.

We will approach the problem stepwise and, at first, restrict the analysis to inhomogeneity in one direction only (called *one-dimensional* or 1D systems) leading

Downloaded from Cambridge Books Online by IP 152.2.176.242 on Mon Apr 29 20:09:13 WEST 2013.
http://dx.doi.org/10.1017/CBO9780511616945.008
Cambridge Books Online © Cambridge University Press, 2013

to a description in terms of ordinary differential equations (ODEs). A generic example of such systems is the plane gravitating plasma slab with inhomogeneities $\rho(x)$, $p(x)$ and $\mathbf{B}(x)$ of the density, pressure and magnetic field, caused by plasma currents and gravitational stratification. We have already encountered the hydrodynamic version of the basic ODE in the wave equation (7.34) of Section 7.2.1. The fundamental wave equation for the gravitating magnetized plasma slab is derived in Section 7.3.2. This equation describes a bewildering variety of waves, continua and instabilities, as will be shown in Sections 7.4 and 7.5.

(a) Transformation of the homogeneous problem As a preliminary to the study of inhomogeneous plasmas, it is expedient to restate the *homogeneous* wave problem of Section 5.2 in a slightly different manner. Recall that the equilibrium background in that case was specified by

$$\mathbf{B} = B\mathbf{e}_z\,, \quad \text{with } \rho\,,\, p\,,\, B = \text{const}\,, \tag{7.59}$$

so that the sound and Alfvén speeds, $c \equiv \sqrt{\gamma p/\rho}$ and $\mathbf{b} \equiv \mathbf{B}/\sqrt{\rho}$, are constant. We have already transformed the eigenvalue problem (5.51) in terms of the force operator and associated displacement vector in the spectral equation (6.31) of Section 6.2.1. Since, for the time being, all equilibrium quantities are considered constant, we may write the normal mode amplitude $\boldsymbol{\xi}(\mathbf{r})$ as a Fourier integral (or a Fourier series if one considers a finite box) of plane wave solutions which do not couple:

$$\boldsymbol{\xi}(\mathbf{r}) = (2\pi)^{-3/2} \iiint \hat{\boldsymbol{\xi}}(\mathbf{k})\, \mathrm{e}^{\mathrm{i}\mathbf{k}\cdot\mathbf{r}}\, d^3k\,. \tag{7.60}$$

The normal modes $\hat{\boldsymbol{\xi}}(\mathbf{k};\omega)\exp \mathrm{i}(\mathbf{k}\cdot\mathbf{r} - \omega t)$ may then be studied separately by substituting $\nabla \to \mathrm{i}\mathbf{k}$ in Eq. (6.31). This leads to the algebraic eigenvalue problem (6.32), which we repeat for convenience:

$$\rho^{-1}\mathbf{F}(\hat{\boldsymbol{\xi}}) = \Big[-(\mathbf{k}\cdot\mathbf{b})^2\,\mathbf{I} - (b^2 + c^2)\,\mathbf{kk} + \mathbf{k}\cdot\mathbf{b}\,(\mathbf{kb} + \mathbf{bk}) \Big] \cdot \hat{\boldsymbol{\xi}} = -\omega^2 \hat{\boldsymbol{\xi}}\,. \tag{7.61}$$

The matrix representation of this equation is identical to Eq. (5.52) with $\hat{v}_{x,y,z}$ replaced by $\hat{\xi}_{x,y,z}$. However, we will now generalize the wave vector $\mathbf{k}$ to have a non-vanishing component k_y in order to be able to distinguish between the two perpendicular directions x and y (Fig. 7.7). This will facilitate the transition to the analysis of the inhomogeneous problem, where x and y will no longer be equivalent since the eventual inhomogeneity will be in the x-direction.

The mentioned transformation amounts to a rotation of the coordinate system through an angle $-\chi \equiv -\arctan(k_y/k_x)$ about the z-axis. (The minus sign appears here because $\mathbf{k}_\perp$ is along the old x'-axis.) We indicate the old representation

Downloaded from Cambridge Books Online by IP 152.2.176.242 on Mon Apr 29 20:09:13 WEST 2013.
http://dx.doi.org/10.1017/CBO9780511616945.008
Cambridge Books Online © Cambridge University Press, 2013

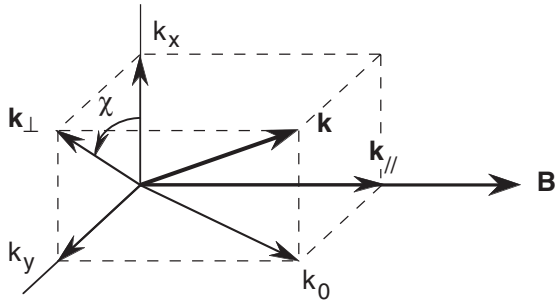

Fig. 7.7. New orientation of the **k** vector.

by primes, $\rho^{-1}\mathbf{F}'\cdot\boldsymbol{\xi}' = -\omega^2\boldsymbol{\xi}'$, where the sans serif bold symbol $\mathbf{F}'$ is used to denote the (old) matrix representation of the operator $\mathbf{F}$. The new representation then becomes

$$\rho^{-1}\mathbf{F}\cdot\boldsymbol{\xi} = -\omega^2\boldsymbol{\xi}\,, \qquad \text{with} \quad \mathbf{F} = \mathbf{R}\cdot\mathbf{F}'\cdot\mathbf{R}^{-1} \ \text{ and } \ \boldsymbol{\xi} = \mathbf{R}\cdot\boldsymbol{\xi}'\,, \tag{7.62}$$

where

$$\mathbf{R} \equiv \begin{pmatrix} \cos\chi & -\sin\chi & 0 \\ \sin\chi & \cos\chi & 0 \\ 0 & 0 & 1 \end{pmatrix}. \tag{7.63}$$

This results in the following matrix representation of the spectral equation (7.61):

$$\begin{pmatrix} -k_x^2(b^2+c^2)-k_z^2b^2 & -k_xk_y(b^2+c^2) & -k_xk_zc^2 \\ -k_xk_y(b^2+c^2) & -k_y^2(b^2+c^2)-k_z^2b^2 & -k_yk_zc^2 \\ -k_xk_zc^2 & -k_yk_zc^2 & -k_z^2c^2 \end{pmatrix}\begin{pmatrix} \xi_x \\ \xi_y \\ \xi_z \end{pmatrix} = -\omega^2\begin{pmatrix} \xi_x \\ \xi_y \\ \xi_z \end{pmatrix}, \tag{7.64}$$

where we have dropped the hats on $\boldsymbol{\xi}$ for notational simplicity. Note that Eq. (5.52) is recovered, as it should, when the limit $k_y \to 0$ is taken. Solutions are obtained by setting the determinant of the system to zero. Of course, this results in the same dispersion equations (5.56) for the Alfvén eigenvalues ω_A^2 and (5.58) for the magneto-sonic eigenvalues $\omega_{s,f}^2$:

$$\omega_A^2 = k_\parallel^2 b^2\,, \qquad \omega_{s,f}^2 = \tfrac{1}{2}k^2(b^2+c^2)\left[1 \pm \sqrt{1 - \frac{4k_\parallel^2 b^2 c^2}{k^2(b^2+c^2)^2}}\right], \tag{7.65}$$

where now

$$k^2 = k_x^2 + k_y^2 + k_z^2\,, \qquad k_\perp = \sqrt{k_x^2+k_y^2}\,, \qquad k_\parallel = k_z\,.$$

Downloaded from Cambridge Books Online by IP 152.2.176.242 on Mon Apr 29 20:09:13 WEST 2013.
http://dx.doi.org/10.1017/CBO9780511616945.008
Cambridge Books Online © Cambridge University Press, 2013

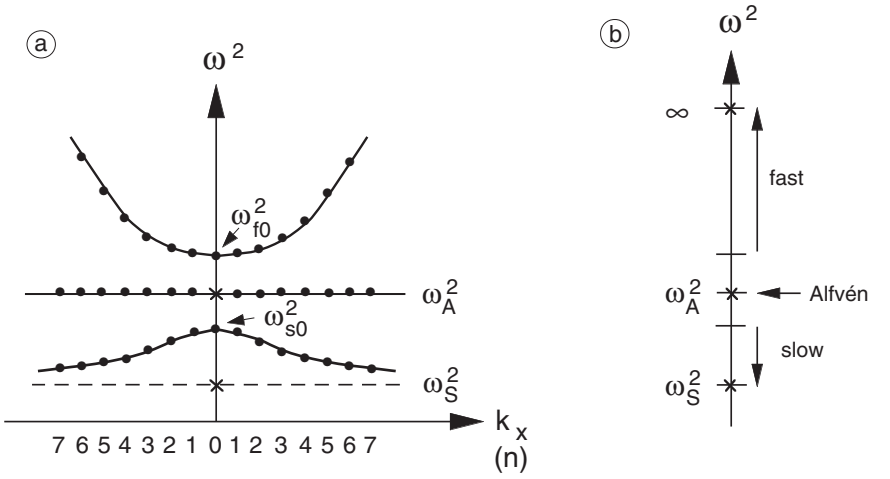

Fig. 7.8. (a) Dispersion diagram $\omega^2 = \omega^2(k_x)$ for k_y and k_z fixed; (b) corresponding structure of the spectrum.

However, the expressions (5.57) and (5.60) for the eigenvectors have to be modified to account for the changed direction of the plane spanned by **k** and **B** (previously, the x'–z' plane) since the Alfvén eigenvectors $\boldsymbol{\xi}_A$ are perpendicular to this plane and the magneto-sonic eigenvectors $\boldsymbol{\xi}_{s,f}$ are lying in it.

(b) Essential spectrum The spectrum of MHD waves is modified significantly by plasma inhomogeneity. If the inhomogeneity is in the x-direction, the assumption of uncoupled plane waves breaks down with respect to the wave number k_x so that we have to replace k_x by $-\mathrm{i}\partial/\partial x$ in Eq. (7.64). Hence, the dispersion equation $\omega^2 = \omega^2(k_x, k_y, k_z)$ loses its meaning with respect to the dependence on k_x . The consequences of this will be worked out in the next section. However, one essential feature of the spectrum remains intact, that was already alluded to in the discussion of the asymptotic properties associated with the group velocity (Section 5.3.3). This relates to *localized wave motion in the direction of inhomogeneity*, which can be understood already from the homogeneous theory by considering the limit $k_x \to \infty$. To that end, we plot ω^2 as a function of k_x, keeping k_y and k_z fixed (Fig. 7.8(a)). Note that this picture is very similar to Fig. 5.7(b), but the degeneracy of Alfvén and fast modes at $k_\perp = 0$ is removed.

The effects of a confined inhomogeneous plasma can now be mimicked, within the context of homogeneous theory, by considering the plasma as a slab of finite extension enclosed by plates at $x = 0$ and $x = a$. The wave number k_x will then be quantized: $k_x = n\pi/a$, where n is the *number of nodes* of the eigenfunction ξ_x considered as a function of x. Hence, the eigenvalues will be labelled by n, rather than by k_x, and this labelling still makes sense for an inhomogeneous medium with

Downloaded from Cambridge Books Online by IP 152.2.176.242 on Mon Apr 29 20:09:13 WEST 2013.
http://dx.doi.org/10.1017/CBO9780511616945.008
Cambridge Books Online © Cambridge University Press, 2013

equilibrium quantities that vary in the x-direction. This quantization produces a discrete spectrum, with three branches that behave distinctly differently (Fig. 7.8(b)). The essential features of these three sub-spectra of point eigenvalues, labelled by n, are the following ones.

(1) The discrete eigenvalues of the fast sub-spectrum monotonically increase, so that

$$\omega_F^2 \equiv \lim_{k_x\to\infty} \omega_f^2 \approx \lim_{k_x\to\infty} k_x^2(b^2+c^2) = \infty \tag{7.66}$$

is a formal *cluster point* of the fast wave point spectrum.

(2) The eigenvalues ω_a^2 of the Alfvén sub-spectrum are *infinitely degenerate*, because they do not depend on k_x, so that

$$\omega_A^2 \equiv \lim_{k_x\to\infty} \omega_a^2 = \omega_a^2 = k_\parallel^2 b^2 \,. \tag{7.67}$$

Hence there is no need to distinguish between the point eigenvalues ω_a^2 and the limit ω_A^2. (That is why we did not even introduce the symbol ω_a^2 before.)

(3) The discrete eigenvalues of the slow wave sub-spectrum monotonically decrease with an *accumulation* or *cluster point* at

$$\omega_S^2 \equiv \lim_{k_x\to\infty} \omega_s^2 = k_\parallel^2 \frac{b^2c^2}{b^2+c^2} \,, \tag{7.68}$$

where the subscript s denotes the slow discrete modes and S their cluster point.

Mathematically speaking, ω_F^2, ω_A^2, and ω_S^2 belong to what is called the *essential spectrum*, which is the manifestation of the continuous spectrum in this context. This turns out to be basic for the discussion of the inhomogeneous case, where the functions vary with x. Then, the infinite degeneracy of the Alfvén eigenvalues is lifted by the appearance of a *continuous spectrum of improper Alfvén modes* instead, and the cluster point of the slow point spectrum is spread out in a *continuous spectrum of improper slow modes*, whereas the fast cluster point $\omega_F^2 = \infty$ is unaffected.

The two values of ω^2 denoted by ω_{s0}^2 and ω_{f0}^2, where the slow and the fast modes cross the vertical axis in Fig. 7.8(a), also turn out to play a special role in the spectral theory of inhomogeneous plasmas. Their values are given by:

$$\omega_{s0,\,f0}^2 \equiv \omega_{s,\,f}^2(k_x=0) = \tfrac{1}{2}k_0^2(b^2+c^2)\left[\,1 \pm \sqrt{1 - \frac{4k_\parallel^2 b^2c^2}{k_0^2(b^2+c^2)^2}}\,\right], \tag{7.69}$$

where $k_0 \equiv \sqrt{k_y^2 + k_z^2}$ is the horizontal wave number (see Fig. 7.7). The function of these *turning point frequencies* ω_{s0}^2 and ω_{f0}^2 appears to be to separate the three

Downloaded from Cambridge Books Online by IP 152.2.176.242 on Mon Apr 29 20:09:13 WEST 2013.
http://dx.doi.org/10.1017/CBO9780511616945.008
Cambridge Books Online © Cambridge University Press, 2013

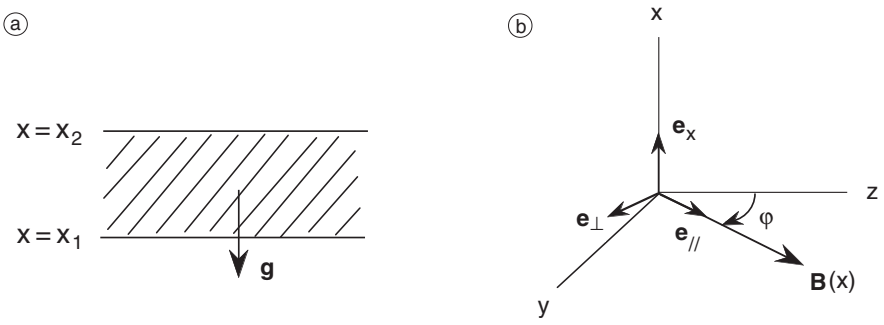

Fig. 7.9. (a) Gravitating plasma slab and (b) magnetic field line projection.

branches of the spectrum, as evidenced by the following sequence of inequalities:

$$0 \le \omega_S^2 \le \omega_s^2 \le \omega_{s0}^2 \;\le\; \omega_A^2 \;\le\; \omega_{f0}^2 \le \omega_f^2 \le \omega_F^2 = \infty\,. \tag{7.70}$$

This clear separation of the three discrete sub-spectra for homogeneous media returns, in a modified form, when the plasma becomes inhomogeneous.

▹ **Exercise.** Check the above expressions to teach yourself the basic steps. All of this trivial algebra returns in operator form in later sections! ◃

7.3.2 Derivation of the MHD wave equation for a gravitating slab

We now introduce genuine inhomogeneity in the model. Consider a plasma slab, infinite and homogeneous in the y- and z-directions, and contained between two planes at $x = x_1$ and $x = x_2$ (Fig. 7.9(a)). The equilibrium is assumed to vary in the x-direction:

$$\mathbf{B} = B_y(x)\,\mathbf{e}_y + B_z(x)\,\mathbf{e}_z\,, \quad \rho = \rho(x)\,, \quad p = p(x)\,. \tag{7.71}$$

The magnetic field is confined to plane layers parallel to the y-z plane, but its direction is assumed to vary with height. This is caused by current layers that are confined to the same planes (to be considered as the *magnetic surfaces* for this configuration):

$$\mathbf{j} = \nabla \times \mathbf{B} = -B_z'(x)\,\mathbf{e}_y + B_y'(x)\,\mathbf{e}_z\,, \tag{7.72}$$

where primes denote differentiation with respect to x. In general, $\mathbf{j}$ has a different direction from $\mathbf{B}$ so that there is a Lorentz force $\mathbf{j} \times \mathbf{B} = (\nabla \times \mathbf{B}) \times \mathbf{B} = -\nabla(\frac{1}{2}B^2)$ in the x-direction. (The latter relation follows by application of Eq. (A.8) where the additional term $\mathbf{B} \cdot \nabla\mathbf{B}$, which is present for curved magnetic fields, vanishes here.) This force is to be balanced by the pressure gradient ∇p and the gravitational force $\rho(x)\mathbf{g}$, due to an external gravitational field Φ with

Downloaded from Cambridge Books Online by IP 152.2.176.242 on Mon Apr 29 20:09:13 WEST 2013.
http://dx.doi.org/10.1017/CBO9780511616945.008
Cambridge Books Online © Cambridge University Press, 2013

constant acceleration

$$\mathbf{g} = -\nabla\Phi = -\hat{g}\mathbf{e}_x\,. \tag{7.73}$$

Here, a hat is put on the gravitational acceleration since the ordinary symbol g will be used for another purpose shortly. Consequently, equilibrium requires satisfaction of just one ODE,

$$(p + \tfrac{1}{2}B^2)' = -\rho\hat{g}\,, \tag{7.74}$$

which is the only restriction to be imposed on the possible choices of the functions $\rho(x)$, $p(x)$, $B_y(x)$, and $B_z(x)$.

In this manner, a generic 1D inhomogeneous model for confined plasmas is obtained. The presence of the two bounding plates may appear to be a rather artificial constituent of the model, in particular for astrophysical plasmas. Their function is to simply model plasma confinement, either by the presence of a conducting shell (as in tokamaks), or by the presence of an immobile (very dense) neighbouring plasma. One could always try to minimize their influence by moving them out to infinity, while keeping their essential role of eliminating the flow of energy in or out of the system. Of course, the ultimate remedy is to extend the analysis to an appropriate choice of one of the models (II)–(VI) of Section 4.6.

The wave and spectral equations for the gravitating plasma slab are obtained from Eqs. (6.23) and (6.28), which we repeat for convenience:

$$\mathbf{F}(\boldsymbol{\xi}) = \rho\frac{\partial^2\boldsymbol{\xi}}{\partial t^2} = -\rho\omega^2\boldsymbol{\xi}\,. \tag{7.75}$$

Clearly, the most laborious part of the problem is the evaluation of the force operator

$$\mathbf{F}(\boldsymbol{\xi}) \equiv -\nabla\pi - \mathbf{B}\times(\nabla\times\mathbf{Q}) + (\nabla\times\mathbf{B})\times\mathbf{Q} + \nabla\Phi\,\nabla\cdot(\rho\boldsymbol{\xi})\,, \tag{7.76}$$

with

$$\pi = -\gamma p\nabla\cdot\boldsymbol{\xi} - \boldsymbol{\xi}\cdot\nabla p\,, \qquad \mathbf{Q} = \nabla\times(\boldsymbol{\xi}\times\mathbf{B})\,. \tag{7.77}$$

This will be done in the following sequence of steps.

(a) Field line projection First, normal modes are studied satisfying the spectral equation (7.75), but now the 3D Fourier representation (7.60) is replaced by a *2D Fourier representation* for the two homogeneous directions only:

$$\boldsymbol{\xi}(\mathbf{r}) = \frac{1}{2\pi}\int\!\!\int \hat{\boldsymbol{\xi}}(x; k_y, k_z)\,\mathrm{e}^{\mathrm{i}(k_y y + k_z z)}\,dk_y dk_z\,. \tag{7.78}$$

Downloaded from Cambridge Books Online by IP 152.2.176.242 on Mon Apr 29 20:09:13 WEST 2013.
http://dx.doi.org/10.1017/CBO9780511616945.008
Cambridge Books Online © Cambridge University Press, 2013

Our task is to find the x-dependence of the separate Fourier components, which simply will be denoted as $\boldsymbol{\xi}(x)\ \exp \mathrm{i}(k_y y + k_z z)$, dropping the hat. The horizontal part of the differential operator ∇ then produces the algebraic substitutions $\partial_y \to \mathrm{i}k_y$ and $\partial_z \to \mathrm{i}k_z$, whereas the component ∂_x in the direction of inhomogeneity will produce (ordinary) differential equations.

Next, all vectors are projected onto the three unit vectors $\mathbf{e}_x$, $\mathbf{e}_\perp$, $\mathbf{e}_\parallel$ (*the field line triad*, Fig. 7.9(b)), which represent the physically relevant directions:

$$\begin{aligned} \mathbf{e}_x &\equiv \nabla x\,, \\ \mathbf{e}_\perp &\equiv (\mathbf{B}/B) \times \mathbf{e}_x = (0,\, B_z/B,\, -B_y/B)\,, \\ \mathbf{e}_\parallel &\equiv \mathbf{B}/B \qquad\quad = (0,\, B_y/B,\, B_z/B)\,. \end{aligned} \tag{7.79}$$

This *orthogonal projection*[3] is based on the physical significance of *magnetic field lines and magnetic surfaces* for the description of perturbations. It may be generalized to more complicated equilibria, like tokamaks with nested magnetic surfaces where $\mathbf{e}_x$ represents the normal, and $\mathbf{e}_\perp$ and $\mathbf{e}_\parallel$ the two tangential directions with respect to these surfaces. Hence, we will call the three directions defined by Eq. (7.79) by generic names, viz. *normal* (with respect to the magnetic surfaces), *perpendicular* (with respect to the field lines, but tangential to the magnetic surfaces so that the symbol $\perp$ is now more restrictive than in Section 7.3.1) and *parallel* (with respect to the field lines). In this projection, the result of the gradient operator on the perturbation $\boldsymbol{\xi}(x)\ \exp \mathrm{i}(k_y y + k_z z)$ may be written as

$$\nabla = \mathbf{e}_x \partial_x + \mathrm{i}\mathbf{e}_\perp(x)\, g + \mathrm{i}\mathbf{e}_\parallel(x)\, f\,, \tag{7.80}$$

where $\partial_x \equiv d/dx$ is the normal derivative, and f and g represent the perpendicular and parallel derivatives:

$$\begin{aligned} g = g(x) &\equiv -\mathrm{i}\mathbf{e}_\perp \cdot \nabla = G/B\,, \qquad G \equiv k_y B_z - k_z B_y\,, \\ f = f(x) &\equiv -\mathrm{i}\mathbf{e}_\parallel \cdot \nabla = F/B\,, \qquad F \equiv k_y B_y + k_z B_z\,. \end{aligned} \tag{7.81}$$

(The lower case g and f will be replaced by the upper case G and F in later chapters where division by B becomes awkward.) The quantities g and f may be considered as the wave vectors in the perpendicular and parallel directions, although

[3] One frequently encounters the statement in the literature that a local field line *coordinate* representation is exploited when, at best, a *projection* like the present one is meant. At worst, the existence of coordinates $u(x, y, z)$, $v(x, y, z)$, $w(x, y, z)$ is really assumed and one of them, say w, is supposed to measure distance along the magnetic field. The existence of such coordinates would imply $\mathbf{B} = f(u, v, w)\nabla w$, where f is some scalar function. Hence $\mathbf{j} = \nabla \times \mathbf{B} = \nabla f \times \nabla w = (1/f)\nabla f \times \mathbf{B}$, so that $j_\parallel = 0$. Of course, such a severe restriction on the equilibrium is not justified in general. In plane slab geometry, that condition implies that $\mathbf{B}$ is uni-directional. Only for such trivial fields could one construct field line coordinates of that kind.

Field line coordinates of an entirely different kind, so-called *Clebsch coordinates* α, β, γ, do exist, though. Here, $\mathbf{B}$ is represented as the vector product of two gradients of them: $\mathbf{B} = \nabla\alpha \times \nabla\beta$. These coordinates are useful for the study of instabilities localized about magnetic field lines.

Downloaded from Cambridge Books Online by IP 152.2.176.242 on Mon Apr 29 20:09:13 WEST 2013.
http://dx.doi.org/10.1017/CBO9780511616945.008
Cambridge Books Online © Cambridge University Press, 2013

they are functions of x in general. However, the magnitude of the resulting horizontal wave vector is constant:

$$k_0 \equiv \sqrt{g^2 + f^2} = \sqrt{k_y^2 + k_z^2}\,. \tag{7.82}$$

We also project $\boldsymbol{\xi}$ on the field line triad:

$$\boldsymbol{\xi} = \xi\,\mathbf{e}_x - \mathrm{i}\eta\,\mathbf{e}_\perp - \mathrm{i}\zeta\,\mathbf{e}_\parallel\,, \tag{7.83}$$

where

$$\begin{aligned}
\xi &\equiv \mathbf{e}_x \cdot \boldsymbol{\xi} \;\; = \xi_x\,,\\
\eta &\equiv \mathrm{i}\mathbf{e}_\perp \cdot \boldsymbol{\xi} = \mathrm{i}(B_z\xi_y - B_y\xi_z)/B\,,\\
\zeta &\equiv \mathrm{i}\mathbf{e}_\parallel \cdot \boldsymbol{\xi} \;\; = \mathrm{i}(B_y\xi_y + B_z\xi_z)/B\,.
\end{aligned}$$

The factors i have been inserted here since this turns out to lead to a representation where ξ, η and ζ may be assumed to be real.

When manipulating with vector equations, it is important to remember that the directions of the unit vectors $\mathbf{e}_\perp$ and $\mathbf{e}_\parallel$ vary with x when $\mathbf{B}$ is not uni-directional:

$$\partial_x \mathbf{e}_\perp = -\varphi' \mathbf{e}_\parallel\,, \qquad \partial_x \mathbf{e}_\parallel = \varphi' \mathbf{e}_\perp\,, \tag{7.84}$$

where $\varphi \equiv \arctan(B_y/B_z)$ is the angle between $\mathbf{B}$ and the z-axis (see Fig. 7.9(b)).

It remains to evaluate the components of the force operator $\mathbf{F}(\boldsymbol{\xi})$ explicitly, i.e. to exploit the consequences of the equilibrium relation (7.74), of the 2D Fourier representation (7.78), and of the orthogonal projection (7.79)–(7.83). This involves straightforward but rather tedious analysis, which is put in small print.

▷ **Explicit construction of the wave equation matrix.** In order to keep the analysis as mechanical as possible, we first derive the x, y, z components of the force operator $\mathbf{F}$ and only at the end compose the perpendicular and parallel components. Writing the different Fourier components of $\mathbf{F}$, we will drop the harmonic factor $\exp \mathrm{i}(k_y y + k_z z)$, but, of course, only after the gradient, divergence and curl operations have been applied. Straightforward application of the operations (7.80)–(7.82) and (7.83) then yields, for example, the important relation

$$\nabla \cdot \boldsymbol{\xi} = \xi' + g\eta + f\zeta\,, \tag{7.85}$$

so that the fluid terms of $\mathbf{F}$ may be written as

$$\begin{aligned}
-\nabla\pi \;&=\; [\,p'\xi + \gamma p(\xi' + g\eta + f\zeta)\,]'\,\mathbf{e}_x\\
&\quad + \mathrm{i}k_y[p'\xi + \gamma p(\xi' + g\eta + f\zeta)]\,\mathbf{e}_y + \mathrm{i}k_z[p'\xi + \gamma p(\xi' + g\eta + f\zeta)]\,\mathbf{e}_z\,,\\
\nabla\Phi\,\nabla\cdot(\rho\boldsymbol{\xi}) \;&=\; \hat{g}\,[(\rho\xi)' + \rho g\eta + \rho f\zeta\,]\,\mathbf{e}_x\,.
\end{aligned} \tag{7.86}$$

The evaluation of the magnetic terms requires some more diligence because of the repeated

Downloaded from Cambridge Books Online by IP 152.2.176.242 on Mon Apr 29 20:09:13 WEST 2013.
http://dx.doi.org/10.1017/CBO9780511616945.008
Cambridge Books Online © Cambridge University Press, 2013

curl operations:

$$\begin{aligned}
\boldsymbol{\xi}\times\mathbf{B} &= -\mathrm{i}B\eta\,\mathbf{e}_x - B_z\xi\,\mathbf{e}_y + B_y\xi\,\mathbf{e}_z\,,\\
\mathbf{Q} &= \mathrm{i}Bf\xi\,\mathbf{e}_x - [(B_y\xi)' - k_zB\eta]\,\mathbf{e}_y - [(B_z\xi)' + k_yB\eta]\,\mathbf{e}_z\,,\\
\nabla\times\mathbf{Q} &= -\mathrm{i}[(Bg\xi)' + k_0^2B\eta]\,\mathbf{e}_x\\
&\quad + [(B_z\xi)'' - k_zBf\xi + k_y(B\eta)']\mathbf{e}_y - [(B_y\xi)'' - k_yBf\xi - k_z(B\eta)']\mathbf{e}_z,\\
-\mathbf{B}\times(\nabla\times\mathbf{Q}) &= [B_y(B_y\xi)'' + B_z(B_z\xi)'' - B^2f^2\xi + Bg(B\eta)']\,\mathbf{e}_x\\
&\quad + \mathrm{i}B_z[(Bg\xi)' + k_0^2B\eta]\,\mathbf{e}_y - \mathrm{i}B_y[(Bg\xi)' + k_0^2B\eta]\,\mathbf{e}_z\,,\\
\mathbf{j}\times\mathbf{Q} &= [B_y'(B_y\xi)' + B_z'(B_z\xi)' + B(Bg)'\eta]\,\mathbf{e}_x + \mathrm{i}BB_y'f\xi\,\mathbf{e}_y + \mathrm{i}BB_z'f\xi\,\mathbf{e}_z\,.
\end{aligned} \tag{7.87}$$

Inserting the above expressions in the spectral equation (7.75), using the equilibrium equation (7.74), produces the three vector components of $\mathbf{F}$ in the x, y, z directions:

$$\begin{aligned}
-\rho\omega^2\xi_x &= [(\gamma p + B^2)\xi']' - B^2f^2\xi + [(\gamma p + B^2)g\eta]' + \rho\hat{g}g\eta + (\gamma pf\zeta)' + \rho\hat{g}f\zeta\,,\\
-\rho\omega^2\xi_y &= \quad \mathrm{i}B_zBg\,\xi' + \mathrm{i}k_y(\gamma p\xi' - \rho\hat{g}\xi) + \mathrm{i}(k_0^2B_zB + k_y\gamma pg)\,\eta + \mathrm{i}k_y\gamma pf\zeta\,,\\
\rho\omega^2\xi_z &= -\mathrm{i}B_yBg\,\xi' + \mathrm{i}k_z(\gamma p\xi' - \rho\hat{g}\xi) - \mathrm{i}(k_0^2B_yB - k_z\gamma pg)\,\eta + \mathrm{i}k_z\gamma pf\zeta\,.
\end{aligned} \tag{7.88}$$

Projecting the last two components onto $\mathbf{e}_\perp$ and $\mathbf{e}_\parallel$ finally yields the required representation given in Eq. (7.89) below. ◁

▷ **Exercise.** If you want to become conversant with spectral analysis of plasmas, you should not only reproduce the above steps, but also find alternative derivations. ◁

(b) Wave equation in field line projection The resulting wave or spectral equation for a plane gravitating slab, in orthogonal field line projection, assumes the following symmetric form:

$$\begin{pmatrix}
\frac{d}{dx}(\gamma p + B^2)\frac{d}{dx} - f^2B^2 & \frac{d}{dx}g(\gamma p + B^2) + g\rho\hat{g} & \frac{d}{dx}f\gamma p + f\rho\hat{g}\\
-g(\gamma p + B^2)\frac{d}{dx} + g\rho\hat{g} & -g^2(\gamma p + B^2) - f^2B^2 & -gf\gamma p\\
-f\gamma p\frac{d}{dx} + f\,\rho\hat{g} & -f\,g\,\gamma p & -f^2\gamma p
\end{pmatrix}
\begin{pmatrix}\xi\\ \eta\\ \zeta\end{pmatrix}
= -\rho\omega^2\begin{pmatrix}\xi\\ \eta\\ \zeta\end{pmatrix}. \tag{7.89}$$

Downloaded from Cambridge Books Online by IP 152.2.176.242 on Mon Apr 29 20:09:13 WEST 2013.
http://dx.doi.org/10.1017/CBO9780511616945.008
Cambridge Books Online © Cambridge University Press, 2013

The most important feature of this matrix representation of the force operator **F** is that it depends on x through $\rho(x)$, $p(x)$, $B^2(x)$, $f(x)$ and $g(x)$. If this dependence is neglected (which implies that the four gravitational terms $\rho\hat{g}$ must be neglected as well), the eigenvalue equation (7.64) for infinite homogeneous plasmas is recovered. The eigenvalue equation (7.32) for the gravito-acoustic modes of Section 7.2.1 is recovered in the limit $B \to 0$.

The matrix eigenvalue problem (7.89) for the three vector components ξ, η, ζ only contains normal differential operators d/dx in the first row and column. Hence, it can be reduced to a single second order differential equation in ξ by eliminating η and ζ by means of the second and third components, which are algebraic in η and ζ :

$$\eta = g\,\frac{[(b^2+c^2)\omega^2 - f^2b^2c^2]\,\xi' - \hat{g}\,\omega^2\,\xi}{D}\,,$$
$$\zeta = f\,\frac{c^2(\omega^2 - f^2b^2)\,\xi' - \hat{g}\,(\omega^2 - k_0^2b^2)\,\xi}{D}\,, \tag{7.90}$$

where $b \equiv B/\sqrt{\rho}$, $c \equiv \sqrt{\gamma p/\rho}$, and D is the determinant of the lower right 2×2 sub-matrix. Substituting these expressions into the first component gives the required *second order differential equation for* ξ, derived by Goedbloed [81](I):

$$\frac{d}{dx}\,\frac{N}{D}\,\frac{d\xi}{dx} + \left[\rho(\omega^2 - f^2b^2) + \rho'\hat{g} - k_0^2\rho\hat{g}^2\,\frac{\omega^2 - f^2b^2}{D}\right.$$
$$\left. - \left\{\rho\hat{g}\,\frac{\omega^2(\omega^2 - f^2b^2)}{D}\right\}'\right]\xi = 0\,, \tag{7.91}$$

where

$$N = N(x;\omega^2) \equiv \rho(\omega^2 - f^2b^2)\left[(b^2+c^2)\,\omega^2 - f^2b^2c^2\right],$$
$$D = D(x;\omega^2) \equiv \omega^4 - k_0^2(b^2+c^2)\,\omega^2 + k_0^2 f^2b^2c^2\,. \tag{7.92}$$

This equation has to be solved subject to the model I boundary conditions

$$\xi(x_1) = \xi(x_2) = 0\,. \tag{7.93}$$

This completes the formulation of this one-dimensional spectral problem.

Note that Eq. (7.91) contains the differential equation (7.34) for gravito-acoustic modes in the limit $b \to 0$. Also, the three MHD wave frequencies ω_s^2, ω_A^2, ω_f^2 for homogeneous plasmas, given in Eq. (7.65), are recovered in the limit $\rho\hat{g} \to 0$ and neglecting all x dependencies, so that $d/dx \to \mathrm{i}k_x$, $g \to k_y$, and $f \to k_z$.

It is of some interest for later generalizations to observe the intriguing difference between the spectral problem posed by the '3D' vector eigenvalue equation (7.89)

Downloaded from Cambridge Books Online by IP 152.2.176.242 on Mon Apr 29 20:09:13 WEST 2013.
http://dx.doi.org/10.1017/CBO9780511616945.008
Cambridge Books Online © Cambridge University Press, 2013

and the equivalent '1D' scalar eigenvalue equation (7.91), supplemented with the algebraic relations (7.90). Whereas the latter formulation is convenient for most of the analysis, and certainly for numerical integration, the eigenvalue character of the problem has been spoiled to a great extent because ω^2 is scattered all over the place in Eq. (7.91). (For that reason, equations of this type are sometimes called 'nonlinear' eigenvalue equations.) Hence, to prove or disprove general properties (like monotonicity of the discrete spectrum) it may be advisable to return to the original formulation (7.89).

(c) Singular frequencies The ordinary differential equation (7.91), with the boundary conditions (7.93), describes all gravito-magnetohydrodynamic modes of a gravitating magnetized plasma slab with completely arbitrary equilibrium profiles. Before trying to solve it by analytical or numerical methods, one first needs to pay attention to the physical meaning of the different terms and, in particular, to the different singularities that occur.

It is clear that the factor N/D in front of the highest derivative of the differential equation plays an important role. We may write this factor in terms of the four special frequencies (that were already introduced) in Eqs. (7.94)–(7.96) for the case of a homogeneous plasma:

$$\frac{N}{D} = \rho(b^2 + c^2)\,\frac{[\,\omega^2 - \omega_A^2(x)\,]\,[\,\omega^2 - \omega_S^2(x)\,]}{[\,\omega^2 - \omega_{s0}^2(x)\,]\,[\,\omega^2 - \omega_{f0}^2(x)\,]}\,. \tag{7.94}$$

The numerator N involves the *asymptotic Alfvén and slow magneto-sonic frequencies*,

$$\omega_A^2(x) \equiv f^2 b^2 \equiv F^2/\rho\,, \qquad \omega_S^2(x) \equiv f^2\frac{b^2c^2}{b^2+c^2} \equiv \frac{\gamma p}{\gamma p + B^2}\,\omega_A^2(x)\,, \tag{7.95}$$

whereas the denominator D involves the *slow and fast turning point frequencies*,

$$\omega_{s0,\,f0}^2(x) \equiv \tfrac{1}{2}k_0^2(b^2+c^2)\left[\,1 \pm \sqrt{1 - \frac{4f^2b^2c^2}{k_0^2(b^2+c^2)^2}}\,\right]. \tag{7.96}$$

For inhomogeneous plasmas, all of these four special frequencies depend on x, through $f^2(x)$, $b^2(x)$ and $c^2(x)$, so that their role is to be determined by a local analysis about the points where the different factors of N and D vanish. In particular, the ODE (7.91) becomes *singular* for $N \to 0$, when $\omega^2 \to \omega_A^2(x)$ or $\omega^2 \to \omega_S^2(x)$, i.e. when the local Alfvén or slow magneto-sonic frequencies are approached. These singularities deserve a separate treatment, given in Section 7.4, where it is shown that they give rise to non-square integrable solutions associated with *continuous spectra*. On the other hand, the ODE only develops *apparent*

Downloaded from Cambridge Books Online by IP 152.2.176.242 on Mon Apr 29 20:09:14 WEST 2013.
http://dx.doi.org/10.1017/CBO9780511616945.008
Cambridge Books Online © Cambridge University Press, 2013

singularities for $D \to 0$, when $\omega^2 \to \omega_{s0}^2(x)$ or $\omega^2 \to \omega_{f0}^2(x)$, i.e. when the local magneto-sonic turning point frequencies are approached. An apparent singularity implies that there are cancellations in the series expansion of the solution, so that it remains finite in the end. This follows directly from the equivalent system of first order differential equations (next subsection), but can also be demonstrated explicitly from the second order differential equation (Section 7.4.1). The history of this topic is summarized at the end of Section 7.4.2.

The function $F(x)$, that occurs in the frequencies $\omega_A(x)$ and $\omega_S(x)$ of the Alfvén and slow continua, deserves special attention since it represents the projection of the gradient operator parallel to the magnetic field:

$$F \equiv -\mathrm{i}\mathbf{B} \cdot \nabla = \mathbf{k}_0 \cdot \mathbf{B}\,. \tag{7.97}$$

The locations in the plasma where $F = 0$ play an important role in the stability of plasmas since the stabilizing magnetic field line bending energy vanishes there, favouring interchange instability (see Section 7.5.2). Accordingly, in stability theory, the continua $\{\omega_A^2(x)\}$ and $\{\omega_S^2(x)\}$ appear in the disguise of the 'interchange' values $\{F^2(x)\}$.

(d) Equivalent system of first order differential equations For numerical integration one usually converts a second order ODE into a pair of first order ODEs for the function and its first derivative. In our case, instead of ξ', it is much better to exploit a physical variable for that purpose, viz. the (Eulerian) *perturbation of the total pressure*:

$$\Pi \equiv \pi + \mathbf{B} \cdot \mathbf{Q} = -\gamma p \nabla \cdot \boldsymbol{\xi} - \boldsymbol{\xi} \cdot \nabla p + \mathbf{B} \cdot \mathbf{Q}\,. \tag{7.98}$$

Converting $\nabla \cdot \boldsymbol{\xi}$ by means of Eq. (7.85), $\mathbf{Q}$ with Eq. (7.87), and exploiting the equilibrium relation (7.74), this expression may be transformed into

$$\begin{aligned} \Pi &= -\rho(b^2 + c^2)\xi' + \rho\hat{g}\xi - \rho g(b^2 + c^2)\eta - \rho f c^2 \zeta \\ &= -\frac{N}{D}\,\xi' + \rho\hat{g}\,\frac{\omega^2(\omega^2 - f^2 b^2)}{D}\,\xi\,, \end{aligned} \tag{7.99}$$

where η and ζ have been eliminated in the second line by means of Eq. (7.90). Hence, the peculiar derivative term in curly brackets in the second order ODE (7.91) comes from this expression for the total pressure perturbation Π.

By means of the expression just derived, we may convert the second order differential equation (7.91) into the following pair of first order differential equations:

$$\begin{pmatrix} \xi \\ \Pi \end{pmatrix}' = -\frac{1}{N} \begin{pmatrix} C & D \\ E & -C \end{pmatrix} \begin{pmatrix} \xi \\ \Pi \end{pmatrix}, \tag{7.100}$$

Downloaded from Cambridge Books Online by IP 152.2.176.242 on Mon Apr 29 20:09:14 WEST 2013.
http://dx.doi.org/10.1017/CBO9780511616945.008
Cambridge Books Online © Cambridge University Press, 2013

where

$$C \equiv -\rho\hat{g}\,\omega^2(\omega^2 - f^2b^2)\,,$$
$$E \equiv -\Big[\,\rho(\omega^2 - f^2b^2) + \rho'\hat{g}\,\Big]N - \rho^2\hat{g}^2(\omega^2 - f^2b^2)^2\,. \tag{7.101}$$

The determinant of the matrix on the RHS of Eq. (7.100) is proportional to N:

$$DE + C^2 = -\Big\{\Big[\,\rho(\omega^2 - f^2b^2) + \rho'\hat{g}\,\Big]D - k_0^2\rho\hat{g}^2(\omega^2 - f^2b^2)\Big\}N\,. \tag{7.102}$$

This guarantees that no additional singularities have been introduced in this formulation. The vector eigenvalue equations (7.89) for ξ, η, ζ, the scalar eigenvalue problem (7.91) for ξ, and the two-variable eigenvalue problem (7.100) for ξ, Π are equivalent.

The formulation in terms of two first order ODEs was first exploited by Appert, Gruber and Vaclavik [9] for the analogous problem in cylindrical geometry. Its merit is that it shows right away that nothing blows up for $D = 0$ so that these singularities of Eq. (7.91) must be *apparent*, whereas the $N = 0$ singularities are genuine.

7.3.3 Gravito-MHD waves

Before we start the investigation of the general structure of the spectrum of MHD waves in a gravitating medium, where the mentioned singularities will be in the centre of our attention, it is useful to discuss one simple but non-trivial example of a complete spectrum where the singularities are still absent (or, rather, degenerate enough to permit a simple representation). This is provided by the generalization of the problem considered in Section 7.2.3 to an *exponentially stratified atmosphere with constant sound and Alfvén speeds*:

$$\rho = \rho_0 \mathrm{e}^{-\alpha x}\,, \quad p = p_0\mathrm{e}^{-\alpha x}\,, \quad \mathbf{B} = B_0\mathrm{e}^{-\frac{1}{2}\alpha x}\mathbf{e}_z\,, \tag{7.103}$$

so that

$$c^2 = \frac{\gamma p}{\rho} = \frac{\gamma p_0}{\rho_0}\,, \qquad b^2 = \frac{B^2}{\rho} = \frac{B_0^2}{\rho_0}\,. \tag{7.104}$$

It is useful to exploit the parameter β as a measure for the relative magnitude of the sound speed with respect to the Alfvén speed:

$$\beta \equiv \frac{2p}{B^2} = \frac{2p_0}{B_0^2}\,, \qquad \text{so that} \quad \frac{c^2}{b^2} = \tfrac{1}{2}\gamma\beta\,. \tag{7.105}$$

Downloaded from Cambridge Books Online by IP 152.2.176.242 on Mon Apr 29 20:09:16 WEST 2013.
http://dx.doi.org/10.1017/CBO9780511616945.008
Cambridge Books Online © Cambridge University Press, 2013

The equilibrium relation (7.74) then fixes the relationship between the parameter α and the gravitational acceleration $\hat{g}$:

$$\alpha = \frac{\rho\hat{g}}{p + \frac{1}{2}B^2} = \frac{\rho_0\hat{g}}{p_0 + \frac{1}{2}B_0^2} = \frac{\gamma\hat{g}}{c^2 + \frac{1}{2}\gamma b^2} = \frac{2}{1+\beta}\frac{\hat{g}}{b^2}. \tag{7.106}$$

Also, the wave numbers f $(= k_z)$ and g $(= k_y)$ are constants now so that the continuous spectra $\omega_S^2 \equiv f^2b^2c^2/(b^2 + c^2)$ and $\omega_A^2 \equiv f^2b^2$, defined in Eq. (7.95), just degenerate into two points on the ω^2-axis.

Through these simplifications, the basic spectral equation (7.91) transforms into a differential equation *with constant coefficients* (after elimination of the factor $\mathrm{e}^{-\alpha x}$):

$$\frac{N_0}{\rho_0 D_0}\frac{d}{dx}\left(\mathrm{e}^{-\alpha x}\frac{d\xi}{dx}\right) + \left[\omega^2 - f^2b^2 - k_0^2\hat{g}^2\frac{\omega^2 - f^2b^2}{D_0} - \alpha\hat{g} + \alpha\hat{g}\frac{\omega^2(\omega^2 - f^2b^2)}{D_0}\right]\mathrm{e}^{-\alpha x}\xi = 0, \tag{7.107}$$

where the numerator and denominator coefficients $N_0 \equiv N(0)$ and $D_0 \equiv D(0)$. This yields an exponential solution $\xi = C\mathrm{e}^{(\frac{1}{2}\alpha \pm \mathrm{i}q)x}$ with a vertical 'wave number'

$$q \equiv \sqrt{-\frac{1}{4}\alpha^2 + \frac{\rho_0}{N_0}\left[(\omega^2 - f^2b^2)(D_0 + k_0^2c^2N_B^2) + \alpha\hat{g}\,g^2b^2\omega^2\right]} = n\frac{\pi}{a} \tag{7.108}$$

that has to satisfy the quantization condition (7.47) because of the model I boundary conditions on ξ. Here, we have introduced the Brunt–Väisäläa frequency N_B again (with an index B on it to avoid confusion with our other symbol N):

$$N_B^2 \equiv -\frac{1}{\rho}\left(\rho'\hat{g} + \frac{\rho^2\hat{g}^2}{\gamma p}\right) = \alpha\hat{g} - \frac{\hat{g}^2}{c^2} = \frac{(\gamma-1)\beta - 1}{1+\beta}\frac{\hat{g}^2}{c^2}. \tag{7.109}$$

Note that in the HD limit ($\beta \to \infty$), the expression (7.44) of Section 7.2.3 is recovered: $N_B^2 \to (\gamma - 1)\hat{g}^2/c^2$. However, due to the finite β MHD modifications of the equilibrium, positivity of N_B^2 is no longer guaranteed now but depends on the value of β:

$$N_B^2 \begin{cases} \geq 0 & \text{for} \quad \beta \geq (\gamma-1)^{-1} \\ < 0 & \text{for} \quad 0 \leq \beta < (\gamma-1)^{-1}. \end{cases} \tag{7.110}$$

This permits some analysis of the MHD version of the convective instability, but one should be aware of the intrinsic limitation of the stability results obtained on the assumption (7.103) of exponential profiles. Obviously, this assumption is not dictated by physical necessity but is just made for analytical convenience.

Downloaded from Cambridge Books Online by IP 152.2.176.242 on Mon Apr 29 20:09:16 WEST 2013.
http://dx.doi.org/10.1017/CBO9780511616945.008
Cambridge Books Online © Cambridge University Press, 2013

(a) Dispersion equation and special solutions Inversion of Eq. (7.108) for q yields the *dispersion equation for the gravito-MHD waves*:

$$(\omega^2 - f^2 b^2)\Big[\,\omega^4 - k_{\rm eff}^2(b^2+c^2)\omega^2 + k_{\rm eff}^2 f^2 b^2 c^2 + k_0^2 c^2 N_B^2\,\Big] + \alpha\hat{g}\, g^2 b^2 \omega^2 = 0\,, \tag{7.111}$$

where $f = k_0 \cos\vartheta$ and $g = k_0 \sin\vartheta$ (with ϑ indicating the angle between $\mathbf{k}_0$ and $\mathbf{B}$) and we recall the definition of the effective total 'wave number',

$$k_{\rm eff}^2 \equiv k_0^2 + q^2 + \tfrac{1}{4}\alpha^2\,.$$

Since the dispersion equation (7.111) is a cubic equation in ω^2, with three independent solutions, we immediately conclude that gravity does not increase the number of degrees of freedom of the MHD system. We had three MHD waves without gravity and we keep three waves with gravity. These waves transform into the ordinary MHD waves of Chapter 5 when $\hat{g} \to 0$ and into the gravito-acoustic waves of Section 7.2.3 when $b \to 0$ ($\beta \to \infty$). However, the latter limit deserves further analysis to clarify how the twofold HD spectral structure of Fig. 7.3 (with clustering at $\omega = \infty$ and $\omega = 0$) relates to the threefold MHD spectral structure (with clustering at $\omega = \infty$, $\omega = \omega_A$ and $\omega = \omega_S$). This will be discussed after we have obtained the MHD counterpart in Fig. 7.10.

Two misleadingly simple expressions are obtained from the dispersion equation (7.111) for the limiting cases of purely parallel and purely perpendicular propagation. For *parallel propagation* ($\mathbf{k}_0 \parallel \mathbf{B} \;\Rightarrow\; \vartheta = 0\,,\; f = k_0\,,\; g = 0$), the following solutions are obtained:

$$\omega_1^2 = k_0^2 b^2\,, \qquad \omega_{2,3}^2 = \tfrac{1}{2}k_{\rm eff}^2(b^2+c^2)\left[\,1 \pm \sqrt{1 - \frac{4k_0^2c^2(k_{\rm eff}^2 b^2 + N_B^2)}{k_{\rm eff}^4(b^2+c^2)^2}}\,\right]. \tag{7.112}$$

These *appear* to be the unaffected Alfvén waves and two gravitational modifications of the fast and slow magneto-sonic waves (one of which will give rise to the Parker instability). For *perpendicular propagation* ($\mathbf{k}_0 \perp \mathbf{B} \;\Rightarrow\; \vartheta = \frac{1}{2}\pi\,,\; f = 0\,,\; g = k_0$) the dispersion equation yields the following solutions:

$$\omega_1^2 = 0\,, \qquad \omega_{2,3}^2 = \tfrac{1}{2}k_{\rm eff}^2(b^2+c^2)\left[\,1 \pm \sqrt{1 - \frac{4k_0^2 N_m^2}{k_{\rm eff}^4(b^2+c^2)}}\,\right], \tag{7.113}$$

where another characteristic expression appears, viz.

$$N_m^2 \equiv -\frac{1}{\rho}\left(\rho'\hat{g} + \frac{\rho^2\hat{g}^2}{\gamma p + B^2}\right) = \alpha\hat{g} - \frac{\hat{g}^2}{b^2+c^2} = \frac{(\gamma-1)\beta + 1}{1+\beta}\,\frac{\hat{g}^2}{b^2+c^2}\,, \tag{7.114}$$

Downloaded from Cambridge Books Online by IP 152.2.176.242 on Mon Apr 29 20:09:16 WEST 2013.
http://dx.doi.org/10.1017/CBO9780511616945.008
Cambridge Books Online © Cambridge University Press, 2013

which is called the magnetically modified Brunt–Väisäläa frequency; see Priest [190]. (Note the different sign in the numerator compared to the expression (7.109) for N_B^2, so that $N_m^2 > 0$ for this class of equilibria, independent of the value of β.) One of the solutions degenerates into a marginal mode and the two other solutions are magnetic compressional modifications of the p- and g-modes given by Eq. (7.49). The dispersion diagram of Fig. 7.3 remains valid for these solutions if we replace the sound speed by the magneto-sonic speed ($c^2 \to b^2 + c^2$), and adapt the definitions of the Lamb and Brunt–Väisäläa frequencies accordingly.

We have termed the expressions (7.112) and (7.113) misleadingly simple since they represent limiting cases of intricate mode couplings where the labels A, s and f may no longer be appropriate (which is why we have used the neutral labels 1, 2 and 3 instead) and they create a false impression on stability (with only the parallel expression admitting unstable solutions, whereas MHD instabilities preferentially operate in the perpendicular direction). To obtain the full spectral picture of the different HD and MHD effects operating in gravitating plasmas, and their relation to stability, we should study the cubic dispersion equation (7.111) for *oblique propagation*. This is done, most effectively, by means of a numerical representation (exploiting Cardano's explicit solutions) for a typical choice of the parameters. Since the latter part of the problem is less trivial than it may appear, we first pay attention to the construction of dimensionless parameters.

(b) Dimensionless scaling of the dispersion equation and general solutions

When handling the final result of an MHD calculation, like the dispersion equation (7.111), it is always useful to convert it to a dimensionless form exploiting the scale independence introduced in Section 4.1.2 to get rid of the trivial dimensional factors. To that end, we exploit the thickness a ($\equiv x_2 - x_1$) of the slab as a measure for lengths, and the density ρ_0 and the magnetic field strength B_0 at $x = 0$ as measures for the density and magnetic field determining the (constant) Alfvén speed $b \equiv B_0/\sqrt{\rho_0}$. The relevant, dimensionless, parameters then become

$$\bar{\omega} \equiv (a/b)\,\omega\,, \quad \bar{k}_{\rm eff} \equiv k_{\rm eff} a\,, \quad \bar{k}_0 \equiv k_0 a\,, \quad \bar{q} \equiv q a\,, \quad \bar{\alpha} \equiv \alpha a\,, \qquad (7.115)$$

in terms of which the implicit form of the dimensionless dispersion equation reads:

$$\begin{aligned} \bar{\omega}^6 &- \Big[\,(1+\tfrac{1}{2}\gamma\beta)\bar{k}_{\rm eff}^2 + \bar{k}_0^2\cos^2\vartheta\,\Big]\bar{\omega}^4 \\ &+ \Big[\,(1+\gamma\beta)\bar{k}_{\rm eff}^2\cos^2\vartheta + \tfrac{1}{4}(1+\beta)(\gamma\beta-\beta+1-2\cos^2\vartheta)\,\bar{\alpha}^2\,\Big]\bar{k}_0^2\,\bar{\omega}^2 \\ &- \Big[\,\tfrac{1}{2}\gamma\beta\bar{k}_{\rm eff}^2\cos^2\vartheta + \tfrac{1}{4}(1+\beta)(\gamma\beta-\beta-1)\,\bar{\alpha}^2\,\Big]\bar{k}_0^4\cos^2\vartheta = 0\,. \end{aligned} \qquad (7.116)$$

Downloaded from Cambridge Books Online by IP 152.2.176.242 on Mon Apr 29 20:09:16 WEST 2013.
http://dx.doi.org/10.1017/CBO9780511616945.008
Cambridge Books Online © Cambridge University Press, 2013

The solution of this cubic provides the explicit dimensionless dispersion equation:

$$\bar{\omega} = \bar{\omega}(\bar{k}_0, \vartheta, \bar{q}; \bar{\alpha}, \beta, \gamma)\,. \tag{7.117}$$

Here, the parameters in front of the semicolon refer to the perturbation and the ones behind it refer to the equilibrium. For the numerical investigation of the stability of a particular equilibrium, one could fix the parameters $\bar{\alpha}, \beta, \gamma\ (= 5/3)$ to correspond to that equilibrium, but one should investigate the full range of the parameters $\bar{q}, \vartheta, \bar{k}_0$, since that is what nature does. Using the scale independence in this manner, we obtain certainty about the completeness of parameter space and avoid useless scanning of redundant parameters.

In terms of the dimensionless parameters, the 'singular' frequencies of Section 7.3.2 become

$$N_0 = 0 \Rightarrow \quad \bar{\omega}_A^2 = \bar{k}_0^2 \cos^2\vartheta\,, \qquad \bar{\omega}_S^2 = \frac{\frac{1}{2}\gamma\beta}{1 + \frac{1}{2}\gamma\beta}\,\bar{k}_0^2 \cos^2\vartheta\,, \tag{7.118}$$

$$D_0 = 0 \Rightarrow \quad \bar{\omega}_{s0,\,f0}^2 = \tfrac{1}{2}\bar{k}_0^2(1 + \tfrac{1}{2}\gamma\beta)\left[\,1 \pm \sqrt{1 - \frac{2\gamma\beta}{(1 + \frac{1}{2}\gamma\beta)^2}\,\cos^2\vartheta}\,\right]. \tag{7.119}$$

The dimensionless expressions of the two kinds of Brunt–Väisäläa frequencies, involving the gravitational parameter $\bar{\alpha}$, read:

$$\bar{N}_B^2 = \tfrac{1}{4}\bar{\alpha}^2\,\frac{(1+\beta)\,[(\gamma-1)\beta - 1]}{\frac{1}{2}\gamma\beta}\,, \qquad \bar{N}_m^2 = \tfrac{1}{4}\bar{\alpha}^2\,\frac{(1+\beta)\,[(\gamma-1)\beta + 1]}{1 + \frac{1}{2}\gamma\beta}\,. \tag{7.120}$$

Whereas the 'singular' frequency expressions (7.118) and (7.119) do not involve $\bar{\alpha}$, they play a decisive role in the clarification of the MHD spectral structure, as we will see.

In Fig. 7.10 we show plots of $\bar{\omega}^2(\bar{k}_0^2)$ for oblique propagation ($\vartheta = \pi/4$) for thirty values of the vertical mode number n. The value of $\bar{\alpha}\ (= 20)$ has been chosen to be approximately the same as for the HD p- and g-modes of Fig. 7.3. To demonstrate the connection with the latter diagram, a high value of β is taken in Fig. 7.10(a), whereas β is chosen to be unity in Fig. 7.10(b) to exhibit the more usual MHD spectral structure. The singular frequencies $\bar{\omega}_A^2$ and $\bar{\omega}_S^2$ are indicated by long dashes and the magneto-sonic turning point frequencies $\bar{\omega}_{s0,\,f0}^2$ are indicated by short dashes. The three dotted lines represent the zeroth ($n = 0$) 'member' of each family of solutions. Those are actually not solutions, since they do not satisfy

Downloaded from Cambridge Books Online by IP 152.2.176.242 on Mon Apr 29 20:09:16 WEST 2013.
http://dx.doi.org/10.1017/CBO9780511616945.008
Cambridge Books Online © Cambridge University Press, 2013

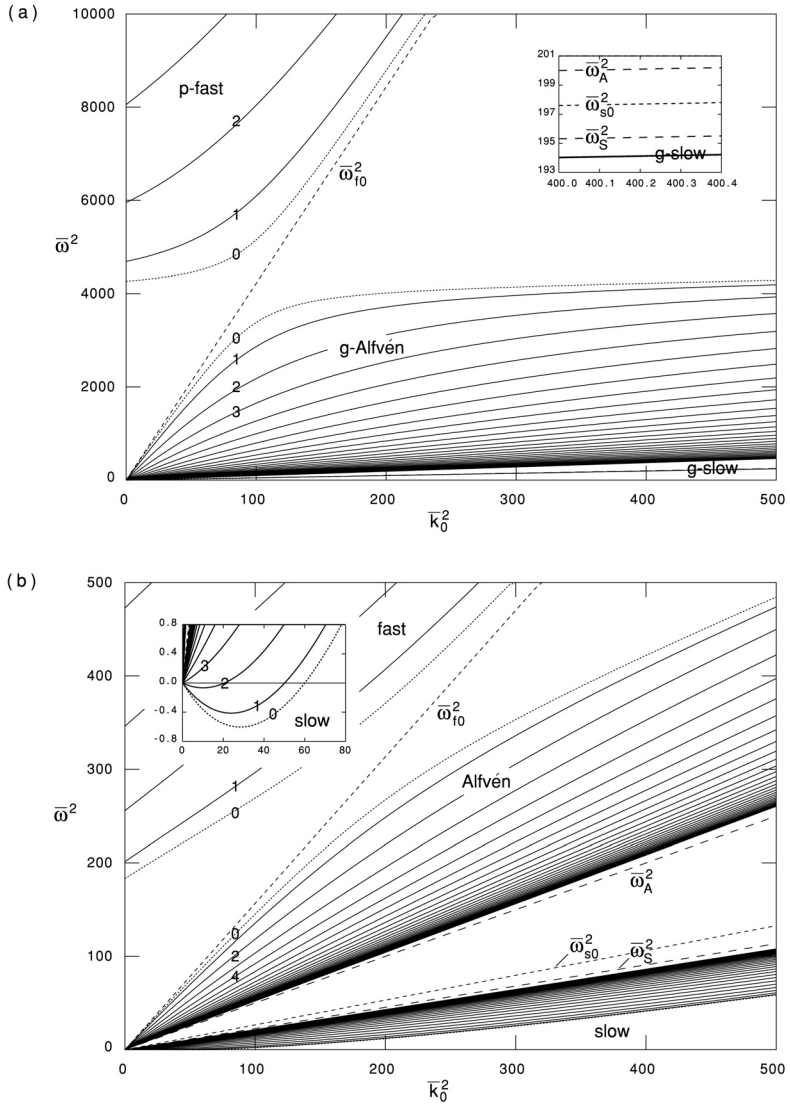

Fig. 7.10. Dispersion diagrams for the oblique gravito-MHD modes of an exponential plane plasma layer. The squared frequencies in normalized units, $\bar{\omega}^2 = \bar{\omega}^2(\bar{k}_0^2, \bar{q}^2, \vartheta)$, are plotted for thirty values of the vertical 'wave number' $\bar{q} = n\pi$ $(n = 1, 2, \ldots, 30)$; $\bar{\alpha} = 20$, $\vartheta = \pi/4$. (a) Near HD regime ($\beta = 50$), inset: blow-up of low-frequencies (slow wave spectrum not yet resolved on this scale); (b) regular MHD regime ($\beta = 1$), inset: unstable slow modes.

the boundary conditions, but they conveniently mark the boundaries of the most global modes. The spectral structure is determined by how these three families of solutions for $\bar{\omega}^2$ are distributed from $n = 1$ to $n \to \infty$, where the latter limit yields the essential spectrum (see Section 7.3.1).

Downloaded from Cambridge Books Online by IP 152.2.176.242 on Mon Apr 29 20:09:16 WEST 2013.
http://dx.doi.org/10.1017/CBO9780511616945.008
Cambridge Books Online © Cambridge University Press, 2013

By means of Fig. 7.10, the following matters may be elucidated:

(1) the relationship between the HD and the MHD spectral structures (Fig. 7.10(a));
(2) the influence of gravity and the essential spectrum in MHD (Fig. 7.10(b));
(3) the convective/Rayleigh–Taylor instability in the presence of a magnetic field.

We will discuss them, one by one.

(1) The HD dispersion equation (7.48) is obtained from the MHD dispersion equation (7.116) by scaling with β, $\widetilde{\omega}^2 \equiv \frac{1}{2}\gamma\beta\,\bar{\omega}^2$ (so that the vertical sizes in Fig. 7.10(a) are a factor $\frac{1}{2}\gamma\beta$ larger than those in Fig. 7.3), and taking the limit $\beta \to \infty$:

$$\widetilde{\omega}^2\Big[\,\widetilde{\omega}^4 - \bar{k}_{\rm eff}^2\,\widetilde{\omega}^2 + \tfrac{1}{4}(\gamma-1)\bar{\alpha}^2\bar{k}_0^2\,\Big] = 0\,. \tag{7.121}$$

This shows that, in addition to the p- and g-modes discussed in Section 7.2.3, the marginal horizontal shifts perpendicular to $\mathbf{k}_0$, that were discarded in Section 7.2.1, are needed to obtain a *threefold essential spectrum* ($\widetilde{\omega}^2_{1,2} \equiv 0$, $\widetilde{\omega}^2_3 \equiv \infty$) that may be connected to the threefold essential spectrum of MHD. In fact, in the limit $\beta \to \infty$, the Alfvén and slow mode frequencies $\bar{\omega}^2_{A,S} \to 0$, where the displacement $\boldsymbol{\xi}$ becomes dominantly horizontal, whereas $\bar{\omega}^2_F \equiv \infty$, corresponding to dominantly vertical displacements. Fig. 7.10(a) shows that, for large but finite β, the p-modes transform into the fast MHD modes and the g-modes transform into the Alfvén modes. In addition, a new branch of gravitational slow MHD modes springs forth in the low-frequency domain. From the inset in Fig. 7.10(a) it is clear that for the value of the gravitational parameter chosen, $\bar{\alpha}^2 \sim \bar{k}_0^2$, the spectrum is strongly affected by gravity both for the Alfvén modes (infinitely degenerate in the absence of gravity) and for the slow modes (anti-Sturmian in the absence of gravity). Notice that there is still quite a lot of empty space left between the lowest Alfvén curve and $\bar{\omega}^2_A$ and between the highest slow curve and $\bar{\omega}^2_S$, which will be occupied by the curves for $n > 30$ (not shown) establishing the link with the essential spectrum.

(2) Decreasing the value of β to unity (Fig. 7.10(b)), the three MHD sub-spectra (separated by empty evanescent regions containing the turning point frequencies $\bar{\omega}^2_{s0}$ and $\bar{\omega}^2_{f0}$) become more clearly distinguished. The three sequences can be labelled as fast, Alfvén and slow by virtue of the monotonicity of $\bar{\omega}^2$ as a function of n (to be proved in general in Section 7.4.3), where $\bar{\omega}^2_F$, $\bar{\omega}^2_A$ and $\bar{\omega}^2_S$ are obtained in the limit $n \to \infty$. By expanding the solutions of the dispersion equation (7.116) around these frequencies, one obtains the following expressions for the *approach*

Downloaded from Cambridge Books Online by IP 152.2.176.242 on Mon Apr 29 20:09:17 WEST 2013.
http://dx.doi.org/10.1017/CBO9780511616945.008
Cambridge Books Online © Cambridge University Press, 2013

to the essential spectrum:

$$\begin{aligned}
\bar{\omega}_f^2 &\approx (1+\tfrac{1}{2}\gamma\beta)\,\bar{q}^2 && \rightarrow \quad \bar{\omega}_F^2 \equiv \infty\,,\\
\bar{\omega}_a^2 &\approx \bar{\omega}_A^2 + \tfrac{1}{2}(1+\beta)\left(\frac{\bar{k}_0}{\bar{q}}\right)^2 \bar{\alpha}^2 \sin^2\vartheta && \rightarrow \quad \bar{\omega}_A^2\,, \qquad (7.122)\\
\bar{\omega}_s^2 &\approx \bar{\omega}_S^2 + \frac{\bar{\omega}_S^4 - \tfrac{1}{4}(1+\beta)(1+\beta-\gamma\beta\cos^2\vartheta)\,\bar{k}_0^2\bar{\alpha}^2}{(1+\tfrac{1}{2}\gamma\beta)\,\bar{q}^2} && \rightarrow \quad \bar{\omega}_S^2\,.
\end{aligned}$$

(For the validity of the expressions for $\bar{\omega}_a^2$ and $\bar{\omega}_s^2$, the second term should be much smaller than the first one so that they are not valid in the limit $\vartheta \to \pi/2$, when $\bar{\omega}_A^2$ and $\bar{\omega}_S^2 \to 0$. This subject abounds with non-uniform limits; the reader is strongly advised to build up experience by studying this dispersion equation in the many different limits, virtually all of which turn out to be physically relevant.) Whereas the deviation from the limiting frequencies is determined by the gravitational parameter $\bar{\alpha}$, the essential spectrum itself is not affected by gravity; it is robust in that sense.

The expressions (7.122) clearly show how the infinite degeneracy of the Alfvén frequencies is lifted by gravity so that an anti-Sturmian sequence ($\bar{\omega}^2 \downarrow \bar{\omega}_A^2$ as $n \to \infty$) is obtained. The slow frequencies, which are anti-Sturmian ($\bar{\omega}^2 \downarrow \bar{\omega}_S^2$) in the absence of gravity, either become Sturmian ($\bar{\omega}^2 \uparrow \bar{\omega}_S^2$), as in the range of $\bar{k}_0^2$ plotted in Fig. 7.10(b), or remain anti-Sturmian when $\bar{k}_0^2$ is large enough (far outside the range shown). However, for monotonicity of $\bar{\omega}^2(n)$ to remain valid, the transition from Sturmian to anti-Sturmian behaviour should occur at a point of *infinite degeneracy of the slow modes*. This is exactly what happens when the numerator of the second term of the expression (7.122)(c) for $\bar{\omega}_s^2$ vanishes. Hence, for this class of equilibria, the sequence of inequalities (7.70) for homogeneous equilibria is modified to permit both Sturmian and anti-Sturmian slow frequencies ($\bar{\omega}_s^2 < \bar{\omega}_S^2$ and $\bar{\omega}_s^2 > \bar{\omega}_S^2$), and anti-Sturmian Alfvén frequencies ($\bar{\omega}_a^2 > \bar{\omega}_A^2$).

Having obtained a rather compelling way of labelling the MHD sub-spectra, we now return to our reservations when discussing the simple expressions (7.112) for parallel propagation. In particular, it would appear logical to associate ω_1^2 with the Alfvén modes and ω_2^2 (the solution with the minus sign) with the slow modes. However, as shown by Adam [3], when $N_B^2 c^2 > \frac{1}{4}\alpha^2 b^4$ (i.e. $\beta > 2$ for $\gamma = 5/3$), the curve for $\omega_2^2(q)$ crosses the value ω_1^2 so that some of the slow frequencies would exceed the Alfvén frequency, in conflict with the very name 'slow'. (There is no conflict with the direction of monotonicity determined by the sign of N_0/D_0 since $\omega_A^2 = \omega_{s0}^2$ in this case, so that two 'singular' frequencies are crossed simultaneously.) We eliminate this paradox by considering near parallel propagation ($|\vartheta| = \epsilon \ll 1$) in the limit $\epsilon \to 0$. For $\epsilon \neq 0$, the two solutions split apart into an

Downloaded from Cambridge Books Online by IP 152.2.176.242 on Mon Apr 29 20:09:17 WEST 2013.
http://dx.doi.org/10.1017/CBO9780511616945.008
Cambridge Books Online © Cambridge University Press, 2013

anti-Sturmian Alfvén branch approaching ω_A^2 for $q \to \infty$ and an anti-Sturmian slow branch starting just below ω_A^2 ($= \omega_{s0}^2$) at $q = 0$ and approaching ω_S^2 for $q \to \infty$. For purely parallel propagation, in the limit $\epsilon \to 0$, these curves develop a kink at the cross-over point $q = q_c$ so that we should call the upper part (consisting of ω_2^2 for $0 \leq q < q_c$ and of ω_1^2 for $q_c \leq q < \infty$) 'Alfvén', and the lower part (consisting of ω_1^2 for $0 \leq q < q_c$ and of ω_2^2 for $q_c \leq q < \infty$) 'slow'.

(3) The transition to Sturmian monotonicity of the slow modes, exhibited by both Figs. 7.10(a) and (b), is crucial for the well-posedness of the ideal MHD stability problem. It guarantees that, for $\bar{\omega}^2 < 0$, *the largest growth rates are obtained for the most global* ($n = 1$) *instability*. (If this were not the case, making the plasma layer thinner by moving in the walls, would make the growth rates larger, in conflict with physical intuition.) For example, as shown by the inset of Fig. 7.10(b), the modes $n = 1$ and $n = 2$ are unstable but all the higher ones ($n \geq 3$) are stable for this particular choice of the parameters.

To systematically investigate the unstable range of parameters, one needs a general stability criterion, which is usually not a closed expression but a rather involved procedure like investigating the quadratic form of the energy (Section 6.4.4). Exceptionally, for the present case of the exponential equilibrium (7.103), an instability criterion is easily obtained from the dispersion equation (7.116). For unstable solutions ($\bar{\omega}^2 < 0$), the last coefficient (including the minus sign) should be positive:

$$\left(\tfrac{1}{2}\gamma\beta\bar{k}_{\rm eff}^2\cos^2\vartheta + \tfrac{1}{2}\gamma\beta\bar{N}_B^2\right)\cos^2\vartheta \equiv$$

$$\left\{\tfrac{1}{2}\gamma\beta(\bar{k}_0^2 + \bar{q}^2)\cos^2\vartheta + \tfrac{1}{4}\Big[(1+\beta)(\gamma\beta - \beta - 1) + \tfrac{1}{2}\gamma\beta\cos^2\vartheta\Big]\bar{\alpha}^2\right\}\cos^2\vartheta < 0. \tag{7.123}$$

This expression shows that gravitational instability is obtained when the first term in square brackets is not only negative (i.e., $\bar{N}_B^2 < 0$) but also dominates over the remaining terms proportional to $\cos^2\vartheta$: the gravitational instability drive should dominate over the stabilizing field-line bending contribution of the slow mode perturbations. Hence, one expects the worst instability for perpendicular propagation ($\vartheta = \pi/2$). On the other hand, recalling from Section 7.2.3 that the exponential atmosphere is stable in the HD limit ($\beta \to \infty$), magnetic field perturbations are apparently essential to create gravitational instability in the MHD domain. Accordingly, the whole potentially negative expression in curly brackets is multiplied by $\cos^2\vartheta$ so that, at worst, marginal stability is obtained for $\vartheta = \pi/2$. Consequently, *for this class of equilibria*, the MHD version of the Rayleigh–Taylor instability occurs in a range of near-perpendicular wave vectors $\mathbf{k}_0$, excluding the direction

Downloaded from Cambridge Books Online by IP 152.2.176.242 on Mon Apr 29 20:09:17 WEST 2013.
http://dx.doi.org/10.1017/CBO9780511616945.008
Cambridge Books Online © Cambridge University Press, 2013

$\mathbf{k}_0 \cdot \mathbf{B} = 0$ itself. This range may even include parallel propagation ($\vartheta = 0$) when $\bar{N}_B^2$ is negative enough, giving rise to the Parker instability (see below). The stabilizing slow mode contributions also vanish in the extreme limit $\beta \to 0$, opposite to HD, when the plasma becomes unstable for all $\vartheta \neq \pi/2$ and any value of $\bar{\alpha}$. We leave it to the reader to derive the expression for the growth rate for that case.

(c) Parker instability According to Parker [175], "the interstellar magnetic field in the general neighbourhood of the Sun is, on average, parallel to the plane of the Galaxy ... This galactic magnetic field must be confined by the weight of the gas (plasma) threaded by the field. This interstellar gas-field system is subject to a universal Rayleigh–Taylor instability such that the interstellar gas tends to concentrate into pockets suspended in the field. The cause of the instability may be thought of as a hydromagnetic self-attraction in the interstellar gas, which may be ten times larger than the gravitational self-attraction of the gas. It is this hydromagnetic self-attraction which produces the observed tendency of the interstellar gas to be confined in discrete clouds."

The gas, which consists of electrons, ions and neutrals, is described by means of the ideal MHD equations, so that the equations of the present section apply. The instability is investigated for motions in the vertical x-z plane only, i.e. longitudinal perturbations ($\vartheta = 0$). Parker also includes the effects of a relativistic cosmic ray particle population on the pressure of the background equilibrium, as well as on the dynamics. Neglecting the latter, we obtain from Eq. (7.123) the criterion for the Parker instability in our notation:

$$\bar{k}_{\text{eff}}^2 + \bar{N}_B^2 < 0 \quad \Rightarrow \quad \bar{k}_0^2 + \bar{q}^2 - \tfrac{1}{4}\bar{\alpha}^2 \cdot \frac{2(1+\beta)(1+\beta-\gamma\beta) - \gamma\beta}{\gamma\beta} < 0\,. \tag{7.124}$$

The growth rate of the instabilities may be obtained from Eq. (7.112) (with the minus sign). This shows the connection with the slow magneto-sonic wave which is essential for the instability since it involves dominant perturbed flows parallel to the magnetic field. Hence, 'the gas tends to drain downward along the magnetic lines of force into the lowest region along each line'.

Obviously, at this point, numerical values for the wave numbers k_0, q and for the equilibrium parameters α, β and γ have to be chosen to demonstrate the viability of the mechanism for the description of cloud formation along galactic spiral arms. We leave the subject here and refer to the original literature [175] and the review paper by Mouschovias [160] for a discussion of all the astrophysical ramifications.

(d) Interchanges and quasi-interchanges We return to the discussion of the full dispersion equation (7.116), for $\vartheta \neq 0$, since perpendicular and near-perpendicular propagation properties are of generic interest for the stability of confined plasmas

Downloaded from Cambridge Books Online by IP 152.2.176.242 on Mon Apr 29 20:09:17 WEST 2013.
http://dx.doi.org/10.1017/CBO9780511616945.008
Cambridge Books Online © Cambridge University Press, 2013

in general. Expanding the dispersion equation for $\vartheta = \pi/2 \pm \epsilon$, with $\epsilon \ll 1$, we obtain two potentially unstable solutions:

$$\bar{\omega}^2 \approx \frac{\bar{k}_0^2}{\bar{k}_{\rm eff}^2}\,\bar{N}_m^2 \qquad \text{(pure interchanges, } \vartheta = \pi/2\text{)},$$
$$\bar{\omega}^2 \approx \frac{\bar{N}_B^2}{\bar{N}_m^2}\,\bar{\omega}_S^2 = \frac{(\gamma-1)\beta - 1}{(\gamma-1)\beta + 1}\,\bar{k}_0^2 \cos^2\vartheta \qquad \text{(quasi-interchanges, } \vartheta \neq \pi/2\text{)}. \tag{7.125}$$

This reveals one of the limitations of the equilibrium with exponential dependence of the background quantities. Pure interchanges, with a maximum growth rate at $\vartheta = \pi/2$, are trivially stable since they require $\bar{N}_m^2 < 0$, which is not possible for these equilibria. However, the second branch, with maximum growth rate at $\vartheta \neq \pi/2$, may be unstable since it requires $\bar{N}_{\rm B}^2 < 0$. They have been called *gravitational quasi-interchanges* by Newcomb [165]. Both the regular and the modified Brunt–Väisäläa frequencies, $\bar{N}_B$ and $\bar{N}_m$, enter the expression for their growth rate, indicating the possibility of intricate stability transitions.

In the stability analysis of general equilibria, the crossing of these two branches of the dispersion equation plays an important role in clarifying the apparent discrepancies that occur in the stability criteria for gravitational interchanges. We defer further discussion to Section 7.5.2, when we are no longer restricted to the choice of uni-directional magnetic field and exponential equilibrium profiles.

7.4 Continuous spectrum and spectral structure

'Singularity is almost invariably a clue.'

(Bender and Orszag [23], at the beginning of their exposition of approximate solutions of linear differential equations, quoting Sherlock Holmes in *The Boscombe Valley Mystery* by Sir Arthur Conan Doyle.)

7.4.1 Singular differential equations

We have obtained important insight in the structure of the MHD spectrum for equilibria with exponential profiles, where the 'singular' frequencies determined by $N_0 = 0$ and $D_0 = 0$ are constant. However, in this manner we have evaded the most important issues of inhomogeneity in MHD, which are, in general, that these frequencies depend on the coordinate x of inhomogeneity and that the magnetic field is not uni-directional: *continuous spectrum* and *magnetic shear* are essential constituents of the MHD description of plasmas. We face these issues in this section and the next.

Downloaded from Cambridge Books Online by IP 152.2.176.242 on Mon Apr 29 20:09:17 WEST 2013.
http://dx.doi.org/10.1017/CBO9780511616945.008
Cambridge Books Online © Cambridge University Press, 2013

When a problem has been reduced to a *non-singular* ordinary second order differential equation it may be considered to have been solved, because one can always obtain the explicit answers numerically to any relevant degree of accuracy. A specific example has just been given in Section 7.3.3. Since this example actually hinges on algebraic simplification through the exponential factor, let us briefly consider how the numerical solution might proceed with a more general inhomogeneity. To that end, we write the basic differential equation (7.91) symbolically as

$$\frac{d}{dx}\left[P(x;\omega^2)\,\frac{d\xi}{dx}\right] - Q(x;\omega^2)\,\xi = 0\,, \tag{7.126}$$

where $P \equiv N/D$, and $Q \equiv -[\cdots]$ with the expression in square brackets as in Eq. (7.91). This equation is to be solved subject to the model I boundary conditions (7.93). Specifying the background equilibrium by a particular choice of the profiles $\rho(x)$, $p(x)$, $B_y(x)$ and $B_z(x)$, satisfying the equilibrium constraint (7.74) of Section 7.3.2, *and prescribing a particular value* $\omega^2 = \omega^{2(0)}$ for the unknown eigenfrequency, the functions $P(x;\omega^2)$ and $Q(x;\omega^2)$ are completely determined. One may then solve Eq. (7.126) by means of a standard numerical library routine, starting from the left boundary condition $\xi(x_1) = 0$ (where the derivative $\xi'(x_1)$ may be prescribed arbitrarily since the differential equation is homogeneous and linear), and stepping towards the right end of the interval $x_1 \le x \le x_2$. Of course, arriving there, the right boundary condition $\xi(x_2) = 0$ will not be satisfied in general. This necessitates the construction of an algorithm for the choice of a new value $\omega^2 = \omega^{2(1)}$ that will bring the solution closer to satisfying that boundary condition in the next iteration. This part of the problem is important for the determination of the eigenvalue, but it does not present any difficulty. The point is that an extremely effective algorithm exists, based on shooting (Section 7.5.1) and the oscillation theorem (Section 7.4.3), which is valid *as long as the ODE is non-singular*. The essential problem left is, therefore, a proper treatment of the singularities of the basic differential equation. Hence, we now resume our discussion of the singularities that was started in Section 7.3.2(c).

In contrast to the non-singular integration procedure just sketched, where the boundary conditions determine the solution on the entire interval $[x_1, x_2]$, a singularity $\omega^2 = \omega_A^2(x_0)$ or $\omega^2 = \omega_S^2(x_0)$ at a point $x = x_0$ splits the interval into two parts that become independent, in a sense to be discussed. Hence, there is no way to produce the singular problem from the non-singular one by a small perturbation. There either is a singular point or there is not, and the presence of such a point changes the analysis completely. For example, in marginal stability theory (where $\omega^2 \equiv 0$, so that the mentioned singularities become zeros of the Alfvén frequency $\omega_A = F/\sqrt{\rho}$ with F defined in Eq. (7.97)) there is always a distinct difference

Downloaded from Cambridge Books Online by IP 152.2.176.242 on Mon Apr 29 20:09:17 WEST 2013.
http://dx.doi.org/10.1017/CBO9780511616945.008
Cambridge Books Online © Cambridge University Press, 2013

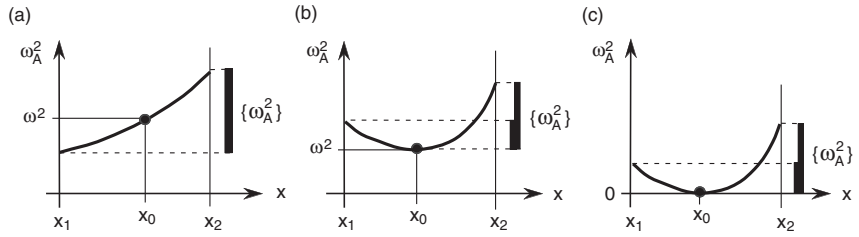

Fig. 7.11. Normal dependence of $\omega_A^2(x)$ determines: (a) continuous spectrum singularity; (b) potential cluster point for stable waves; (c) potential cluster point at marginal stability.

between configurations with magnetic shear ($F' \neq 0$) and without ($F' = 0$), where the limit $F' \to 0$ produces complicated boundary layers. We will analyse this in Section 7.5.

Before we delve into the singularity theory of Eq. (7.126), an explicit example may illustrate the different kinds of singularities encountered in MHD of inhomogeneous plasmas. For that purpose, we concentrate on the Alfvén singularity. In Fig. 7.11 three generic cases are depicted for the distribution of $\omega_A^2(x)$, where the slow singularities $\omega_S^2(x)$ (not shown) may be assumed to be well separated from the Alfvén ones (cases (a) and (b)), but they necessarily coalesce at the marginal point (case (c)).

(a) If $\omega_A^2(x)$ is monotonic, any choice of ω^2 in the range $\omega_A^2(x_1) \leq \omega^2 \leq \omega_A^2(x_2)$ will lead to a singular point $x_1 \leq x_0 \leq x_2$ where the Alfvén factor of the function P may be expanded as follows:

$$\omega^2 - \omega_A^2 \approx -(\omega_A^{2\prime})_0 (x - x_0) \quad \Rightarrow \quad P \sim x - x_0 \,. \tag{7.127}$$

This range will determine the *continuous spectrum* $\{\omega_A^2\}$ of Alfvén modes, and similarly for the frequency range $\{\omega_S^2\}$ of the slow modes, as will be shown in Section 7.4.2.

(b) If $\omega_A^2(x)$ is not monotonic, the continuous spectrum develops a maximum or minimum at some point x_0 where it starts to fold over onto itself. Choosing ω^2 to correspond to that extremum permits expansion of the Alfvén factor as

$$\omega^2 - \omega_A^2 \approx -\tfrac{1}{2}(\omega_A^{2\prime\prime})_0 (x - x_0)^2 \quad \Rightarrow \quad P \sim (x - x_0)^2. \tag{7.128}$$

The value $\omega^2 = \omega_A^2(x_0)$ corresponds to an internal edge of the continuous spectrum which may become a *cluster point* of the discrete spectrum, depending on further conditions, as will be discussed in Section 7.4.4.

(c) For marginal stability ($\omega^2 = 0$), such candidate cluster points always occur in sheared magnetic fields at an *interchange point* $F^2(x_0) = 0$, where both the

Downloaded from Cambridge Books Online by IP 152.2.176.242 on Mon Apr 29 20:09:18 WEST 2013.
http://dx.doi.org/10.1017/CBO9780511616945.008
Cambridge Books Online © Cambridge University Press, 2013

Alfvén and the slow continuum reach the origin: $\omega_S^2 \equiv \gamma p(\gamma p + B^2)^{-1}\omega_A^2 = 0$. Since, according to Eq. (7.96), also $\omega_{s0}^2 \approx \omega_S^2$ there, the factor ω_S^2 of the numerator $N(\omega^2 = 0)$ is cancelled by the leading order of the factor ω_{s0}^2 of the denominator $D(\omega^2 = 0)$ so that the Alfvén factor determines the behaviour at the singularity:

$$-\omega_A^2 \approx -\tfrac{1}{2}({\omega_A^2}'')_0\,(x - x_0)^2 = -({\omega_A}')_0^2\,(x - x_0)^2 \quad \Rightarrow \quad P \sim (x - x_0)^2\,. \tag{7.129}$$

By means of this expansion, the conditions for *local interchange stability* may be derived, as will be demonstrated in Section 7.5.2.

We are now prepared to appreciate the physical significance of the different steps in the following mathematical analysis of Eq. (7.126).

Singularity of this differential equation is best discussed in terms of the standard form used in classical texts (i.e. dating from the pre-electronic computing era, e.g. Ince [115]) as well as in modern ones (e.g. Bender and Orszag [23]) on linear differential equations:

$$\xi'' + \frac{P'}{P}\,\xi' - \frac{Q}{P}\,\xi = 0\,. \tag{7.130}$$

This equation is non-singular if the two functions P'/P and Q/P are analytic on the whole domain of interest, i.e. in a finite region of the complex z-plane containing the interval $x_1 \le x \le x_2$ of the real axis (where the prime is redefined as differentiation with respect to z). Theoretically, the solution may be carried from (ordinary) point to (ordinary) point by Taylor series expansion with a radius of convergence determined by the distance to the nearest singularity of the two mentioned functions. Hence, such singularities interfere with the numerical procedure described earlier. Obviously, the zeros of

$$N \equiv \rho(b^2 + c^2)\Big[\omega^2 - \omega_A^2(x)\Big]\Big[\omega^2 - \omega_S^2(x)\Big] \sim (x - x_0)^l\,, \quad (l = 1 \text{ or } l = 2)\,, \tag{7.131}$$

produce singularities of the kind $P'/P \sim z^{-1}$ and $Q/P \sim z^{-l}$. Here, z is the complex continuation of the real variable $x - x_0$, which is the distance to a point x_0 where either ω_A^2 or ω_S^2 coincides with the eigenvalue parameter ω^2. We have seen above that it is sufficient for virtually all cases of interest to consider $l = 1$ and $l = 2$ only, i.e. *regular singularities*. In the neighbourhood of such singularities, the differential equation may be written as

$$\xi'' + \frac{1}{z}\,p(z)\,\xi' - \frac{1}{z^2}\,q(z)\,\xi = 0\,, \tag{7.132}$$

Downloaded from Cambridge Books Online by IP 152.2.176.242 on Mon Apr 29 20:09:19 WEST 2013.
http://dx.doi.org/10.1017/CBO9780511616945.008
Cambridge Books Online © Cambridge University Press, 2013

where $p(z)$ and $q(z)$ are analytic functions with the following Taylor expansion:

$$\begin{cases} p(z) \equiv z\,\dfrac{P'}{P} = p_0 + p_1 z + \cdots \\ q(z) \equiv z^2\,\dfrac{Q}{P} = q_0 + q_1 z + \cdots \end{cases}, \quad \text{where} \begin{cases} p_0 = 1\,,\ q_0 = 0 \ \ (l = 1) \\ p_0 = 2\,,\ q_0 \neq 0 \ \ (l = 2). \end{cases} \tag{7.133}$$

The behaviour of the solutions in the neighbourhood of such points may be obtained by means of the *Frobenius method of expansion*.

The Frobenius expansion about a regular singularity assumes

$$\xi = z^{\nu} \sum_{n=0}^{\infty} a_n z^n\,, \tag{7.134}$$

where, in general, the index ν is not an integer and may even be complex. The values of ν and the coefficients a_n are obtained by substituting the expansion into the differential equation (7.132):

$$\sum_{n=0}^{\infty} (\nu+n)(\nu+n-1) a_n z^{\nu+n-2} + (p_0 + p_1 z + \cdots) \sum_{n=0}^{\infty} (\nu+n) a_n z^{\nu+n-2} - (q_0 + q_1 z + \cdots) \sum_{n=0}^{\infty} a_n z^{\nu+n-2} = 0\,. \tag{7.135}$$

Balancing the different powers yields the following sequence of equalities:

$$\begin{aligned} z^{\nu-2} &: \ [\nu^2 + (p_0 - 1)\nu - q_0]\, a_0 = 0\,, \\ z^{\nu-1} &: \ [(\nu+1)\nu + p_0(\nu+1) - q_0]\, a_1 = (-\nu p_1 + q_1)\, a_0\,, \quad \text{etc.} \end{aligned} \tag{7.136}$$

Hence, in general, the two solutions ξ_1 and ξ_2 start off with a term $a_0 z^{\nu_{1,2}}$, where a_0 is arbitrary and the indices $\nu_{1,2}$ are the solutions of the *indicial equation*, obtained by putting the factor in square brackets of (7.136)(a) equal to zero. The coefficients a_n $(n \geq 1)$ follow by recursion from the relations (7.136)(b), etc. The solutions of the indicial equation, and hence the solutions ξ_1 and ξ_2 themselves, are qualitatively different for the case (a) and the cases (b), (c) illustrated in Fig. 7.11:

$$l = 1 \ \text{(continuous spectrum)}: \qquad \nu_1 = \nu_2 = 0\,, \tag{7.137}$$

$$l = 2 \ \text{(cluster points)}: \qquad \nu_{1,2} = -\tfrac{1}{2} \pm \tfrac{1}{2}\sqrt{1 + 4q_0}\,. \tag{7.138}$$

For the cluster point analysis ($l = 2$), this is virtually sufficient information. It will

Downloaded from Cambridge Books Online by IP 152.2.176.242 on Mon Apr 29 20:09:19 WEST 2013.
http://dx.doi.org/10.1017/CBO9780511616945.008
Cambridge Books Online © Cambridge University Press, 2013

be completed in Section 7.4.4 for the waves (case (b)) and in Section 7.5.2 for the marginal states (case (c)). For the analysis of the continuous spectrum ($l = 1$), however, we are not done at all since we have just obtained one value ($\nu = 0$) corresponding to an analytic function (called the 'small' solutions) which obviously does not exhibit singular behaviour. The 'large' solution, revealing the singularity, is to be obtained yet.

To complete the analysis for the first case, with equal indices $\nu_1 = \nu_2 = 0$, the quoted literature (Ince [115], p. 397, Bender and Orszag [23], p. 73) shows how the 'large' solution is obtained. This involves the special trick of writing the small solution obtained as a function of ν, not substituting the value $\nu_1 = 0$ yet, differentiating it with respect to ν, and then inserting the value $\nu = 0$. This produces a second, independent, solution containing a logarithmic contribution, since

$$\frac{\partial}{\partial \nu}(z^\nu) = \frac{\partial}{\partial \nu}\left(\mathrm{e}^{\nu \ln z}\right) = z^\nu \ln z \;\rightarrow\; \ln z \quad \text{for} \quad \nu \rightarrow 0\,. \tag{7.139}$$

Hence, in the neighbourhood of the regular singular point $z = x - x_0 = 0$, two solutions are obtained:

$$\begin{aligned} &\xi_1 = u(z)\,, && u = u_0 + u_1 z + \cdots\,, && \text{('small' solution)}\,, \\ &\xi_2 = u(z)\,\ln z + v(z)\,, && v = v_0 + v_1 z + \cdots\,, && \text{('large' solution)}\,, \end{aligned} \tag{7.140}$$

where the explicit form of the coefficients u_n and v_n is much less important than the appearance of the logarithmic factor. The latter introduces a branch point at $z = 0$ where a decision is to be taken on how to continue the solution past this point. This choice depends on the physical context in which the singularity is encountered.

In the solution of the initial value problem by means of the Laplace transform, as sketched in Section 6.3.2 and elaborated in Chapter 10, the parameter ω is assumed to be complex and the continuation is obtained by deforming the Laplace contour around the singularity. This procedure is completely analogous to that exploited by Landau in his solution of the initial value problem for the Vlasov equation (Section 2.3.3), where the velocity variable v of the Vlasov problem corresponds to the spatial coordinate x of the MHD problem.

In the determination of the spectrum of ideal MHD, since there is no dissipation, ω^2 remains real, so that we should consider the solutions (7.140) along the real axis, exploiting the principal value of $\ln z$, i.e. $\ln|x - x_0|$. The logarithmic singularity at $x = x_0$ then divides the real x-interval in two parts such that the solution ξ obtains just enough additional freedom (compared to that at an ordinary point) to satisfy the boundary conditions for any value of ω^2. This produces the continuous spectrum, as will be demonstrated in the next section.

Downloaded from Cambridge Books Online by IP 152.2.176.242 on Mon Apr 29 20:09:19 WEST 2013.
http://dx.doi.org/10.1017/CBO9780511616945.008
Cambridge Books Online © Cambridge University Press, 2013

▷ **Apparent singularities** $D = 0$ singularities occur when either one of the factors $\omega^2 - \omega_{s0}^2$ or $\omega^2 - \omega_{f0}^2$ vanishes on the interval:

$$D \equiv \Big[\omega^2 - \omega_{s0}^2(x)\Big]\Big[\omega^2 - \omega_{f0}^2(x)\Big] \sim x - x_0 \quad \Rightarrow \; P \sim (x - x_0)^{-1}, \; Q \sim (x - x_0)^{-2}. \tag{7.141}$$

This also produces singularities of the kind $P'/P \sim z^{-1}$ and $Q/P \sim z^{-1}$. The coefficients of the analytic functions $p(z)$ and $q(z)$ then yield solutions of the indicial equation with an integer difference between the indices:

$$p_0 = -1\,, \; q_0 = 0 \quad \Rightarrow \quad \nu_1 = 2\,, \; \nu_2 = 0\,. \tag{7.142}$$

This implies that only one 'small' solution $\sim z^2$ is obtained, whereas the other one again contains a logarithmic contribution, unless the coefficients of the expansion of $p(z)$ and $q(z)$ possess the very special property

$$(p_1 - q_1)q_1 - (p_0 - q_0)q_2 = 0\,. \tag{7.143}$$

In that case, none of the solutions is singular; see Ince [115], p. 404. The MHD wave equation (7.91) turns out to have precisely that property! This follows from the way in which the expression D appears in the functions P and Q:

$$P \equiv \frac{N}{D}\,, \qquad Q \equiv -U - \frac{V}{D} - \left(\frac{W}{D}\right)'\,, \tag{7.144}$$

where the explicit expressions for U, V, and W can be read off from Eq. (7.91). These coefficients are related by

$$W^2 + NV = \rho^2 \hat{g}^2 (\omega^2 - f^2 b^2)^2 \, D \to 0 \quad \text{as } x \to x_0\,. \tag{7.145}$$

Translated in terms of the functions p and q, this produces the equality (7.143). Consequently, *the $D = 0$ singularities are apparent*. ◁

7.4.2 Alfvén and slow continua

For simplicity, we choose the equilibrium quantities such that the singular frequency functions $\omega_A^2(x)$ and $\omega_S^2(x)$ are well separated and monotonically increasing, as in Fig. 7.11(a). We will prove that the collection of frequencies $\omega^2 \in \{\omega_A^2(x) | \, x_1 \le x \le x_2\}$ and $\omega^2 \in \{\omega_S^2(x) | \, x_1 \le x \le x_2\}$ constitutes the continuous spectrum, i.e. the set of *improper eigenvalues* of the MHD force operator $\rho^{-1}\mathbf{F}$, with associated non-square integrable 'eigenfunctions'.

We concentrate again on the Alfvén singularities $\omega^2 \in \{\omega_A^2(x)\}$, noting that the analysis for the slow singularities $\omega^2 \in \{\omega_S^2(x)\}$, lying in a narrow band below the Alfvén ones, is completely analogous. For a given value of $\omega^2 = \omega_0^2$ from this set, the ODE (7.91) is singular ($N = 0$) at the position $x = x_0$ where $\omega_A^2(x_0) = \omega_0^2$, as shown once more in Fig. 7.12(a). The monotonically increasing function $\omega_A^2 = \omega_A^2(x)$ may be inverted to give a monotonically increasing function $x_A = x_A(\omega^2)$, as illustrated in Fig. 7.12(b). In this manner, the position x

Downloaded from Cambridge Books Online by IP 152.2.176.242 on Mon Apr 29 20:09:19 WEST 2013.
http://dx.doi.org/10.1017/CBO9780511616945.008
Cambridge Books Online © Cambridge University Press, 2013

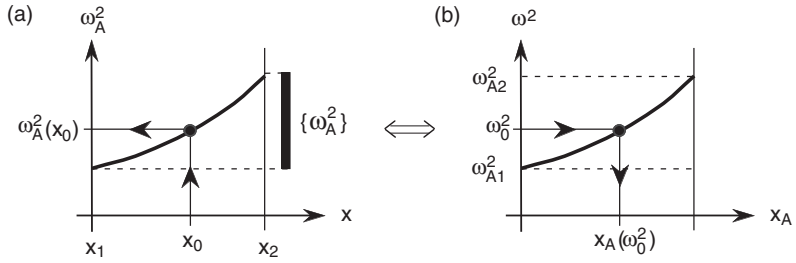

Fig. 7.12. Inversion of the Alfvén frequency function: (a) $\omega_A^2 = \omega_A^2(x)$; (b) $x_A = x_A(\omega^2)$.

of the singularity becomes a function of ω^2. As we have seen in Section 7.4.1, expansion about the singularity gives the dominant coefficient of the differential equation:

$$\omega^2 - \omega_A^2(x) \approx -(\omega_A^{2\prime})_0(x - x_0) = -(\omega_A^{2\prime})_0 s\,, \tag{7.146}$$

where, since everything is real now, the complex variable z is replaced by the real variable s, which is the distance to the singularity:

$$s \equiv x - x_0 = x - x_A(\omega^2)\,. \tag{7.147}$$

Instead of the complex expressions (7.140), we now obtain real independent solutions of the form

$$\begin{cases} \xi_1 = u(s;\omega^2) & \text{('small' solution)}\,, \\ \xi_2 = u(s;\omega^2)\ln|s| + v(s;\omega^2) & \text{('large' solution)}\,, \end{cases} \tag{7.148}$$

to the right ($s > 0$) as well as to the left ($s < 0$) of the singularity.

The most important consequence of the singularities $N = 0$ of the differential equation (7.91) is that certain jumps of the solutions are permitted, so that satisfaction of the boundary conditions (7.93) is always possible for ω^2 in the singular domain. To prove this, we exploit the series expansions just obtained. Because of the assumed monotonicity of $\omega_A^2(x)$, the interval (x_1, x_2) contains only one singular point for a fixed value of ω^2 so that the general solution may be written as

$$\xi = \Big[A_1 u + C_1(u\ln|s| + v)\Big]H(-s) + \Big[A_2 u + C_2(u\ln|s| + v)\Big]H(s)\,, \tag{7.149}$$

where $H(s)$ is the Heaviside step function (defined as $H \equiv 0$ for $s < 0$ and $H \equiv 1$ for $s > 0$), and we have to determine the values of A_1, C_1, A_2, and C_2. Of course, for a non-singular second order differential equation the solution should be continuous, so that $A_1 = A_2$ and $C_1 = C_2$. We will now prove that *the small*

Downloaded from Cambridge Books Online by IP 152.2.176.242 on Mon Apr 29 20:09:20 WEST 2013.
http://dx.doi.org/10.1017/CBO9780511616945.008
Cambridge Books Online © Cambridge University Press, 2013

solution may jump whereas the large solution has to be continuous: $A_1 \neq A_2$, $C_1 = C_2$.

▷ **Proof** Write the original differential equation (7.91) as

$$(P\xi')' - Q\xi = 0\,, \tag{7.150}$$

where

$$P \approx P_1 s + \cdots\,, \qquad Q \approx Q_0 + \cdots\,.$$

Substitution of a 'small' solution $\xi = uH(s)$ leads to the following expressions, successively:

$$\begin{aligned}
\xi' &= u'H(s) + u\delta(s)\,,\\
P\xi' &= Pu'H(s) + Pu\delta(s) = Pu'H(s)\,,\\
(P\xi')' &= (Pu')'H(s) + Pu'\delta(s) = (Pu')'H(s)\,,\\
(P\xi')' - Q\xi &= \big[(Pu')' - Qu\big]H(s) = 0\,,
\end{aligned}$$

by virtue of the fact that $u(s)$ is a solution of Eq. (7.150), and properties such as $H'(s) = \delta(s)$ and $s\delta(s) = 0$. Consequently, $A_1 uH(-s)$ is a solution of Eq. (7.150) but, likewise, $A_2 uH(s)$ is also a solution, so that the small solutions left and right are totally unrelated: $A_1 \neq A_2$. Performing a similar analysis for the large solution, one finds that the term $u \ln|s| H(s)$ produces a δ-function contribution that does not vanish, so that $C_1 = C_2$, QED. ◁

Consequently, the general solution to Eq. (7.150) may be written as

$$\xi = A_1 u\, H(-x + x_A) + A_2 u\, H(x - x_A) + C\,[u \ln|x - x_A| + v]\,. \tag{7.151}$$

Due to the fact that we have now three (rather than the usual two) constants available, the two boundary conditions $\xi(x_1) = 0$ and $\xi(x_2) = 0$ may always be satisfied for $\omega^2 \in \omega_A^2(x)$, i.e. when there is a singular point on the interval (x_1, x_2). By imposing these two boundary conditions, the two constants A_1 and A_2 may be eliminated so that *the improper eigenfunctions for an Alfvén continuum mode* become:

$$\begin{aligned}
\xi_A(x;\omega^2) = C(\omega^2)\Bigg\{&\left[\ln\frac{x - x_A(\omega^2)}{x_1 - x_A(\omega^2)} - \frac{v_1(\omega^2)}{u_1(\omega^2)}\right] u(x;\omega^2) H(-x + x_A(\omega^2))\\
&+ \left[\ln\frac{x - x_A(\omega^2)}{x_2 - x_A(\omega^2)} - \frac{v_2(\omega^2)}{u_2(\omega^2)}\right] u(x;\omega^2) H(x - x_A(\omega^2)) + v(x;\omega^2)\Bigg\},
\end{aligned} \tag{7.152}$$

where

$$u(x;\omega^2) \equiv u(x - x_A(\omega^2))\,, \qquad u_1(\omega^2) \equiv u(x_1;\omega^2)\,, \quad \text{etc.}$$

Downloaded from Cambridge Books Online by IP 152.2.176.242 on Mon Apr 29 20:09:20 WEST 2013.
http://dx.doi.org/10.1017/CBO9780511616945.008
Cambridge Books Online © Cambridge University Press, 2013

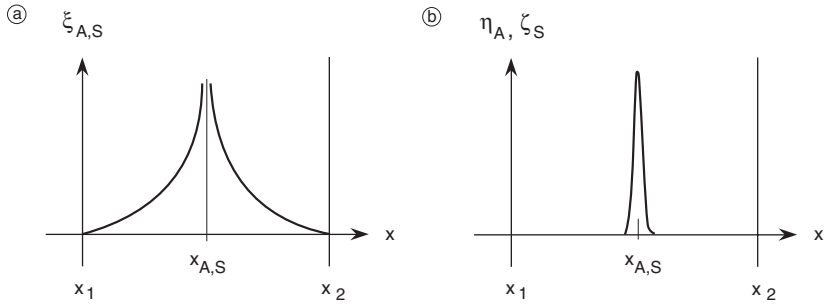

Fig. 7.13. Schematic representation of the (a) normal and (b) tangential components of the improper Alfvén and slow continuum 'eigenfunctions'.

The factor $C(\omega^2)$ may be fixed by 'normalizing' the eigenfunctions:

$$\langle\, \boldsymbol{\xi}_A(x;\omega^2), \boldsymbol{\xi}_A(x;\widetilde{\omega}^2)\,\rangle = \delta(\omega^2 - \widetilde{\omega}^2)\,. \tag{7.153}$$

Similar expressions may be derived for the improper eigenfunctions of the slow continuum modes. Therefore, 'solutions' have been obtained which satisfy the boundary conditions (see Fig. 7.13(a)) for any $\omega^2 \in \{\omega_A^2(x)\}$ and $\omega^2 \in \{\omega_S^2(x)\}$, QED. The continuous ranges of frequencies $[\,\omega^2_{A\,\min}, \omega^2_{A\,\max}\,]$ and $[\,\omega^2_{S\,\min}, \omega^2_{S\,\max}\,]$ are called *the Alfvén continuum* and *the slow magneto-sonic continuum*, respectively.

This appears to establish the existence of two continuous spectra, but the most characteristic part of the eigenfunctions is not yet discussed. Actually, if we restrict the analysis to the normal component of that function, we cannot even prove that we have 'improper' eigenfunctions because the singularities $\ln|s|$ and $H(s)$ are square integrable. The dominant, non-square integrable, part of the 'improper' eigenfunction resides in the tangential components η and ζ, given by Eqs. (7.90), which involve the derivative $\xi' \gg \xi/a$. From Eq. (7.151), this derivative produces a $1/(x - x_A)$ singularity and a δ-function:

$$\begin{aligned}
\xi'_A &= C\left\{\left[\mathcal{P}\,\frac{1}{x - x_A(\omega^2)} - \frac{A_1 - A_2}{C}\,\delta(x - x_A(\omega^2))\right]u\right. \\
&\quad \left. + \left[\frac{A_1}{C}H(-x + x_A(\omega^2)) + \frac{A_2}{C}H(x - x_A(\omega^2)) + \ln|x - x_A(\omega^2)|\right]u' + v'\right\} \\
&\approx C(\omega^2)\left\{\mathcal{P}\,\frac{1}{x - x_A(\omega^2)} + \mu(\omega^2)\,\delta(x - x_A(\omega^2))\right\},
\end{aligned} \tag{7.154}$$

Downloaded from Cambridge Books Online by IP 152.2.176.242 on Mon Apr 29 20:09:20 WEST 2013.
http://dx.doi.org/10.1017/CBO9780511616945.008
Cambridge Books Online © Cambridge University Press, 2013

where $\mathcal{P}$ indicates that the principal part is to be taken when integrating this function, and $\mu(\omega^2)$ is a function involving the boundary data of u and v:

$$\mu \equiv \frac{-A_1 + A_2}{C} = \ln \left| \frac{x_2 - x_A(\omega^2)}{x_1 - x_A(\omega^2)} \right| - \frac{v_1(\omega^2)}{u_1(\omega^2)} + \frac{v_2(\omega^2)}{u_2(\omega^2)} \,. \tag{7.155}$$

For the Alfvén continuum modes, the tangential component η perpendicular to the magnetic field dominates (since ξ_A' is multiplied by $\omega^2 - \omega_A^2$ in the expression for ζ):

$$\eta_A \approx \frac{g(b^2 + c^2)(\omega_A^2 - \omega_S^2)}{D(\omega_A^2)} \xi_A' = -\frac{1}{g} \xi_A' \gg \xi_A \sim \zeta_A \quad \text{for} \quad \omega^2 \to \omega_A^2 \,. \tag{7.156}$$

Similarly, for the slow continuum modes, the component ζ parallel to the magnetic field dominates (since ξ_S' is multiplied by $\omega^2 - \omega_S^2$ in the expression for η):

$$\zeta_S \approx \frac{f c^2(\omega_S^2 - \omega_A^2)}{D(\omega_S^2)} \xi_S' = -\frac{1}{f} \frac{b^2 + c^2}{c^2} \xi_S' \gg \xi_S \sim \eta_S \quad \text{for} \quad \omega^2 \to \omega_S^2 \,, \tag{7.157}$$

where the formal expression for ξ_S' is obtained from Eq. (7.154) by replacing the subscripts A by S. The tangential components of these 'improper' eigenfunctions are represented schematically in Fig. 7.13(b).

In conclusion: the continuum modes are characterized by *a non-square integrable tangential component perpendicular to the magnetic field for the Alfvén modes* and *a non-square integrable parallel tangential component for the slow modes*. This shows the extreme anisotropy of ideal MHD waves as regards motion inside and across magnetic surfaces. This is a quite general property which remains true for other plasma geometries, like cylindrical and toroidal ones.

We appear to have obtained the generalization of the essential spectrum, represented by the three cluster point singularities for the simpler inhomogeneous plasmas discussed in Section 7.3.3. What about the *fast magneto-sonic singularities* in the high frequency limit? In that limit, as we will show below, ξ' also blows up but the normal component itself still dominates over the tangential components:

$$\xi_F' \gg \xi_F \gg \eta_F \sim \zeta_F \quad \text{for} \quad \omega^2 \to \omega_F^2 \equiv \infty \,. \tag{7.158}$$

Hence, the three expressions (7.156)–(7.158) for the slow and Alfvén continuum modes and the fast cluster modes together establish the generalization for inhomogeneous plasmas of the orthogonality property (5.63) and of the asymptotic properties (5.88) for the three MHD waves that were introduced in Chapter 5.

Downloaded from Cambridge Books Online by IP 152.2.176.242 on Mon Apr 29 20:09:20 WEST 2013.
http://dx.doi.org/10.1017/CBO9780511616945.008
Cambridge Books Online © Cambridge University Press, 2013

▷ **Fast magneto-sonic cluster point singularities** For large ω^2, the derivatives with respect to x also become large, so that the differential equation for ξ reduces to

$$\xi'' + \frac{\omega^2}{b^2 + c^2}\,\xi = 0\,. \tag{7.159}$$

The solution of this equation may be obtained by means of WKB analysis; see e.g. Bender and Orszag [23], p. 484. The leading order solution reads:

$$\xi \approx C(b^2 + c^2)^{1/4} \sin\left[\omega_n \int_{x_1}^{x} (b^2 + c^2)^{-1/2}\, dx\right], \qquad \omega_n \approx \frac{n\pi}{\displaystyle\int_{x_1}^{x_2} (b^2 + c^2)^{-1/2}\, dx}\,. \tag{7.160}$$

Although the sequence (7.160) contains functions of finite norm, it does not converge to an element of Hilbert space for $n \to \infty$ (see Section 6.3.1). Hence, the fast cluster point $\omega_F^2 \equiv \lim_{n\to\infty} \omega_n^2 = \infty$ belongs to the continuous or essential spectrum. From these expressions, the singular behaviour (7.158) of the fast magnetosonic modes follows directly. ◁

▷ **Historical note** It is clear now that the proper description of the singularities of the MHD wave equation is crucial for the theory of inhomogeneous plasmas. The correct picture gradually evolved, mostly from the analysis of the analogous problem in cylinder geometry with various simplifying assumptions. The presence of a continuous spectrum of Alfvén waves in MHD was pointed out by Uberoi [233], who also drew attention to the analogy with the problem of electrostatic oscillations in inhomogeneous cold plasmas (another fluid model). The latter was analysed by Barston [16] by means of singular ('improper') normal modes, like the Van Kampen modes [237] in the Vlasov description of plasmas, and by Sedláček [206] by means of the Laplace transform of the initial value problem, like in the celebrated Landau solution of the damping [136]. All this made it clear that these kinds of singularities are not restricted to the microscopic velocity space details of a kinetic description of plasmas, but also occur in fluid descriptions when the plasma is inhomogeneous in ordinary space. (Of course, always with the caveat, also made in Section 7.2.4 on the analogy with quantum mechanical spectral theory, that the analogy is through the mathematics of linear operators, not necessarily through the physics.) Accordingly, the possibility of dissipationless damping of Alfvén waves was pointed out by Tataronis and Grossmann [225], and the complementary theory of heating by Alfvén waves was developed by Chen and Hasegawa [54]. From there, applications to laboratory and astrophysical plasmas multiplied. These topics will be discussed in Chapters 10 and 11. In the meanwhile, Grad [99] had put the subject, including stability, in the context of MHD spectral theory, pointing out the presence of four types of singularities (for $N = 0$ and $D = 0$) and, unfortunately, associating a continuous spectrum with each of them. The mistake concerning the $D = 0$ singularities was pointed out immediately by Appert, Gruber and Vaclavik [9] (by means of the system of first order differential equations discussed in Section 7.3.2), but Grad maintained that this was insufficient proof since a full construction of the resolvent operator (appearing in the solution of the initial value problem; see Section 6.3) would be required. Such a proof was given by Goedbloed in a memorandum, that was only published 24 years later [85] when the mistake was repeated by other

Downloaded from Cambridge Books Online by IP 152.2.176.242 on Mon Apr 29 20:09:20 WEST 2013.
http://dx.doi.org/10.1017/CBO9780511616945.008
Cambridge Books Online © Cambridge University Press, 2013

authors. Since the form of the resolvent operator is another manifestation of the consistency of MHD spectral theory, it is reproduced in Section 10.2. ◁

7.4.3 Oscillation theorems

In Section 7.3.1, we have shown that the sequence of inequalities (7.70) already exhibits the central position of the essential spectrum for homogeneous plasmas, where it just consists of the single frequencies ω_S^2, ω_A^2, and ω_F^2. In the MHD wave equation (7.91) for inhomogeneous plasmas, these frequencies returned in the form of the *genuine singularities* $\omega_S^2(x)$ and $\omega_A^2(x)$, which give rise to continuous spectra consisting of their values on the entire plasma interval $x_1 \le x \le x_2$. In addition, certain *apparent singularities* $\omega_{s0}^2(x)$ and $\omega_{f0}^2(x)$ turned up, which could be proved not to give rise to logarithmic contributions in the normal component, nor to any non-square integrable contributions in the tangential components, so that they do not represent continuous spectra. In this section, we will get to appreciate the positive role they play in the determination of the spectral structure. For inhomogeneous plasmas, similar to the inequalities (7.70) (of course, omitting the discrete eigenvalues ω_s^2, ω_a^2, ω_f^2 since they are unknown now), one easily demonstrates that the mentioned frequencies are well ordered at each position x of the plasma slab:

$$0 \le \omega_S^2(x) \le \omega_{s0}^2(x) \le \omega_A^2(x) \le \omega_{f0}^2(x) \le \omega_F^2 = \infty\,. \tag{7.161}$$

Hence, for a weakly inhomogeneous plasma, or for a thin slice of the plasma not containing points $F = 0$ (since ω_S, ω_{s0}, and ω_A coalesce there), the values of the frequencies (7.161) on the interval $x_1 \le x \le x_2$ might be distributed along the real ω^2-axis as schematically illustrated in Fig. 7.14. In the present section, we wish to determine how the empty spaces of this diagram will be filled up (or not) by the discrete spectrum.

(a) Sturm's theorems To do that, we need to study the qualitative behaviour of the eigenfunctions ξ of the differential equation (7.91), subject to the boundary conditions (7.93), as a function of the eigenvalue parameter ω^2. The kind of qualitative behaviour we envision is exemplified by the classical *Sturm–Liouville system* (see, e.g. Morse and Feshbach [159], p. 719) which is described by the non-singular

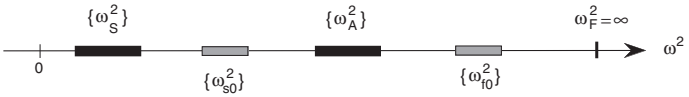

Fig. 7.14. Schematic representation of the ranges of the genuine (black) and apparent (grey) singularities of the MHD spectral equation for a weakly inhomogeneous plasma.

Downloaded from Cambridge Books Online by IP 152.2.176.242 on Mon Apr 29 20:09:21 WEST 2013.
http://dx.doi.org/10.1017/CBO9780511616945.008
Cambridge Books Online © Cambridge University Press, 2013

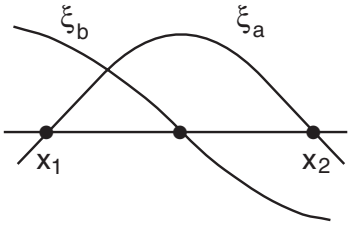

Fig. 7.15. Sturm's separation theorem.

second order differential equation

$$(P\xi')' - (Q - \lambda R)\,\xi = 0\,, \tag{7.162}$$

where λ is the eigenvalue parameter, P, Q and R are functions of x, with $P > 0$ and $R > 0$.

Let $\xi^{(1)}$ and $\xi^{(2)}$ be two linearly independent solutions of Eq. (7.162) for a fixed value of λ. Denote the two linear combinations of these two solutions by

$$\xi_a = a_1\xi^{(1)} + a_2\xi^{(2)}\,, \qquad \xi_b = b_1\xi^{(1)} + b_2\xi^{(2)}\,. \tag{7.163}$$

If $b_2/b_1 \neq a_2/a_1$, these solutions are linearly independent, i.e. the Wronski determinant $\xi_a\xi_b' - \xi_a'\xi_b \neq 0$ on the interval considered. *Sturm's separation theorem* states that the zeros of these solutions separate each other: *if x_1 and x_2 are consecutive zeros of ξ_a, then ξ_b vanishes once in the open interval* (x_1, x_2) (Ince [115], p. 223; see Fig. 7.15). (Temporarily, we use x_1 and x_2 to indicate a sub-interval of the complete interval.)

Proof Suppose ξ_b does not vanish on (x_1, x_2). Then, x_1 and x_2 are consecutive zeros of the finite function ξ_a/ξ_b. Hence, $d(\xi_a/\xi_b)/dx$ must vanish at least once on the interval. However,

$$\frac{d}{dx}\left(\frac{\xi_a}{\xi_b}\right) = \frac{\xi_a\xi_b' - \xi_a'\xi_b}{\xi_b^2} \tag{7.164}$$

cannot vanish because that would imply that the Wronski determinant vanishes somewhere. This contradiction proves that ξ_b must vanish at least once. It cannot vanish more than once since then we could interchange the roles of ξ_a and ξ_b and again get a contradiction. Hence, ξ_b vanishes once, and only once; QED.

As far as the oscillatory properties of Eq. (7.162) are concerned, one could say that all solutions oscillate equally fast if λ is kept fixed. Considering solutions of Eq. (7.162) for different values of λ, one may compare their oscillatory behaviour by means of *Sturm's fundamental oscillation theorem* stating the following. *If x_1 and x_2 are two consecutive zeros of the function ξ_1 satisfying*

$$(P\xi_1')' - (Q - \lambda_1 R)\,\xi_1 = 0\,, \tag{7.165}$$

Downloaded from Cambridge Books Online by IP 152.2.176.242 on Mon Apr 29 20:09:21 WEST 2013.
http://dx.doi.org/10.1017/CBO9780511616945.008
Cambridge Books Online © Cambridge University Press, 2013

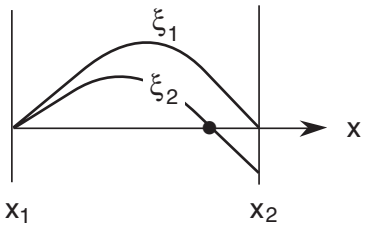

Fig. 7.16. Sturm's oscillation theorem.

then the solutions ξ_2 of the equation

$$(P\xi_2')' - (Q - \lambda_2 R)\,\xi_2 = 0 \tag{7.166}$$

oscillate faster than ξ_1 if $\lambda_2 > \lambda_1$ (Ince [115], p. 224; see Fig. 7.16). Here, 'faster oscillating' means that the solution ξ_2 that vanishes at the left endpoint $x = x_1$ vanishes at least once on the interval (x_1, x_2). (Note that λ_1 is an eigenvalue if the interval (x_1, x_2) corresponds to the complete interval of the problem.)

Proof Multiply Eq. (7.165) by ξ_2 and Eq. (7.166) by ξ_1, integrate over (x_1, x_2) and subtract:

$$\begin{aligned}\int_{x_1}^{x_2} \left[\xi_2(P\xi_1')' - \xi_1(P\xi_2')'\right] dx &= \left[\xi_2 P\xi_1' - \xi_1 P\xi_2'\right]_{x_1}^{x_2} \\ &= \left(\xi_2 P\xi_1'\right)\Big|_{x=x_2} = (\lambda_2 - \lambda_1)\int_{x_1}^{x_2} R\,\xi_1\xi_2\,dx\,. \end{aligned} \tag{7.167}$$

Suppose that the solution ξ_2, which vanishes at $x = x_1$, does not vanish in the open interval (x_1, x_2). Then, the LHS of Eq. (7.167) is negative, whereas the RHS is positive. This contradiction proves that ξ_2 has to vanish at least once on the open interval (x_1, x_2); QED.

Sturm's oscillation theorem gives the behaviour of the solutions of the differential equation (7.162) on any sub-interval of the interval (x_1, x_2). Such an equation, with the property that the solutions oscillate faster upon increasing the eigenvalue parameter λ, is called *Sturmian*. We will call differential equations that have the opposite property (e.g. Eq. (7.162) when the sign of λ is reversed) *anti-Sturmian*. An immediate consequence of these properties is that one can label different discrete modes by just counting the number of nodes on the interval (x_1, x_2). If the system is Sturmian the eigenvalue λ is an increasing function of the number of nodes n, whereas for anti-Sturmian systems λ decreases as a function of n (Fig. 7.17). The classical example of the first kind of behaviour is the vibrating string with characteristic wave speed c and length L, described by the equation $c^2\partial^2\xi/\partial x^2 = \partial^2\xi/\partial t^2 = -\omega^2\xi$, having the eigenvalues $\omega^2 = n^2\pi^2c^2/L^2$.

Downloaded from Cambridge Books Online by IP 152.2.176.242 on Mon Apr 29 20:09:21 WEST 2013.
http://dx.doi.org/10.1017/CBO9780511616945.008
Cambridge Books Online © Cambridge University Press, 2013

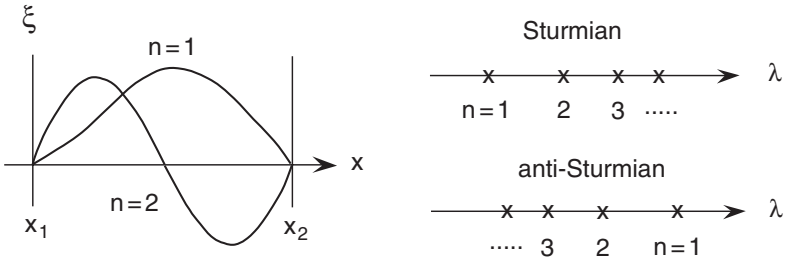

Fig. 7.17. Sturmian and anti-Sturmian dependence of the eigenvalue λ on the number of nodes of the eigenfunctions.

Examples of the second kind of behaviour are much less familiar. However, in Sections 7.2.3 and 7.3.3, we have encountered some significant ones for the HD and MHD waves in a gravitating exponential atmosphere. We will now generalize these properties to arbitrary inhomogeneity.

(b) Oscillation theorem for the MHD wave equation Turning to the MHD wave equation (7.91), it is immediately clear that it is not an equation of the simple Sturm–Liouville kind (7.162). Nevertheless, we may ask whether it still has the Sturmian, or anti-Sturmian, property. It is clear that in order to prove such a property we certainly have to exclude regions of ω^2 corresponding to the continuous spectrum, where the differential equation becomes singular, i.e. where the coefficient N/D in front of the highest derivative develops zeros ($N = 0$). Moreover, it turns out that we also will have to exclude the regions of ω^2 corresponding to the apparent singularities, where N/D becomes infinite ($D = 0$). Let us then study the monotonicity properties, if any, of the discrete spectrum of Eq. (7.91) for values of ω^2 outside the continua $\{\omega_A^2\}$ and $\{\omega_S^2\}$ and also outside the ranges $\{\omega_{s0}^2\}$ and $\{\omega_{f0}^2\}$ shown in Fig. 7.14. For those values of ω^2 the wave equation is free of both genuine and apparent singularities, but the way in which ω^2 appears in the equation makes it virtually impossible to prove anything directly from the equation itself. The reason is, of course, that the wave equation (7.91) has been derived by reducing the original vector eigenvalue problem (with linear dependence on ω^2) to a scalar one. In such a case, the only hope to prove general properties about the spectrum is to go back to first principles and, in particular, to exploit the only general property of the original operator $\rho^{-1}\mathbf{F}$ that we have, viz. that it is self-adjoint.

We prove the following theorem (Goedbloed and Sakanaka [89]). *If x_1 and x_2 are two consecutive zeros of the function ξ_1 satisfying the MHD wave equation (7.91) for $\omega^2 = \omega_1^2$, then the solutions ξ_2 of the MHD wave equation for $\omega^2 = \omega_2^2$*

Downloaded from Cambridge Books Online by IP 152.2.176.242 on Mon Apr 29 20:09:21 WEST 2013.
http://dx.doi.org/10.1017/CBO9780511616945.008
Cambridge Books Online © Cambridge University Press, 2013

oscillate faster than ξ_1 *if* $\omega_2^2 > \omega_1^2$ *and* $N/D > 0$ *(Sturmian), and slower if* $N/D < 0$ *(anti-Sturmian).*

Proof Recall the proof of self-adjointness of the operator $\rho^{-1}\mathbf{F}$ in Section 6.2.3. In particular, let us start from the expression (6.57) for the inner product involving the two displacement vectors $\boldsymbol{\xi}$ and $\boldsymbol{\eta}$, which we now replace by $\boldsymbol{\xi}_1$ and $\boldsymbol{\xi}_2$:

$$\langle \boldsymbol{\xi}_2, \rho^{-1}\mathbf{F}(\boldsymbol{\xi}_1)\rangle - \langle \boldsymbol{\xi}_1, \rho^{-1}\mathbf{F}(\boldsymbol{\xi}_2)\rangle = \tfrac{1}{2}\int \mathbf{n}\cdot\boldsymbol{\xi}_2 \left(\gamma p \nabla\cdot\boldsymbol{\xi}_1 + \boldsymbol{\xi}_1\cdot\nabla p - \mathbf{B}\cdot\mathbf{Q}_1\right) dS$$
$$- \tfrac{1}{2}\int \mathbf{n}\cdot\boldsymbol{\xi}_1 \left(\gamma p \nabla\cdot\boldsymbol{\xi}_2 + \boldsymbol{\xi}_2\cdot\nabla p - \mathbf{B}\cdot\mathbf{Q}_2\right) dS. \quad (7.168)$$

For simplicity, we here exploit the inner product definition (6.35) but assume the vectors to be real. The surface S bounding the plasma actually consists of two surfaces, viz. the planes $x = x_1$ and $x = x_2$. Note that the expressions in the brackets on the RHS correspond to the Eulerian perturbation Π of the total pressure defined in Eq. (7.98), and reduced in Eq. (7.99). Therefore, we may write

$$\begin{aligned}\langle \boldsymbol{\xi}_2, \rho^{-1}\mathbf{F}(\boldsymbol{\xi}_1)\rangle - \langle \boldsymbol{\xi}_1, \rho^{-1}\mathbf{F}(\boldsymbol{\xi}_2)\rangle &= -\tfrac{1}{2}\int \mathbf{n}\cdot\boldsymbol{\xi}_2 \Pi(\boldsymbol{\xi}_1)\, dS + \tfrac{1}{2}\int \mathbf{n}\cdot\boldsymbol{\xi}_1 \Pi(\boldsymbol{\xi}_2)\, dS \\ &= -\tfrac{1}{2}\Big[\xi_2\, \Pi(\boldsymbol{\xi}_1)\Big]_{x_1}^{x_2} + \tfrac{1}{2}\Big[\xi_1\, \Pi(\boldsymbol{\xi}_2)\Big]_{x_1}^{x_2} \\ &= \tfrac{1}{2}\left[\xi_2 \left.\frac{N}{D}\right|_{\omega_1^2} \xi_1'\right]_{x_1}^{x_2} - \tfrac{1}{2}\left[\xi_1 \left.\frac{N}{D}\right|_{\omega_2^2} \xi_2'\right]_{x_1}^{x_2},\end{aligned} \quad (7.169)$$

where we have suppressed the (infinite) area $A \equiv \int dS$ of the y-z plane by tacitly renormalizing the quadratic forms.

Let us now consider two solutions $\boldsymbol{\xi}_1$ and $\boldsymbol{\xi}_2$ of the MHD normal mode equation corresponding to different values ω_1^2 and ω_2^2 of the eigenvalue parameter:

$$\begin{aligned}\mathbf{F}(\boldsymbol{\xi}_1) &= -\rho\omega_1^2\, \boldsymbol{\xi}_1\,, \\ \mathbf{F}(\boldsymbol{\xi}_2) &= -\rho\omega_2^2\, \boldsymbol{\xi}_2\,,\end{aligned} \quad (7.170)$$

but not necessarily satisfying the boundary conditions (7.93). Then, the LHS of Eq. (7.169) transforms to

$$(\omega_2^2 - \omega_1^2)\, \langle \boldsymbol{\xi}_1, \boldsymbol{\xi}_2\rangle\,.$$

Consider a sub-interval (x_1, x_2) of the complete physical interval, temporarily exploiting x_1 and x_2 again to indicate two consecutive zeros of the normal component ξ_1 of $\boldsymbol{\xi}_1$. Let ω_2^2 be close to ω_1^2, so that $\boldsymbol{\xi}_2$ is close to $\boldsymbol{\xi}_1$ and, hence, $\langle \boldsymbol{\xi}_1, \boldsymbol{\xi}_2\rangle > 0$. We will also choose $\boldsymbol{\xi}_2$ such that ξ_2 vanishes at $x = x_1$. We now wish to find out

Downloaded from Cambridge Books Online by IP 152.2.176.242 on Mon Apr 29 20:09:21 WEST 2013.
http://dx.doi.org/10.1017/CBO9780511616945.008
Cambridge Books Online © Cambridge University Press, 2013

whether or not ξ_2 has another zero on (x_1, x_2), i.e., we want to investigate whether ξ_2 oscillates faster or slower than ξ_1 for a given difference of ω_1^2 and ω_2^2. Under the mentioned conditions all that remains of Eq. (7.169) is

$$(\omega_2^2 - \omega_1^2)\,\langle \boldsymbol{\xi}_1, \boldsymbol{\xi}_2 \rangle = \tfrac{1}{2}\left(\xi_2 \frac{N}{D}\bigg|_{\omega_1^2} \xi_1' \right)\bigg|_{x=x_2} . \tag{7.171}$$

Let $\xi_1 > 0$ on the open interval (x_1, x_2) so that $\xi_1'(x = x_2) < 0$. If $N/D > 0$ and $\omega_2^2 - \omega_1^2 > 0$, this implies that $\xi_2(x = x_2) < 0$ so that ξ_2 oscillates faster than ξ_1 (Sturmian behaviour). If, on the other hand, $N/D < 0$, ξ_2 oscillates slower than ξ_1 (anti-Sturmian behaviour); QED.

An important property, directly following from Eq. (7.171), concerns the *orthogonality* of the eigenfunctions of the discrete spectrum. Returning again to using x_1 and x_2 for the complete physical interval, if ξ_1 and ξ_2 both satisfy the left and the right hand boundary conditions (7.93), the RHS of Eq. (7.171) vanishes, so that

$$\langle \boldsymbol{\xi}_1, \boldsymbol{\xi}_2 \rangle = 0 \qquad \text{for} \quad \omega_1^2 \neq \omega_2^2 . \tag{7.172}$$

Hence, the discrete eigenfunctions form an orthogonal set, which may also be normalized to obtain an orthonormal set.

(c) Spectral structure From the oscillation theorem it follows that the discrete spectrum outside the ranges $\{\omega_A^2\}$, $\{\omega_S^2\}$, $\{\omega_{s0}^2\}$, $\{\omega_{f0}^2\}$ shown in Fig. 7.14 is Sturmian for $N/D > 0$, so that the eigenvalue ω^2 increases with the number of nodes of the eigenfunction, and anti-Sturmian for $N/D < 0$, with opposite behaviour of the eigenfunctions. Consequently, the discrete spectrum changes from Sturmian to anti-Sturmian, and vice versa, every time ω^2 crosses one of those four special frequency regions. Thus, the frequency regions $\{\omega_{s0}^2\}$ and $\{\omega_{f0}^2\}$ act as separators of the discrete spectra where non-monotonicity may occur. Consequently, the spectrum of an inhomogeneous plasma slab schematically may look like that shown in Fig. 7.18; see Goedbloed [82].

In conclusion, compared to the spectrum of eigenoscillations of a uniform plasma, the spectrum of an inhomogeneous plasma slab exhibits the following features.

- The infinite degeneracy of the Alfvén point spectrum is lifted and replaced by a continuum of improper modes; in addition, a finite or infinite number of Sturmian, as well as anti-Sturmian, discrete Alfvén modes may occur.
- The accumulation point of the slow magneto-sonic point eigenvalues is spread out into a continuum of improper slow magneto-sonic modes; in addition, a finite or infinite number of Sturmian discrete slow modes may occur.
- The fast magneto-sonic point spectrum still accumulates at infinity.

Downloaded from Cambridge Books Online by IP 152.2.176.242 on Mon Apr 29 20:09:21 WEST 2013.
http://dx.doi.org/10.1017/CBO9780511616945.008
Cambridge Books Online © Cambridge University Press, 2013

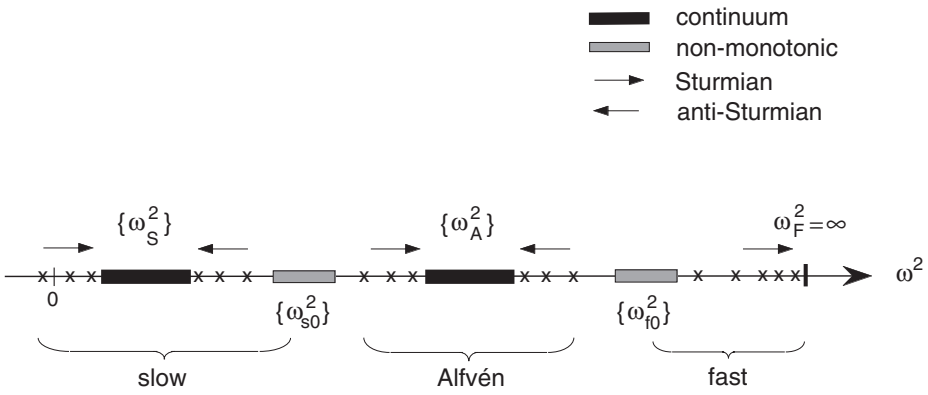

Fig. 7.18. Schematic structure and monotonicity properties of the spectrum of a slightly inhomogeneous plasma layer with gravity. (Without gravity the Sturmian slow modes and all discrete Alfvén modes are missing.)

– The cutoff frequencies ω_{s0}^2 and ω_{f0}^2 are spread out into ranges, which are *not* part of the spectrum, where the discrete spectrum may be non-monotonic.

The clear separation of the sub-spectra shown in Fig. 7.18 is only obtained if the inhomogeneity is not too strong. For strong inhomogeneity the different parts of the spectrum, and their separators, in general fold over each other so that very complicated structures may result. To analyse those, one could consider the inhomogeneous plasma as consisting of a sequence of thin layers, each of which is only weakly inhomogeneous. For each of those layers the local modes (continua and cluster spectra) are well ordered according to the inequalities (7.161), but the non-local discrete modes may appear at apparently arbitrary positions in the spectrum since they may be due to composite structures displaying Alfvénic properties in one part of the plasma and magneto-sonic properties in another part.

To study the problem of stability, in particular to compute the growth rates of instabilities ($\omega^2 < 0$), the relevant part of the spectral structure is extremely simple. There are no continuous spectra for $\omega^2 < 0$ and the discrete modes are Sturmian there. This is exploited in the shooting method, discussed in Section 7.5.1(b).

7.4.4 Cluster spectra*

To show that all four branches of the Alfvén and slow discrete sub-spectra actually may occur, we now derive the conditions for clustering at the edges of the Alfvén and slow continua. To that end, we continue with the analysis of case (b) of Section 7.4.1, where ω^2 is chosen to correspond with the maximum or minimum of the Alfvén or slow continuum; see Fig. 7.11(b). According to Eq. (7.128), at such

Downloaded from Cambridge Books Online by IP 152.2.176.242 on Mon Apr 29 20:09:21 WEST 2013.
http://dx.doi.org/10.1017/CBO9780511616945.008
Cambridge Books Online © Cambridge University Press, 2013

an extremum the expression for the singular Alfvén factor

$$\omega^2 - \omega_A^2 \approx -\tfrac{1}{2}(\omega_A^{2\,\prime\prime})_0\, s^2\,, \tag{7.173}$$

and there is a similar expression for the singular slow factor, which yields a Frobenius expansion with indices $\nu_{1,2}$ given by Eq. (7.138). These indices become complex when the factor under the square root sign is negative, i.e. for

$$q_0 \equiv \left(\frac{s^2 Q}{P}\right)_0 < -\frac{1}{4}\,. \tag{7.174}$$

We will show in Section 7.5.2, for the similar case (c) of a cluster point at marginal stability, that complex indices imply that ξ oscillates infinitely rapidly when the singular point is approached ($s \to \infty$). This implies, through the application of the oscillation theorem, that an infinity of discrete modes is found accumulating at the chosen values of ω^2. We will work out the explicit forms of this inequality for the extrema of the Alfvén and slow continua.

Recall that $P \equiv N/D$. For the Alfvén continuum, one then finds from the expressions (7.91) and (7.92) that

$$\left(\frac{N}{s^2}\right)_0 = f^2 b^4 \cdot -\tfrac{1}{2}\rho(\omega_A^2)''\,, \quad D_0 = -f^2 g^2 b^4\,, \qquad Q_0 = -\rho'\hat{g}\,, \tag{7.175}$$

so that

$$q_0 = -\frac{g^2 \cdot \rho'\hat{g}}{\frac{1}{2}\rho(\omega_A^2)''}\,. \tag{7.176}$$

Hence, in order to have a *Sturmian sequence of discrete Alfvén modes clustering at the lower edge of the Alfvén continuum*, i.e. at the minimum of ω_A^2 (where $\omega_A^{2\,\prime\prime} > 0$), the following condition should be satisfied:

$$g^2 \cdot \rho'\hat{g} \;>\; \frac{1}{8}\,\rho(\omega_A^2)'' \;>\; 0\,; \tag{7.177}$$

vice versa, for an *anti-Sturmian sequence at the upper edge of the Alfvén continuum*, i.e. at the maximum of ω_A^2 (where $\omega_A^{2\,\prime\prime} < 0$):

$$g^2 \cdot \rho'\hat{g} \;<\; \frac{1}{8}\,\rho(\omega_A^2)'' \;<\; 0\,. \tag{7.178}$$

We have encountered an example of the latter in Fig. 7.10, with the cluster spectrum given by Eq. (7.122)(b), for the constant α exponential atmosphere (where $\omega_A^{2\,\prime\prime} = 0$). The counterpart of a Sturmian Alfvén sequence was missing there because that requires an inverted density profile (which is very well possible for more general equilibria).

Downloaded from Cambridge Books Online by IP 152.2.176.242 on Mon Apr 29 20:09:21 WEST 2013.
http://dx.doi.org/10.1017/CBO9780511616945.008
Cambridge Books Online © Cambridge University Press, 2013

Similarly, for extrema of the slow continua, one finds the following expressions:

$$\left(\frac{N}{s^2}\right)_0 = f^2 b^4 \cdot \tfrac{1}{2}\rho(\omega_S^2)'', \quad D_0 = -\omega_S^4,$$
$$Q_0 = \frac{\rho b^2}{c^2\omega_S^2}(\omega_S^4 - k_0^2\hat{g}^2) - \left(\frac{b^2+c^2}{c^2}\,\rho\hat{g}\right)'. \tag{7.179}$$

Hence, in order to have a *Sturmian sequence of discrete slow modes clustering at the lower edge of the slow continuum*, the following condition should be satisfied:

$$\frac{1}{b^2+c^2}\left[-\rho(\omega_S^4 - k_0^2\hat{g}^2) + \frac{c^2}{b^2}\,\omega_S^2\left(\frac{b^2+c^2}{c^2}\,\rho\hat{g}\right)'\right] > \frac{1}{8}\,\rho(\omega_S^2)'' > 0\,; \tag{7.180}$$

vice versa, for an *anti-Sturmian sequence at the upper edge of the slow continuum*:

$$\frac{1}{b^2+c^2}\left[-\rho(\omega_S^4 - k_0^2\hat{g}^2) + \frac{c^2}{b^2}\,\omega_S^2\left(\frac{b^2+c^2}{c^2}\,\rho\hat{g}\right)'\right] < \frac{1}{8}\,\rho(\omega_S^2)'' < 0\,. \tag{7.181}$$

We have encountered an example of the latter behaviour for homogeneous plasmas (where the gravity terms are missing) and of the forms in Fig. 7.10(b), with the cluster spectrum given by Eq. (7.122)(c), for the exponential atmosphere (where $\omega_S^{2\prime\prime} = 0$). Also recall from that example that transition from Sturmian to anti-Sturmian behaviour occurs for a value of $\bar{k}_0^2$ far to the right of the plotted region in Fig. 7.10(b).

Hence, for general equilibria, the five discrete cluster spectra indicated in Fig. 7.18 do actually occur. In the absence of complex indices, the Alfvén and slow cluster points plus the high n modes will be missing, but global (lower n) modes may still be present. To compute those requires numerical solution of the MHD wave equation (7.91).

7.5 Gravitational instabilities of plasmas with magnetic shear

In this section, we apply the stability theory by means of the *energy principle*, as presented in Chapter 6, to the plane inhomogeneous gravitating plasma slab. This also provides another opportunity to illustrate the equivalence of the variational approach with that of the differential equations, as developed in Sections 7.2–7.4.

We have seen that gravity does not influence the continua (i.e. the essential spectrum), but it does influence the appearance or disappearance of discrete cluster spectra (Section 7.4.4). This is clear from the fact that gravity does not appear in the expressions (7.95) and (7.96) for the genuine and apparent singularities ω_A^2, ω_S^2, ω_{s0}^2, ω_{f0}^2 of the basic differential equation (7.91). However, gravity does appear in

Downloaded from Cambridge Books Online by IP 152.2.176.242 on Mon Apr 29 20:09:21 WEST 2013.
http://dx.doi.org/10.1017/CBO9780511616945.008
Cambridge Books Online © Cambridge University Press, 2013

the other coefficients of the ODE determining whether the edge of a continuum is a cluster point or not. Hence, in the logical exposition of the theory, we first had to pay attention to the more difficult issue of the singularities (Section 7.4) whereas the simpler problems of local (related to cluster points) and global stability could be delayed until the present section.

7.5.1 Energy principle for a gravitating plasma slab

Recall that stability can be determined by just studying the sign of the quadratic form $W[\boldsymbol{\xi}]$ for the potential energy for all possible perturbations $\boldsymbol{\xi}$. For convenience, we here repeat the general expression (6.85):

$$W = \tfrac{1}{2}\int \Big[\, \gamma p\, |\nabla\cdot\boldsymbol{\xi}|^2 + |\mathbf{Q}|^2 + (\boldsymbol{\xi}^*\cdot\nabla p)\nabla\cdot\boldsymbol{\xi} \\ + \mathbf{j}\cdot\boldsymbol{\xi}^*\,\mathbf{Q} - (\boldsymbol{\xi}^*\cdot\nabla\Phi)\,\nabla\cdot(\rho\boldsymbol{\xi}) \,\Big] dV\,.$$

We now reduce this expression for the special case of a gravitating plasma slab. This will be the quadratic forms counterpart of the differential equation analysis of Sections 7.3 and 7.4. Of course, the starting point is the same, so that the equilibrium equations (7.71)–(7.74), the 2D Fourier expressions (7.78) for the perturbations, and the projections (7.79)–(7.83) can be maintained. Again, we study separate harmonics, denoted by $\boldsymbol{\xi}(x)\,\exp \mathrm{i}(k_y y + k_z z)$.

Note that the integrand of the expression (6.85) for W consists of products of the unknowns with their complex conjugates. Of course, the energy itself has to be real so that it should be equal to its complex conjugate. This follows from the self-adjointness of the force operator. When working out quadratic forms, it is important to keep track of this reality of the final expression.

(a) Reduction to a one-dimensional variational problem Consider the different contributions to the integrand of W. Recall that we defined the three components ξ, η and ζ such that they can be assumed to be real. Hence, the expression for the compressibility,

$$\nabla\cdot\boldsymbol{\xi} = \xi' + g\eta + f\zeta\,, \tag{7.182}$$

is real. The Cartesian components of the magnetic field perturbation $\mathbf{Q}$ were worked out in Eq. (7.87):

$$Q_x = \mathrm{i}\,f B\,\xi\,, \qquad Q_y = -(B_y\xi)' + k_z B\,\eta\,, \qquad Q_z = -(B_z\xi)' - k_y B\,\eta\,, \tag{7.183}$$

Downloaded from Cambridge Books Online by IP 152.2.176.242 on Mon Apr 29 20:09:22 WEST 2013.
http://dx.doi.org/10.1017/CBO9780511616945.008
Cambridge Books Online © Cambridge University Press, 2013

so that Q_x is imaginary, whereas Q_y and Q_z are real. A typical term of the integrand,

$$\begin{aligned}\mathbf{j}\cdot\boldsymbol{\xi}^*\times\mathbf{Q} &= j_y(\xi_z^* Q_x - \xi_x^* Q_z) + j_z(\xi_x^* Q_y - \xi_y^* Q_x)\\ &= -B_z{}'\left[-\frac{\mathrm{i}}{B}(B_y\eta - B_z\zeta)\,Q_x - \xi\,Q_z\right] + B_y{}'\left[\xi\,Q_y - \frac{\mathrm{i}}{B}(B_z\eta + B_y\zeta)\,Q_x\right],\end{aligned}$$

is now easily seen to be real when the expressions (7.183) are inserted. The remaining contributions to the integrand are also real:

$$\begin{aligned}(\boldsymbol{\xi}^*\cdot\nabla p)\,\nabla\cdot\boldsymbol{\xi} &= p'\xi\,\nabla\cdot\boldsymbol{\xi}\,,\\ (\boldsymbol{\xi}^*\cdot\nabla\Phi)\,\nabla\cdot(\rho\boldsymbol{\xi}) &= -\hat{g}\xi\,(\rho\nabla\cdot\boldsymbol{\xi} + \rho'\xi)\,.\end{aligned}$$

Putting everything together, and cancelling terms by exploiting the equilibrium relation (7.74), the following expression for W is obtained:

$$\begin{aligned}W = \tfrac{1}{2}\int\Bigg[&\frac{f^2B^2}{k_0^2}\xi'^2 + \left(f^2B^2 - \rho'\hat{g} - \frac{\rho^2\hat{g}^2}{\gamma p}\right)\xi^2\\ &+ B^2\left(k_0\eta + \frac{g}{k_0}\xi'\right)^2 + \gamma p\left(\nabla\cdot\xi - \frac{\rho\hat{g}}{\gamma p}\xi\right)^2\Bigg]dV.\end{aligned}\tag{7.184}$$

This quadratic form only depends on ξ, ξ', η and ζ so that, upon minimization, one may expect a differential equation for ξ, and algebraic relations for η and ζ.

▷ **Exercise.** Check all of the above steps for yourself! ◁

In fact, minimization with respect to the transverse variables η and ζ is algebraic and, hence, trivial:

$$\eta = -\frac{g}{k_0^2}\,\xi'\,,\quad\text{and}\qquad \nabla\cdot\boldsymbol{\xi} = \frac{\rho\hat{g}}{\gamma p}\,\xi\quad\Rightarrow\quad \zeta = -\frac{f}{k_0^2}\,\xi' + \frac{\rho\hat{g}}{\gamma p f}\,\xi\,.\tag{7.185}$$

Consequently, only the first two terms remain in the expression (7.184) for the energy:

$$W = \tfrac{1}{2}\int_{x_1}^{x_2}\left[\frac{f^2B^2}{k_0^2}\xi'^2 + \left(f^2B^2 - \rho'\hat{g} - \frac{\rho^2\hat{g}^2}{\gamma p}\right)\xi^2\right]dx,\tag{7.186}$$

where we have suppressed again the infinite area A of the horizontal plane by renormalizing ($\overline{W} \equiv W/A$) and dropping the bar. One immediately notices that the plasma slab is trivially stable in the absence of gravity ($\hat{g} = 0$) since $W \geq 0$ then. An inequality like this illustrates a typical use of the energy principle since it has no simple counterpart in the differential equation approach.

Downloaded from Cambridge Books Online by IP 152.2.176.242 on Mon Apr 29 20:09:22 WEST 2013.
http://dx.doi.org/10.1017/CBO9780511616945.008
Cambridge Books Online © Cambridge University Press, 2013

Systematic minimization of the remaining 1D problem (7.186) is a standard variational problem, as explained in Section 6.6.4, Eqs. (6.198)–(6.201). For a general quadratic form

$$W = \tfrac{1}{2}\int_{x_1}^{x_2} \left(P_0 \xi'^2 + Q_0 \xi^2 \right) dx \,, \tag{7.187}$$

the minimizing solution is a solution of the *Euler–Lagrange equation*

$$\frac{d}{dx}\left(P_0 \frac{d\xi}{dx} \right) - Q_0 \, \xi = 0 \,, \tag{7.188}$$

subject to the boundary conditions

$$\xi(x_1) = \xi(x_2) = 0 \,. \tag{7.189}$$

For the present problem, the Euler–Lagrange equation corresponding to the quadratic form (7.186) reads

$$\frac{d}{dx}\left(\frac{F^2}{k_0^2} \frac{d\xi}{dx} \right) - \left(F^2 - \rho' \hat{g} - \frac{\rho^2 \hat{g}^2}{\gamma p} \right) \xi = 0 \,, \tag{7.190}$$

where we now start to exploit the notation $F \equiv -\mathrm{i}\mathbf{B} \cdot \nabla \equiv k_y B_y + k_z B_z$, already introduced in Eq. (7.97), to stress the central importance of the parallel gradient operator in stability theory.

Note that the Euler–Lagrange equation (7.190) is just the *marginal equation of motion*, obtained from the general MHD wave equation (7.91) by substituting $\omega^2 = 0$:

$$P_0 \equiv P(\omega^2 = 0) \,, \qquad Q_0 \equiv Q(\omega^2 = 0) \,. \tag{7.191}$$

(In contrast to Section 7.4, the index 0 on P_0 and Q_0 now denotes this substitution.) This connection nearly closes the circle of our presentation. We just need to interpret the physical meaning of the 'solutions' of Eq. (7.190) and of the singularities that occur when $F = \mathbf{k}_0 \cdot \mathbf{B} = 0$ somewhere. The latter problem will be addressed in Section 7.5.2.

(b) Variational procedure (absence of singularities) We put quotation marks on 'solutions' since, in general, it is impossible to solve Eq. (7.190) if the boundary conditions (7.189) are imposed. This follows from the simple fact that *there is no eigenvalue parameter* in that differential equation. Hence, all one can do is, for example, start from the left by satisfying the left boundary condition and then integrate to the right and check whether or not more zeros are encountered on the interval (x_1, x_2). Of course, in general, the right boundary condition will not be satisfied for that 'solution'. By means of the calculus of variations, as carried out

Downloaded from Cambridge Books Online by IP 152.2.176.242 on Mon Apr 29 20:09:22 WEST 2013.
http://dx.doi.org/10.1017/CBO9780511616945.008
Cambridge Books Online © Cambridge University Press, 2013

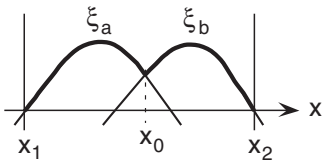

Fig. 7.19. Composite trial function.

systematically by Newcomb [164] for the analogous case of a cylindrical plasma, one may relate the oscillatory behaviour of ξ to stability as follows.

Insert the 'solution' ξ of the Euler–Lagrange equation (7.188) in Eq. (7.187) for the energy W, and integrate by parts:

$$W = \tfrac{1}{2}\int_{x_1}^{x_2} \left(P_0\,\xi'^2 + Q_0\,\xi^2\right) dx$$

$$= \tfrac{1}{2}\int \left[P_0\,\xi'^2 + \xi\,(P_0\xi')'\right] dx = \tfrac{1}{2}\Big[P_0\,\xi\,\xi'\Big]_{x_1}^{x_2}. \qquad (7.192)$$

If the interval (x_1, x_2) is larger than the distance between two consecutive zeros of a solution to the Euler–Lagrange equation, one may split it into two sub-intervals (x_1, x_0) and (x_0, x_2) such that a solution ξ_a which vanishes at $x = x_1$ does not vanish again on (x_1, x_0) and a solution ξ_b which vanishes at $x = x_2$ does not vanish a second time on (x_0, x_2). At $x = x_0$ the amplitudes of the two solutions may be chosen equal (Fig. 7.19). By applying Eq. (7.192) to a solution composed of ξ_a on (x_1, x_0) and ξ_b on (x_0, x_2), one then obtains

$$W = \tfrac{1}{2}\big(P_0\,\xi_a\xi_a'\big)\Big|_{x=x_0} - \tfrac{1}{2}\big(P_0\,\xi_b\xi_b'\big)\Big|_{x=x_0} = \tfrac{1}{2}\Big(P_0\,\xi(\xi_a' - \xi_b')\Big)\Big|_{x=x_0} < 0\,, \qquad (7.193)$$

so that the contribution to the energy is negative. In conclusion:

(1) if the 'solution' ξ_0 of the Euler–Lagrange equation (7.190) (i.e. the marginal equation of motion) that satisfies the left boundary condition $\xi_0(x_1) = 0$ has another zero on the interval (x_1, x_2), then a trial function ξ_1 can be constructed (the composite function of Fig. 7.19) that satisfies both boundary conditions and for which the energy $W(\xi_1) < 0$: the system is unstable;

(2) if ξ_0 has no other zeros on the interval, that construction fails and $W(\xi_1) \geq 0$ for all trial functions: the system is stable.

This is the simple part of Newcomb's variational procedure, valid in the absence of singularities ($F \neq 0$ on the entire interval). The complicated part is the proper handling of those singularities.

Downloaded from Cambridge Books Online by IP 152.2.176.242 on Mon Apr 29 20:09:22 WEST 2013.
http://dx.doi.org/10.1017/CBO9780511616945.008
Cambridge Books Online © Cambridge University Press, 2013

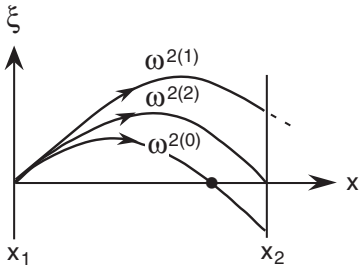

Fig. 7.20. 'Shooting' for discrete eigenvalues.

(c) 'Shooting' method By means of the oscillation theorem of Section 7.4.3, the variational procedure can be replaced by a more transparent one related to the calculation of the *growth rates of the instabilities*. This approach is just a special case of solving for the discrete modes for values of ω^2 outside the ranges of $\omega_A^2(x)$, $\omega_S^2(x)$, $\omega_{s0}^2(x)$, $\omega_{f0}^2(x)$ on the interval $x_1 \leq x \leq x_2$ depicted in Fig. 7.14. In that case, as already alluded to in the introduction of Section 7.4.1, the full MHD wave equation (7.91) is non-singular and a straightforward method to find discrete eigenvalues is to apply the so-called *shooting method*. This amounts to a procedure in which the second order differential equation (7.91) is first solved as an initial value problem where a value of ω^2 is guessed, say $\omega^2 = \omega^{2(i)}$, so that the functions appearing in Eq. (7.91) are determined, and the differential equation is solved numerically starting from the left 'initial' data $\xi(x_1) = 0$, $\xi'(x_1) = \text{const.}$ By some numerical integration scheme the solution $\xi(x; \omega^{2(i)})$ is found. Since the RHS boundary condition (7.93) will not be satisfied in general, $\xi(x_2; \omega^{2(i)}) \neq 0$, one needs to shoot again until this boundary condition is satisfied as well (see Fig. 7.20). To stay with the metaphor: this is not done by changing the inclination of the gun (i.e., by changing the value of $\xi'(x_1)$, which would just change the amplitude of the solution and not the location of the zeros) but by changing the amount of gun powder (i.e., by changing the value of ω^2). Since, according to the oscillation theorem, the eigenvalue ω^2 is monotonic in the distance between the zeros of ξ, one knows precisely in which direction this change has to go: for Sturmian frequency ranges, one should decrease ω^2 to move out the next zero to the position $x = x_2$ to get a genuine eigenfunction, for anti-Sturmian frequency ranges one should increase ω^2.

Unstable discrete modes are always Sturmian because $N/D < 0$ for $\omega^2 < 0$. Since the Euler–Lagrange equation (7.190) is just the marginal form ($\omega^2 = 0$) of the general MHD wave equation (7.91), the connection with the variational procedure for stability is obvious. Referring to Fig. 7.20: if one shoots with $\omega^2 = 0$ and one finds a zero (the curve labelled $\omega^{2(0)}$), there will be a genuine eigenvalue $\omega^{2(2)} < 0$ so that the system is unstable. On the other hand, if one shoots with

Downloaded from Cambridge Books Online by IP 152.2.176.242 on Mon Apr 29 20:09:22 WEST 2013.
http://dx.doi.org/10.1017/CBO9780511616945.008
Cambridge Books Online © Cambridge University Press, 2013

$\omega^2 = 0$ and one finds no zero (the curve labelled $\omega^{2(1)}$), the eigenvalue $\omega^{2(2)} > 0$ so that the system is stable. Hence, the shooting method not only supplies an answer to the stability problem, but also an answer to the question about the 'danger' of the instabilities, i.e. a value for their growth rate. In this manner, the global stability problem appears to have been solved completely for one-dimensional inhomogeneities.

The singularities $F = 0$ of the marginal stability equation are absent in the shooting method as long as $\omega^2 < 0$. From a practical point of view, this is sufficient to solve any stability problem because one can always exploit the σ-stability concept (Section 6.5.3) to stay away from these singularities (any small σ^2 suffices). However, singularities also offer the advantage of increased analytical insight in stability problems, as will be shown in the next section.

7.5.2 Interchange instabilities in sheared magnetic fields

The remaining problem in the stability theory of gravitating plasmas is the proper interpretation of the *singularities* $F \equiv \mathbf{k}_0 \cdot \mathbf{B} = 0$ of the marginal equation (7.190). This is again related to the continuous spectrum since the expressions (7.95) for the Alfvén and slow continuum frequencies both degenerate into the marginal frequency $\omega^2 = 0$ when $F = 0$. Hence, if there is such a point on the interval $[x_1, x_2]$, the Alfvén and slow continua both extend to the origin $\omega^2 = 0$. The physical significance of these points is that the horizontal wave vector $\mathbf{k}_0$ is perpendicular to $\mathbf{B}$, so that the perturbations do not disturb the magnetic field. The magnetic part of the potential energy of the Alfvén wave perturbations vanishes there because the field lines are not bent. Consequently, these are the positions where the driving forces of instability are minimally counterbalanced by magnetic tensions so that instabilities are predominantly localized there.

On the other hand, by means of *magnetic shear* ($F' \neq 0$), the region of minimal field line bending can be minimized so that stability can be restored, as we will see. We have already encountered this effect in Section 6.6.4 when discussing the stabilization of the Rayleigh–Taylor instability of interface plasmas by means of a magnetic field with different directions in the plasma and the vacuum (Fig. 6.21). In that particular case, the magnetic shear was entirely localized in the infinitely narrow surface layer separating plasma and magnetic field. In the present section, we deal with diffuse plasmas where shear is present everywhere.

To establish the significance of the singularities $F(x_0) = 0$, we expand all functions in the neighbourhood of that singularity. Hence, we continue the analysis of case (c) of Section 7.4.1, with the expansion (7.129) of the Alfvén factor, illustrated in Fig. 7.11(c). Introducing the variable angle $\varphi(x) \equiv \arccos(B_z/B)$

Downloaded from Cambridge Books Online by IP 152.2.176.242 on Mon Apr 29 20:09:22 WEST 2013.
http://dx.doi.org/10.1017/CBO9780511616945.008
Cambridge Books Online © Cambridge University Press, 2013

between the magnetic field and the z-axis (Fig. 7.9(b)), and the constant angle $\theta \equiv \arccos(k_z/k_0)$ between the horizontal wave vector and the z-axis, we have

$$F \equiv \mathbf{k}_0 \cdot \mathbf{B} = k_0 B(x) \cos[\,\varphi(x) - \theta\,]\,. \tag{7.194}$$

At the singularity

$$\varphi(x_0) = \theta \pm \pi/2 \quad \Rightarrow \; F'(x_0) = \mp k_0 (B\varphi')_0\,, \tag{7.195}$$

so that

$$\rho\omega_A^2 \equiv F^2(x) \approx (F'^2)_0\, s^2 = k_0^2 (B^2\varphi'^2)_0\, s^2\,, \tag{7.196}$$

where $s \equiv x - x_0$. The quantity φ' represents *the shear of the magnetic field*, which is the change of the angle φ when x is increased. This is caused by the parallel component of the current: $\varphi' = (B_y B_z' - B_y' B_z)/B^2 = -\mathbf{j}\cdot\mathbf{B}/B^2$, according to Eq. (7.72).

In the neighbourhood of the singularity, the marginal stability equation (7.190) is approximated by

$$\frac{d}{ds}\left[\, s^2\,(1 + \cdots)\,\frac{d\xi}{ds}\,\right] - q_0\,(1 + \cdots)\,\xi = 0\,, \qquad q_0 \equiv -\left(\frac{\rho'\hat{g} + \dfrac{\rho^2\hat{g}^2}{\gamma p}}{B^2\varphi'^2}\right)_0\,, \tag{7.197}$$

which has the form of the standard differential equation (7.132) of Section 7.4.1. Consequently, the Frobenius expansion (7.134) may be exploited. To leading order, the solutions of equation (7.197) behave as s^{ν_1} and s^{ν_2}, where ν_1 and ν_2 are the roots of the indicial equation $\nu(\nu+1) - q_0 = 0$, as given by Eq. (7.138). Depending on whether $1 + 4q_0$ is positive or negative, the indices are real or complex.

(a) Local stability (complex indices) The most interesting case is obtained for $1 + 4q_0 < 0$, *when the indices are complex*, because the real solutions of the marginal stability equation are oscillatory then:

$$\begin{aligned} \xi_1 &= s^{-1/2+\mathrm{i}w} + s^{-1/2-\mathrm{i}w} \;\; = 2s^{-1/2}\cos(w\ln s)\,, \\ \xi_2 &= \mathrm{i}(s^{-1/2+\mathrm{i}w} - s^{-1/2-\mathrm{i}w}) = -2s^{-1/2}\sin(w\ln s)\,, \end{aligned} \tag{7.198}$$

where $w \equiv \frac{1}{2}\sqrt{-(1+4q_0)}$. The kind of oscillatory behaviour obtained is quite extreme, since the solutions not only oscillate infinitely rapidly but their amplitude also blows up when $s \to 0$, as schematically illustrated in Fig. 7.21(a). According to the oscillation theorem of Section 7.4.3(b), such marginal 'solutions' signal instability, since the zeros of the solutions of the full MHD spectral equation are peeled off one by one as the value of ω^2 is decreased from 0 to the actual growth

Downloaded from Cambridge Books Online by IP 152.2.176.242 on Mon Apr 29 20:09:22 WEST 2013.
http://dx.doi.org/10.1017/CBO9780511616945.008
Cambridge Books Online © Cambridge University Press, 2013

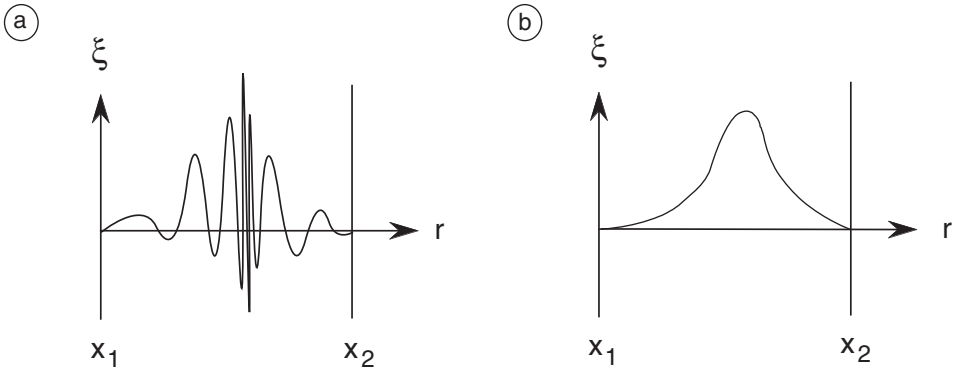

Fig. 7.21. Violation of the interchange criterion: (a) marginal mode ($\omega^2 = 0$, $n = \infty$), (b) associated most global mode ($\omega^2 < 0$, $n = 1$).

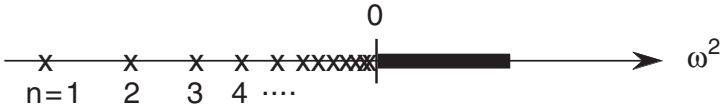

Fig. 7.22. Violation of the interchange criterion: appearance of a cluster point at $\omega^2 = 0$.

rate(s). Consequently, one obtains an infinity of unstable point eigenvalues, accumulating at $\omega^2 = 0$ for $n \to \infty$, where n is the number of nodes of the corresponding eigenfunctions: *when the indices are complex, the marginal point is a cluster point of the unstable modes of the discrete spectrum* (Fig. 7.22). This should not distract the attention from the most important physical fact, viz. that the fastest growing instability is obtained for $n = 1$. Although the condition for instability is local, that $n = 1$ instability need not be local at all, as illustrated by Fig. 7.21(b). Generally, the width of this mode is determined by the width of the region over which the local stability criterion is violated.

To avoid these instabilities, one should demand that $1 + 4q_0 > 0$, so that the indices are real. This leads to the following *stability criterion for interchange modes*:[4]

$$\rho' \hat{g} + \frac{\rho^2 \hat{g}^2}{\gamma p} \quad \left(\equiv -\rho N_B^2 \right) \leq \tfrac{1}{4} B^2 \varphi'^2 \,. \tag{7.199}$$

The three respective terms represent the driving force of the *gravitational* or *Rayleigh–Taylor instability* (heavy fluid on top of a lighter one), *modified by adiabatic effects* (term with γ), and *stabilized by magnetic shear* (term on the right

[4] A rather imprecise term dating from the early days of fusion research when there were hopes of confining extremely high-β plasmas, where the plasma and the magnetic field are nearly completely separated in space. Such plasmas are virtually always unstable with respect to 'interchange' of plasma and magnetic field.

Downloaded from Cambridge Books Online by IP 152.2.176.242 on Mon Apr 29 20:09:22 WEST 2013.
http://dx.doi.org/10.1017/CBO9780511616945.008
Cambridge Books Online © Cambridge University Press, 2013

hand side). To return to our introductory discussion of Section 6.1.1: a glass of magnetized plasma may be turned upside down without the contents dropping out, if the magnetic shear is large enough! Note that the criterion reduces to the HD criterion (7.40) of Section 7.2.2 for convective stability, $N_B^2 > 0$, when $\varphi' = 0$. Here, N_B^2 is the square of the Brunt–Väisäläa frequency, which also turned up in the condition (7.110) of Section 7.3.3 for the stability of gravito-MHD modes.

The analysis has been a *local* one, so that it may be repeated for every point on the interval $[x_1, x_2]$. Hence, for overall stability, one should at least demand that the inequality (7.199) is satisfied everywhere: the criterion is a necessary one for stability. A local criterion of this kind, known as *Suydam's criterion*, was first derived by Suydam (1958) [222] for a diffuse cylindrical plasma column (pinch) where the driving force of the instability is the pressure gradient in combination with curvature of the magnetic field lines. The derivation is completely analogous to the one given here. We will discuss it more extensively in Chapter 9.

(b) Global stability (real indices) For $1 + 4q_0 > 0$, when *the indices are real*, the two solutions at the singularity behave as

$$\begin{aligned} &\xi_s \sim s^{\nu_s}, \qquad \nu_s = -\tfrac{1}{2} + \tfrac{1}{2}\sqrt{1+4q_0} \;>\; -\tfrac{1}{2} \qquad (\text{'small' solution}), \\ &\xi_\ell \sim s^{\nu_\ell}, \qquad \nu_\ell = -\tfrac{1}{2} - \tfrac{1}{2}\sqrt{1+4q_0} \;<\; -\tfrac{1}{2} \qquad (\text{large solution}). \end{aligned} \tag{7.200}$$

Hence, the large solution ξ_ℓ always blows up at $s = 0$, whereas the 'small' solution may or may not blow up depending on whether the square root is smaller or larger than 1. Similar to the singularities for $\omega^2 > 0$, discussed in Section 7.4.2, the present ones (at $\omega^2 = 0$) also split the interval (x_1, x_2) into independent sub-intervals (x_1, x_0) and (x_0, x_2), in the following sense. Consider the sub-interval to the left of the singularity. According to Eq. (7.192), the contribution of that sub-interval to the energy is:

$$W(x_1, x_0) = \tfrac{1}{2}\Big[\, P_0 \xi \xi' \,\Big]_{x_1}^{x_0}. \tag{7.201}$$

At the singularity, this expression behaves as

$$W(x_0) = \tfrac{1}{2}\Big(P_0 \xi \xi'\Big)(x_0) \;\sim\; s^{2\nu+1} \;\rightarrow\; \begin{cases} 0 & \text{for } \nu = \nu_s, \\ \infty & \text{for } \nu = \nu_\ell, \end{cases} \tag{7.202}$$

Downloaded from Cambridge Books Online by IP 152.2.176.242 on Mon Apr 29 20:09:22 WEST 2013.
http://dx.doi.org/10.1017/CBO9780511616945.008
Cambridge Books Online © Cambridge University Press, 2013

so that the energy contribution of the large solution diverges, but that of the 'small' one vanishes (hence: 'small', also when $-\frac{1}{2} < \nu_s < 0$). Consequently, testing for stability while keeping the energy of the perturbations finite implies that we have to exclude the large solution. This means that a kind of internal boundary condition is to be imposed at the singularity, viz. that ξ should be 'small' there. This can be done since jumps in the 'small' solution are allowed by an argument similar to that of Section 7.4.2. Such jumps do not contribute to the energy:

$$P_0\xi_s\, H(s)\left[\xi_s H(s)\right]' \sim s^{\nu+2}H(s)\left[\nu s^{\nu-1}H(s) + s^{\nu}\delta(s)\right]$$
$$= s^{2\nu+1}\left[\nu H(s) + s\delta(s)\right]H(s) \;\to\; 0\,. \qquad (7.203)$$

Therefore, the intervals (x_1, x_0) and (x_0, x_2) may be tested separately with respect to stability (i.e. the sign of W) by means of trial functions that are 'small' at $x = x_0$ and vanish identically either to the right or to the left of $x = x_0$.

The stability test is carried out with the following modification of the non-singular case (described in Section 7.5.1(b), Fig. 7.19), where we now exploit the symbol x_s for the singularity and x_0 for an ordinary interior point. Consider a solution ξ_a of the Euler–Lagrange equation (7.190) which vanishes on the left interval (x_1, x_s), is 'small' to the right of the singularity $x = x_s$, and vanishes once in the interval (x_s, x_2). Such a solution may be joined at a point x_0 in between the singularity x_s and the zero point of ξ_a to another solution ξ_b which vanishes at the right endpoint $x = x_2$, but does not vanish in the open interval (x_0, x_2) (Fig. 7.23). The energy of the Euler–Lagrange solution consisting of $\xi = 0$ on $(0, x_s)$, $\xi = \xi_a$ on (x_s, x_0), and $\xi = \xi_b$ on (x_0, x_2) may be shown to be negative by a completely analogous argument to that used in the derivation of Eq. (7.193). Hence, on independent sub-intervals the 'smallness' of a solution should be counted as a zero,

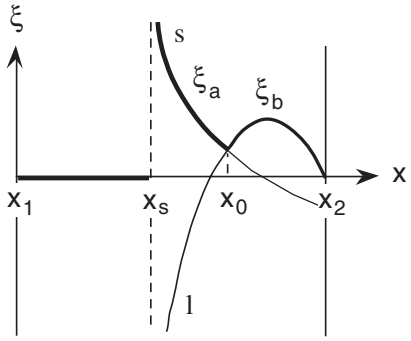

Fig. 7.23. Composite trial function in the presence of a singularity.

Downloaded from Cambridge Books Online by IP 152.2.176.242 on Mon Apr 29 20:09:22 WEST 2013.
http://dx.doi.org/10.1017/CBO9780511616945.008
Cambridge Books Online © Cambridge University Press, 2013

so that for stability a solution that is 'small' at the singularity should not vanish somewhere in the interval. Thus, using Newcomb's wording, we obtain the following stability theorem for the case that the interval (x_1, x_2) contains one singularity $F = 0$ at $x = x_s$.

Theorem. *For specified values of k_y and k_z such that $F \equiv k_y B_y + k_z B_z = 0$ at some point $x = x_s$ of the interval (x_1, x_2), the gravitating plasma slab is stable if, and only if, (1) the interchange criterion (7.199) is satisfied at $x = x_s$; (2) the non-trivial solution ξ_L of the Euler–Lagrange equation (7.190) that is 'small' to the left of $x = x_s$ does not vanish in the open interval (x_1, x_s); (3) the non-trivial solution ξ_R that is 'small' to the right of $x = x_s$ does not vanish in the open interval (x_s, x_2).*

Of course, if there is more than one singularity, there will be more than two independent sub-intervals that have to be tested for oscillatory behaviour in the extended sense.

7.5.3 Interchanges in the absence of magnetic shear

A special case occurs when the magnetic field has *no shear*, i.e. it is uni-directional (like the exponential atmosphere considered in Section 7.3.3). Then, perturbations may be found with $F \equiv 0$ over the whole domain, so that the horizontal wave vector $\mathbf{k}_0$ is perpendicular to the magnetic field everywhere. Naively, one would expect this to be the worst case scenario with stability determined by the condition (7.199) in the no-shear limit ($\varphi' = 0$), i.e. the familiar condition $N_B^2 \geq 0$. However, if $F \equiv fB = 0$, the variable ζ disappears from the expression (7.182) for $\nabla \cdot \boldsymbol{\xi}$ and, thereby, also from the expression (7.184) for the energy. Hence, the two last terms of Eq. (7.184) cannot be considered as independent, so that the minimization proceeds differently than for the case with shear. For $f = 0$, $g = k_0$, the expression for the energy reduces to

$$
\begin{aligned}
W &= \tfrac{1}{2}\int\left[-\left(\rho'\hat{g} + \frac{\rho^2\hat{g}^2}{\gamma p}\right)\xi^2 + B^2\left(k_0\eta + \xi'\right)^2 + \gamma p\left(\xi' + k_0\eta - \frac{\rho\hat{g}}{\gamma p}\xi\right)^2\right]dV \\
&= \tfrac{1}{2}\int\left\{-\left(\rho'\hat{g} + \frac{\rho^2\hat{g}^2}{B^2 + \gamma p}\right)\xi^2\right. \\
&\quad \left. + k_0^2(B^2 + \gamma p)\left[\eta + \frac{(B^2 + \gamma p)\xi' - \rho\hat{g}\xi}{k_0(B^2 + \gamma p)}\right]^2\right\}dV. \qquad (7.204)
\end{aligned}
$$

Downloaded from Cambridge Books Online by IP 152.2.176.242 on Mon Apr 29 20:09:22 WEST 2013.
http://dx.doi.org/10.1017/CBO9780511616945.008
Cambridge Books Online © Cambridge University Press, 2013

By minimization with respect to η, the last term disappears and we get

$$W = -\tfrac{1}{2}\int\left(\rho'\hat{g} + \frac{\rho^2\hat{g}^2}{B^2+\gamma p}\right)\xi^2\,dx\,, \tag{7.205}$$

so that the stability criterion becomes

$$\rho'\hat{g} + \frac{\rho^2\hat{g}^2}{B^2+\gamma p}\quad\left(\equiv -\rho N_m^2\right)\;\leq 0\,. \tag{7.206}$$

Consequently, the stability criterion obtained, for stability with respect to *pure interchanges*, is less severe than the condition (7.199) in the no-shear limit. The expression is again familiar: $N_m^2 \geq 0$, where N_m^2 is the square of the magnetically modified Brunt–Väisäläa frequency defined in Eq. (7.114) of Section 7.3.3.

The criterion $N_m^2 \geq 0$ is automatically satisfied for the exponential atmosphere analysed in that section, consistent with the stability of the solutions (7.113) for perpendicular propagation. However, we also found out there, in the intriguing equation (7.125) where both N_B^2 and N_m^2 appeared, that *the worst instabilities sometimes occur for near-perpendicular*, not for purely perpendicular, *propagation*. This subtlety in the stability of general (not restricted to exponential profiles) shearless magnetic fields was already pointed out in 1961 by Newcomb [165]. We summarize the results of that paper since it throws light on the relationship between stability and spectral analysis.

As is clear from Section 7.3.3, the relevant modes for instability are the low-frequency Alfvén and slow modes. Hence, it is expedient to get rid of the high-frequency fast modes by means of an ordering. This we do by introducing a scale length L of the equilibrium variations,

$$L^{-1} \equiv \frac{\rho\hat{g}}{p+\frac{1}{2}B^2} \tag{7.207}$$

(the parameter α of Section 7.3.3), and imposing the following ordering on the frequencies and wave numbers:

$$\rho\omega^2 \sim L^{-1}\rho\hat{g} \sim f^2b^2 \ll k_0^2b^2\,. \tag{7.208}$$

This implies that we assume near perpendicular propagation of the modes ($|f| \ll |g|$). The MHD wave equation (7.91) then reduces to

$$\frac{d}{dx}\,\rho(\omega^2 - f^2b^2)\,\frac{d\xi}{dx} - k_0^2\left[\,\rho(\omega^2-f^2b^2) + \rho'\hat{g} + \rho\hat{g}^2\,\frac{\omega^2-f^2b^2}{(b^2+c^2)\omega^2 - f^2b^2c^2}\,\right]\xi = 0. \tag{7.209}$$

Downloaded from Cambridge Books Online by IP 152.2.176.242 on Mon Apr 29 20:09:22 WEST 2013.
http://dx.doi.org/10.1017/CBO9780511616945.008
Cambridge Books Online © Cambridge University Press, 2013

This equation still contains the exact marginal stability equation (7.190) for $\omega^2 \to 0$. We solve it for local modes, varying rapidly over the length scale L:

$$\xi \sim \mathrm{e}^{\mathrm{i}qx}, \qquad qL \gg 1\,. \tag{7.210}$$

This yields the following dispersion equation:

$$\omega^4 - \left(\frac{b^2+2c^2}{b^2+c^2}\, f^2b^2 + \frac{k_0^2}{k_0^2+q^2}N_m^2\right)\omega^2 + \frac{c^2}{b^2+c^2}\, f^2b^2\left(f^2b^2 + \frac{k_0^2}{k_0^2+q^2}N_B^2\right) = 0\,, \tag{7.211}$$

having two qualitatively different solutions. For $F^2/\rho \equiv f^2b^2 \ll |N_B^2| \sim |N_m^2|$, we recover the solutions (7.125) found in Section 7.3.3:

$$\omega_1^2 \approx \frac{k_0^2}{k_0^2+q^2}\,N_m^2\,, \qquad \omega_2^2 \approx \frac{\gamma p}{\gamma p + B^2}\,\frac{N_\mathrm{B}^2}{N_m^2}\,F^2/\rho\,. \tag{7.212}$$

The first mode is a *pure interchange* ($F = 0$) which becomes unstable when $N_m^2 < 0$. The second mode is called a *quasi-interchange* ($F \neq 0$) since only finite segments of the field lines can be involved in interchanging plasma and magnetic field. They become unstable when $N_B^2 < 0$. Since this is the more severe criterion, it should be considered as the overall boundary for stability of gravitational instabilities in shearless magnetic fields. With the consideration of the quasi-interchanges, the discrepancy in the stability criteria between sheared magnetic fields in the limit $\varphi \to 0$ and shearless magnetic fields disappears.

To establish the danger of instabilities, it is not sufficient to derive stability criteria, one should also calculate the maximum growth rate to find out which mode dominates. This involves maximizing the growth rate obtained from Eq. (7.211) with respect to the mode numbers f, g and q. This is left as an exercise for the reader. It is expedient to introduce the following notation:

$$\Gamma \equiv -\frac{\rho'}{\rho}\,\hat{g}\,, \qquad \Gamma_B \equiv \frac{\rho\hat{g}^2}{\gamma p}\,, \qquad \Gamma_m \equiv \frac{\rho\hat{g}^2}{\gamma p + B^2}\,, \qquad \Gamma_0 \equiv \frac{\gamma p\,\rho\hat{g}^2}{(\gamma p + B^2)^2}\,, \tag{7.213}$$

where it is to be noted that $\Gamma_B \geq \Gamma_m \geq \Gamma_0$. The result of the optimization can then be summarized as follows:

(1) if $\Gamma \geq \Gamma_B$, the plasma is stable;

(2) if $\Gamma_0 \leq \Gamma < \Gamma_B$, the most unstable mode is a quasi-interchange ($k_\parallel \neq 0$) with

Downloaded from Cambridge Books Online by IP 152.2.176.242 on Mon Apr 29 20:09:22 WEST 2013.
http://dx.doi.org/10.1017/CBO9780511616945.008
Cambridge Books Online © Cambridge University Press, 2013

growth rate

$$\omega^2 = -\frac{\rho \hat{g}^2}{B^2}\left(1 - \sqrt{\Gamma/\Gamma_B}\right)^2 ; \tag{7.214}$$

(3) if $\Gamma \leq \Gamma_0$, the most unstable mode is a pure interchange ($k_\parallel = 0$) with growth rate

$$\omega^2 = \Gamma - \Gamma_m \equiv N_m^2 . \tag{7.215}$$

Hence, calculating the eigenfrequencies of the modes not only removes apparent discrepancies from stability theory, but also introduces new transitions ($\Gamma = \Gamma_0$) that are relevant for the description of the dynamics. Spectral theory is not only a mathematical beauty but also a physical necessity for understanding the dynamics of inhomogeneous plasmas.

7.6 Literature and exercises

Notes on literature

Hydrodynamics of the solar interior and corona:

- Priest, *Solar Magnetohydrodynamics* [190], Chapter 4 on waves.
- Stix, *The Sun* [217], Chapter 2 on internal structure of the Sun, Chapter 5 on oscillations.
- Christensen-Dalsgaard, *Stellar Oscillations* [56], Chapter 2 on the analysis of oscillation data, Chapter 5 on properties of solar and stellar oscillations.

Spectral theory of gravitating plasma slab:

- Goedbloed [81], in a series of papers on 'Stabilization of magnetohydrodynamic instabilities by force-free magnetic fields', derives the MHD wave equation for a gravitating plasma slab (I), and discusses quasi-interchanges in shearless magnetic fields (III).
- Goedbloed & Sakanaka [89], in a 'New approach to magnetohydrodynamic stability', prove the oscillation theorem for the MHD wave equation and introduce the concept of σ-stability.
- Lifschitz, *Magnetohydrodynamics and Spectral Theory* [146], Chapter 7 on MHD oscillations of a gravitating plasma slab.

Singular differential equations:

- Ince, *Ordinary Differential Equations* [115], Chapter 18 on the solution of linear differential equations in series.
- Bender & Orszag, *Advanced Mathematical Methods for Scientists and Engineers* [23], Chapter 3 on approximate solutions of linear differential equations.

Gravitational instabilities:

- Newcomb [165], on quasi-interchanges in 'Convective instability induced by gravity in a plasma with a frozen-in magnetic field'.

Downloaded from Cambridge Books Online by IP 152.2.176.242 on Mon Apr 29 20:09:22 WEST 2013.
http://dx.doi.org/10.1017/CBO9780511616945.008
Cambridge Books Online © Cambridge University Press, 2013

– Parker [175], on the Parker instability in 'The dynamical state of the interstellar gas and field'.
– Mouschovias [160], on 'The Parker instability in the interstellar medium'.

Exercises

[7.1] *The Sun – energy source*

The Sun appears to be a regularly shaped sphere subject to the laws of hydrodynamics.

– Describe the mechanism which produces this shape. Looking at the Sun more carefully, it appears flattened at the poles. Why is that?

Before nuclear physics was understood, it was thought that the energy of the Sun comes from slow contraction due to gravity.

– Using the Sun's luminosity and Newton's law of gravity, estimate the speed at which the Sun would have to shrink. How long would the Sun be able to burn like this?

The light emanating from the Sun exerts pressure.

– Using physical arguments, find the maximum luminosity (called the Eddington luminosity) the Sun could have before it would blow away its outer layers.
– Using the luminosity of the Sun, calculate the heat flux at the Earth. Estimate the surface of exposed skin on your body. When sunbathing for 15 minutes, how much energy would have been transported to your body? How long could a light bulb of 60 watts burn on that amount of energy?

The source of all this radiation is not located near the surface of the Sun.

– Draw a cross-section of the Sun, indicate how and where this energy is produced, and name the different regions resulting from that.

[7.2] *The Sun – radiative transport*

The transport of radiation through a medium can be regarded as a random walk process. On average, a photon will travel one mean free path λ_{mfp} and collide with a particle, which redistributes it into a random direction. Due to the gradient in particle density, the net flux of radiation will be pointing outward. (This process is often compared to a drunkard trying to make his way through a crowded room.)

– The mean free path is defined by $\lambda_{\mathrm{mfp}} \equiv (\kappa\rho)^{-1}$. Choosing the value $\kappa = 0.12\,\mathrm{m^2\ kg^{-1}}$ for the opacity (also called the Rosseland absorption coefficient), calculate the mean free path of a photon, using the solar radius and mass.
– In n steps, the photon travels a distance $d = \sqrt{n}\,\lambda_{\mathrm{mfp}}$. Estimate the number of steps needed for a photon to travel one solar radius and the time needed to cover this distance.

[7.3] *The Sun – convection*

At some radius, the energy produced no longer escapes as radiation, but is transported by convection. We are going to derive the Schwarzschild criterion for the onset of convection.

– Write down the equation of state for an ideal gas in terms of ρ and T, and derive the temperature gradient from this.
– The bulk motion of gas is only stable if the specific entropy, $S \equiv p\rho^{-\gamma}$, is constant in space. Derive the density gradient and the isentropic temperature gradient from this.

Downloaded from Cambridge Books Online by IP 152.2.176.242 on Mon Apr 29 20:09:23 WEST 2013.
http://dx.doi.org/10.1017/CBO9780511616945.008
Cambridge Books Online © Cambridge University Press, 2013

– By comparing these temperature gradients, the criterion for instability is obtained. Convert this criterion by means of the gravitational equilibrium equation to another form, relating to an apparently different instability. Which one is it?

[7.4] *Waves in a gravitating hydrodynamic slab*

Derive the HD wave equation for a plane parallel atmosphere from the nonlinear equations for the density, pressure, and velocity, ignoring non-adiabatic effects.

– What does the latter assumption imply for the description of the Sun?
– Using the Cowling approximation (what does that mean?), derive the differential equations in terms of the displacement field $\boldsymbol{\xi}$ for the appropriate horizontal Fourier modes.
– Rotate the coordinate system such that one of the axes is in the direction of the horizontal wave vector (why is that expedient?), and then derive the second order differential equation for the vertical displacement.

[7.5] *HD waves in an exponentially stratified atmosphere*

We continue with the HD wave equation obtained in the previous exercise.

– What is the physical significance of choosing exponential dependence on height, $\mathrm{e}^{-\alpha x}$, for both the pressure and the density? What does it imply for the sound speed? Using the equilibrium condition, express α in the gravitational parameter $\hat{g}$.
– Derive the second order differential equation for ξ_x in terms of the Brunt–Väisäläa frequency, $N_B^2 = \alpha\hat{g} - \hat{g}^2/c^2$. Obtain the dispersion equation from it and solve it.

[7.6] *MHD waves in an exponentially stratified atmosphere*

Look up the MHD wave equation for general one-dimensional inhomogeneity.

– In addition to the exponential pressure and density profiles of the previous exercise, introduce the appropriate form of the magnetic field as a function of the vertical coordinate to have an atmosphere with constant Alfvén speed. Calculate the new expression for α and use it to simplify the MHD wave equation and resulting dispersion equation.
– For these magnetic field, pressure, and density profiles, calculate the different MHD singularities. What do they represent?
– Give the solutions for purely parallel and purely perpendicular propagation of the waves, exploiting the magnetically modified Brunt–Väisäläa frequency, $N_m^2 = \alpha\hat{g} - \hat{g}^2/(b^2 + c^2)$, as well as N_B^2. Which wave may become unstable? Why not the other one as well?

[7.7]* *Dispersion equation for gravito-MHD waves*

Write a numerical program, exploiting the explicit solutions given in the text, to solve for the three gravito-MHD waves in an exponential atmosphere of magnetized plasma.

– Plot the three branches $\bar{\omega}^2(\bar{k}_0^2)$, similar to Fig. 7.10, for $\bar{\alpha} = 20$, $\beta = 1$, $\vartheta = \pi/2 - 0.1$ with $\bar{q} = \pi, 2\pi, \ldots$. How wide is the unstable region? What kind of modes are they?
– Estimate the value of $\bar{k}_0^2$ where the slow modes change from Sturmian to anti-Sturmian. Continue the numerical scan to that value to check the answer. What do you learn?

Downloaded from Cambridge Books Online by IP 152.2.176.242 on Mon Apr 29 20:09:23 WEST 2013.
http://dx.doi.org/10.1017/CBO9780511616945.008
Cambridge Books Online © Cambridge University Press, 2013

[7.8]★ Continuous spectra and spectral structure

Assuming weak inhomogeneity of the equilibrium, make a sketch of a possible normal dependence of the singular frequencies ω_A^2 and ω_S^2. Also make a sketch of the associated MHD spectrum, indicating continua, discrete spectra, and the separating non-monotonicity regions.

- Starting with the first picture: the second order differential equation $(P\xi')' - Q\xi = 0$ for the MHD spectrum becomes singular at a point $x = x_0$ where $\omega = \omega_A(x_0)$, giving rise to the Alfvén continuum. Expand $\omega^2 - \omega_A^2$ around that singularity, use it to express $P \equiv N/D \sim s \equiv x - x_0$, and expand the other function, Q, as well (only the constant is needed). Solve the differential equation by means of Frobenius' method and discuss the meaning of the two solutions obtained.
- Concerning the second picture: what is the difference between the solutions of the Alfvén and slow continua and those of the turning point frequencies?
- Indicate Sturmian and anti-Sturmian regions in the diagram. (What do those terms mean?) How does the picture change when gravity is introduced? Show that gravity does not influence the continua, but it may effect the appearance of discrete spectra.

[7.9] *Spectrum of an incompressible gravitating slab*

Derive the MHD wave equation for an incompressible ($\gamma \to \infty$) gravitating plasma slab from the general wave equation. (This is a significant simplification, but watch out with the confluences!)

- Show that the Alfvén and slow singularities coincide so that the two continua are degenerate. How do the associated 'improper' modes differ?
- Neglecting gravity, assuming $\rho = \text{const}$, and a linear dependence of $\omega_A^2(x)$ about the singularity at $x = x_0$, show that the wave equation reduces to the zero order modified Bessel equation,

$$\xi'' + z^{-1}\xi' - \xi = 0\,, \quad z \equiv k_0(x - x_0)\,,$$

  with solutions

$$I_0 = 1 + \tfrac{1}{4}z^2 + \tfrac{1}{32}z^4 + \cdots\,,$$

$$K_0 = -[\ln(\tfrac{1}{2}z) + \gamma_0]\, I_0(z) + \tfrac{1}{4}z^2 + \tfrac{3}{128}z^4 + \cdots \quad (\gamma_0 \approx 0.5772 \text{ is Euler's constant})\,.$$

  Are there any 'solutions' other than the ones associated with the continua?
- What changes when you allow for gravity?

[7.10]★ *Shooting method*

One can investigate the discrete spectrum without worrying about the singular solutions by exploiting the 'shooting method', outside the ranges of the continua.

- Explain how this method works.
- In a numerical shooting procedure, what complications do you foresee when solving in the ranges of the turning point frequencies? How would you handle that?

[7.11] *Interchange instabilities*

Unstable modes have frequencies that are automatically outside the ranges of the continua, at least when their growth rate is finite. At $\omega^2 = 0$, one may exploit the potential energy of the perturbations to investigate stability, but one has to worry about a particular singularity.

Downloaded from Cambridge Books Online by IP 152.2.176.242 on Mon Apr 29 20:09:23 WEST 2013.
http://dx.doi.org/10.1017/CBO9780511616945.008
Cambridge Books Online © Cambridge University Press, 2013

– Assume we have a plane gravitating plasma with a sheared magnetic field. Write down the expression for the potential energy, W, and reduce it to a one-dimensional form.
– Explain why, usually, instabilities are localized at positions $x = x_0$ where $F(x_0) = 0$, when $F \equiv \mathbf{k}_0 \cdot \mathbf{B}$. Expand F around $x = x_0$ exploiting the angle $\varphi(x) \equiv \arccos(B_z/B)$.
– Insert this expansion in the Euler–Lagrange equation, and solve by means of a Frobenius expansion. Show that this yields a leading order equation of the form $(s^2\xi')' - q_0\xi = 0$ with indicial equation $\nu(\nu+1) - q_0 = 0$, where $q_0 \equiv -(\rho'\hat{g} + \rho^2\hat{g}^2/\gamma p)_0/(B^2\varphi'^2)_0$.
– How do you obtain the stability criterion for interchange modes from that equation? Explain the meaning of the three terms.

Downloaded from Cambridge Books Online by IP 152.2.176.242 on Mon Apr 29 20:09:23 WEST 2013.
http://dx.doi.org/10.1017/CBO9780511616945.008
Cambridge Books Online © Cambridge University Press, 2013